10.1071/CH23130
Australian Journal of Chemistry

Supplementary Material

The synthesis and manipulation of certain Diels–Alder adducts of levoglucosenone and *iso*-levoglucosenone

Brett Pollard[A], *Xin Liu*[A], *Luke A. Connal*[A], *Martin G. Banwell*[B,*] and *Michael G. Gardiner*[A]

[A]Research School of Chemistry, Institute of Advanced Studies, The Australian National University, Canberra, ACT 2601, Australia

[B]Institute for Advanced and Applied Chemical Synthesis, Jinan University, Guangzhou, 510632, PR China

*Correspondence to: Email: mgbanwell@jnu.edu.cn, mgbanwell@gmail.com

Plots derived from the single-crystal X-ray analyses of compounds 10, 12, 14, 15, 16, 18, 19, 20, 22, 23, 24, 25, 29, 30, 32, 33 and the aggregate of compounds 33 and 34

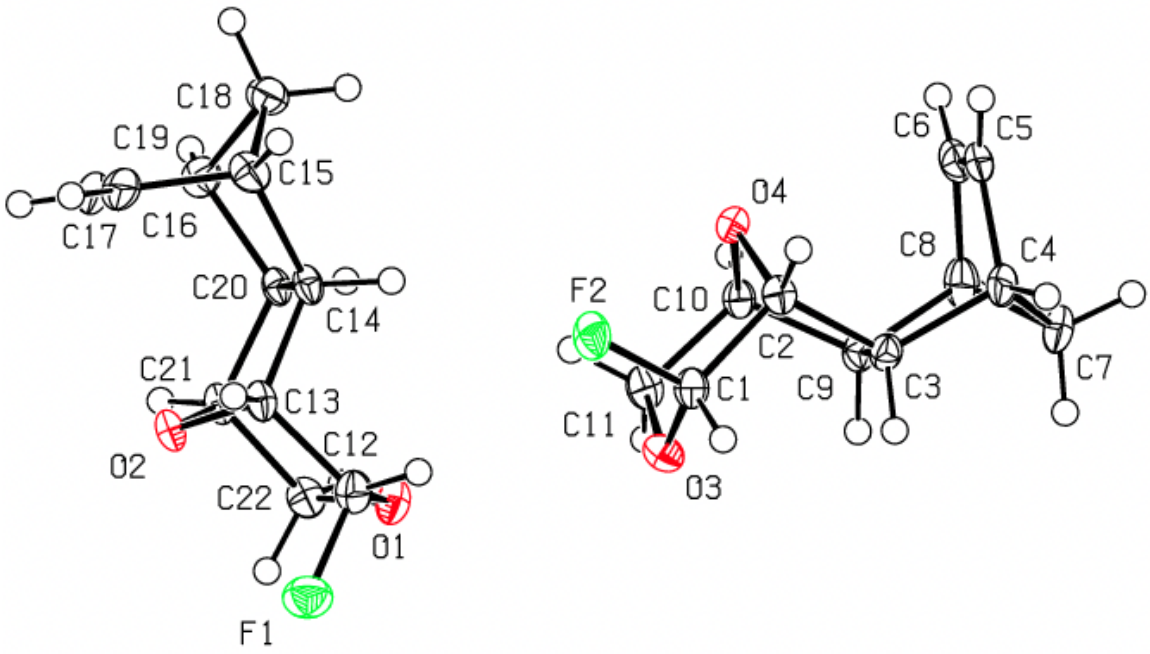

Figure S1: Molecular structure of compound **10** (CCDC 2268350) showing both crystallographically independent molecules in the asymmetric unit. Atomic displacement parameters shown at 50% probability level (crystal grown from hexane).

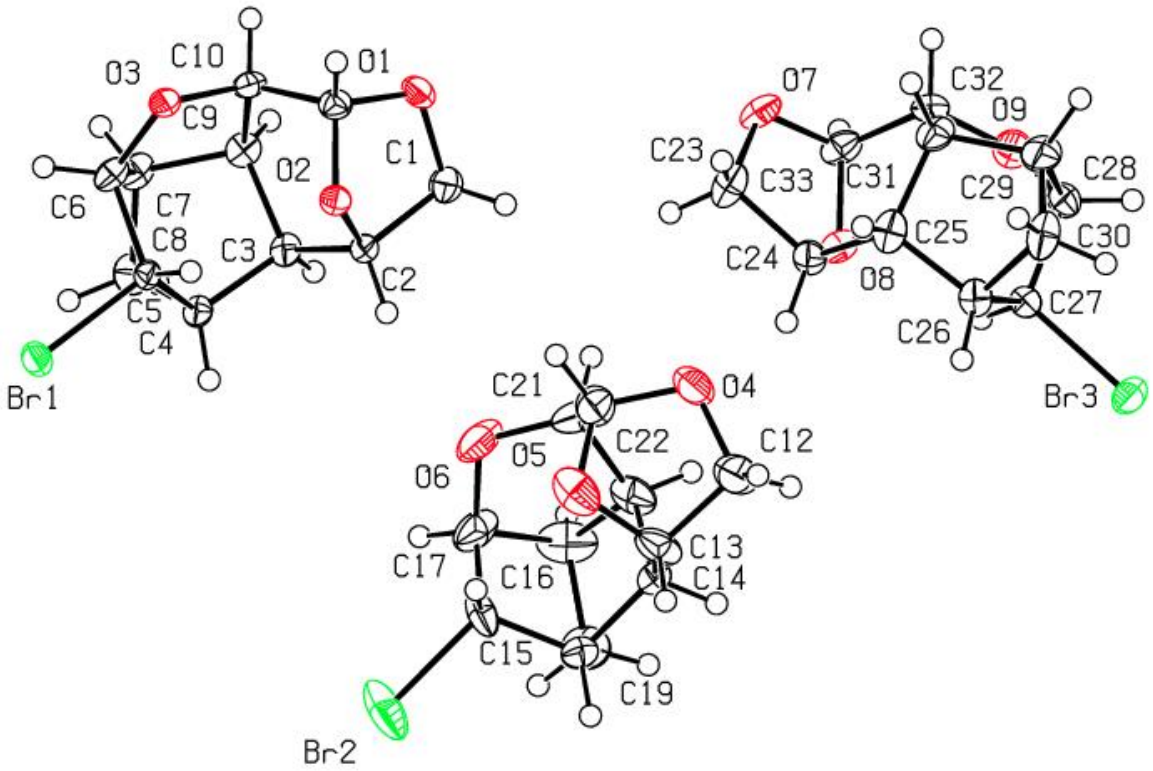

Figure S2: Molecular structure of compound **12** (CCDC 2268351) and showing the three crystallographically independent molecules in the asymmetric unit. Atomic displacement parameters shown at 50% probability level (crystal grown from methanol–dichloromethane).

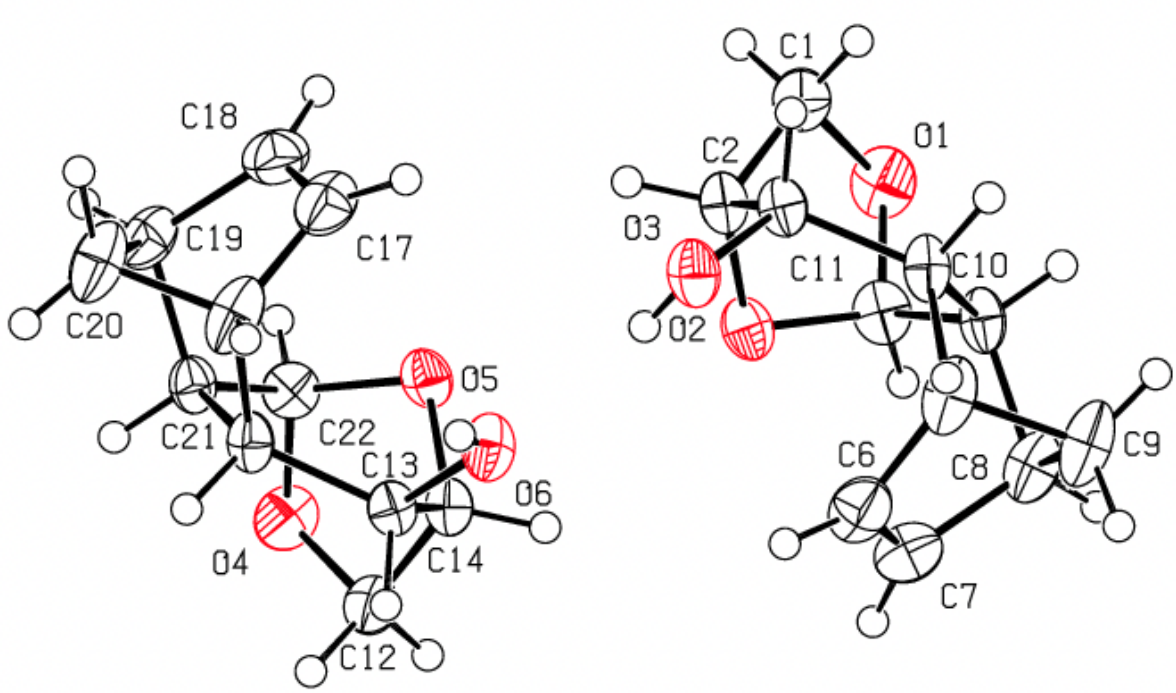

Figure S3: Molecular structure of compound **14** (CCDC 2268353) and showing both crystallographically independent molecules in the asymmetric unit (hydrogen bonding is not shown and the extended structure arising from hydrogen bonding is also not shown). Atomic displacement parameters shown at 50% probability level (crystal grown from diethyl ether–petroleum ether).

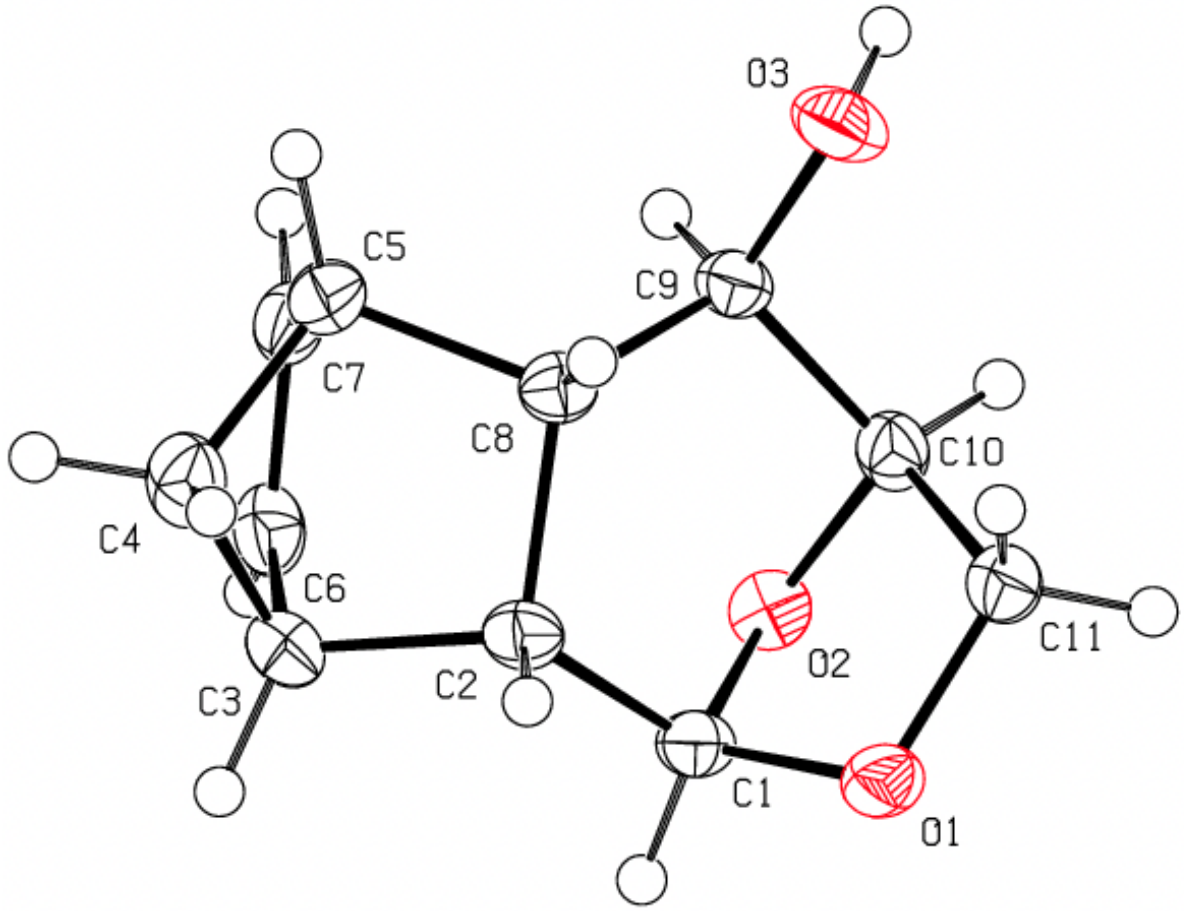

Figure S4: Molecular structure of compound **15** (CCDC 2268352). The extended structure arising from hydrogen bonding is not shown. Atomic displacement parameters shown at 50% probability level (crystal grown from ethyl acetate–petroleum ether).

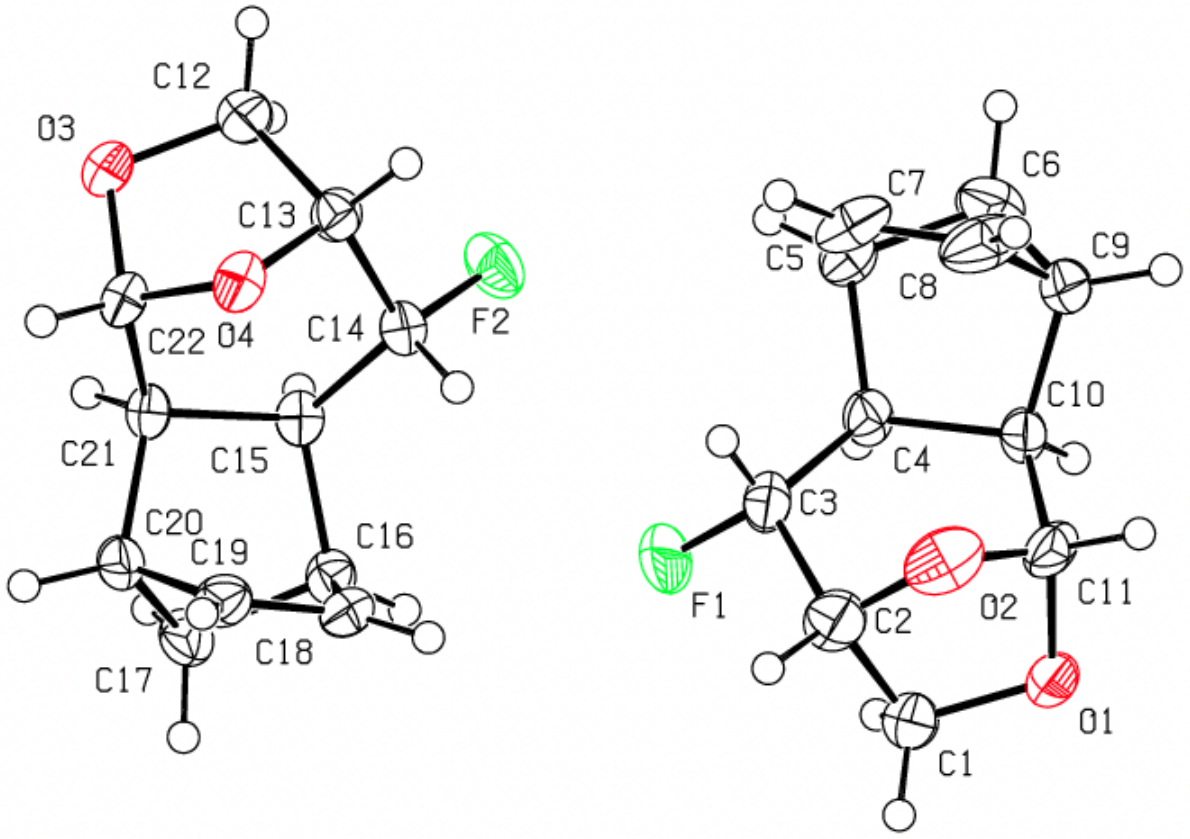

Figure S5: Molecular structure of compound **16** (CCDC 2268354) showing both crystallographically independent molecules in the asymmetric unit. Atomic displacement parameters shown at 50% probability level (crystal grown from hexane).

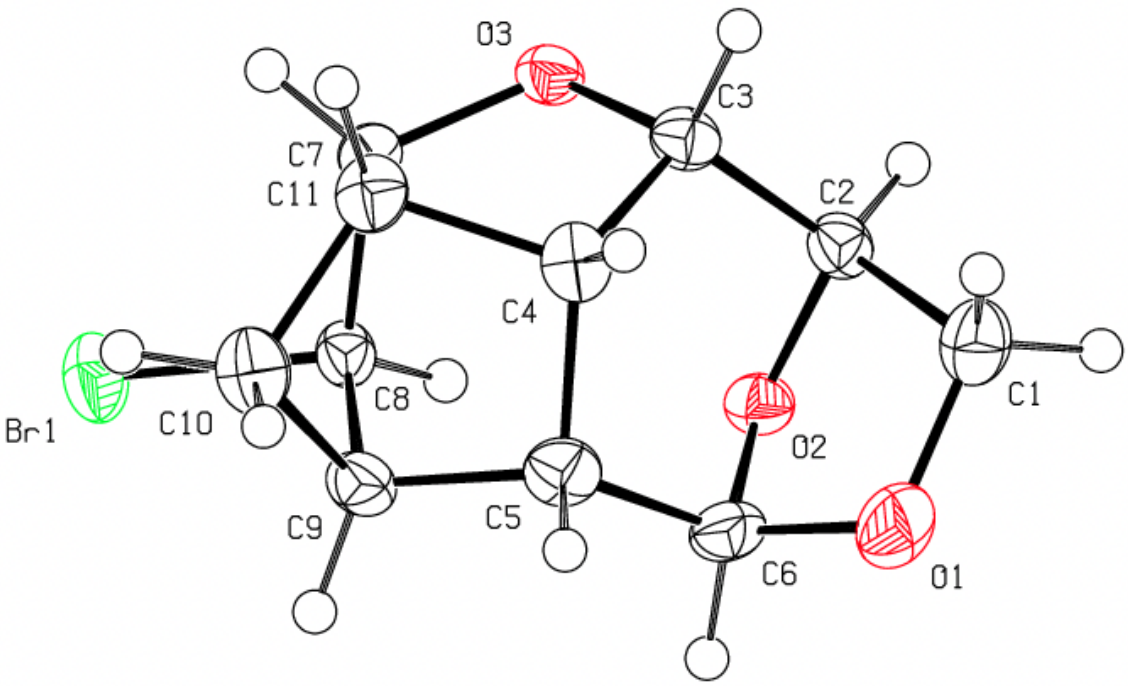

Figure S6: Molecular structure of compound **18** (CCDC 2268355). Atomic displacement parameters shown at 50% probability level (crystal grown from ethyl acetate–hexane–methanol).

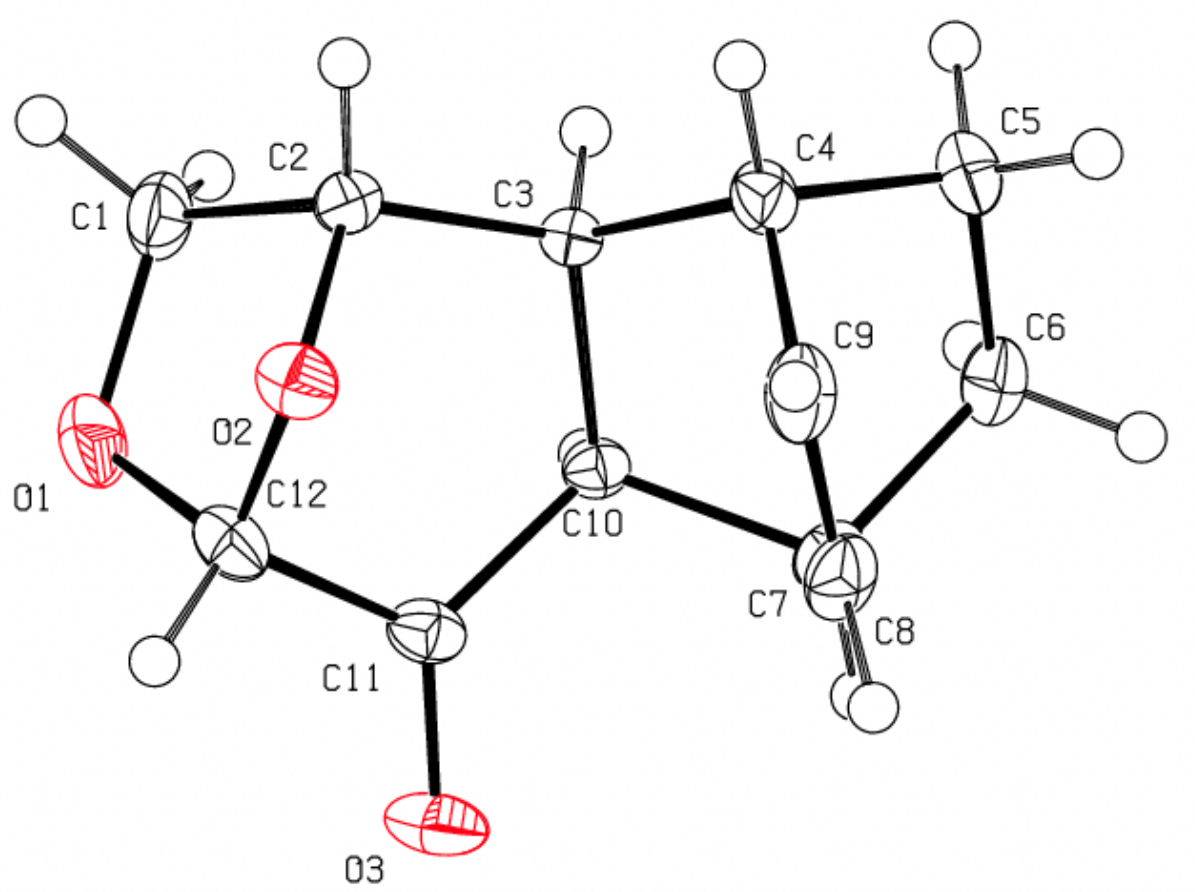

Figure S7: Molecular structure of compound **19** (CCDC 2268356). Atomic displacement parameters shown at 50% probability level (crystal grown from diethyl ether–hexane).

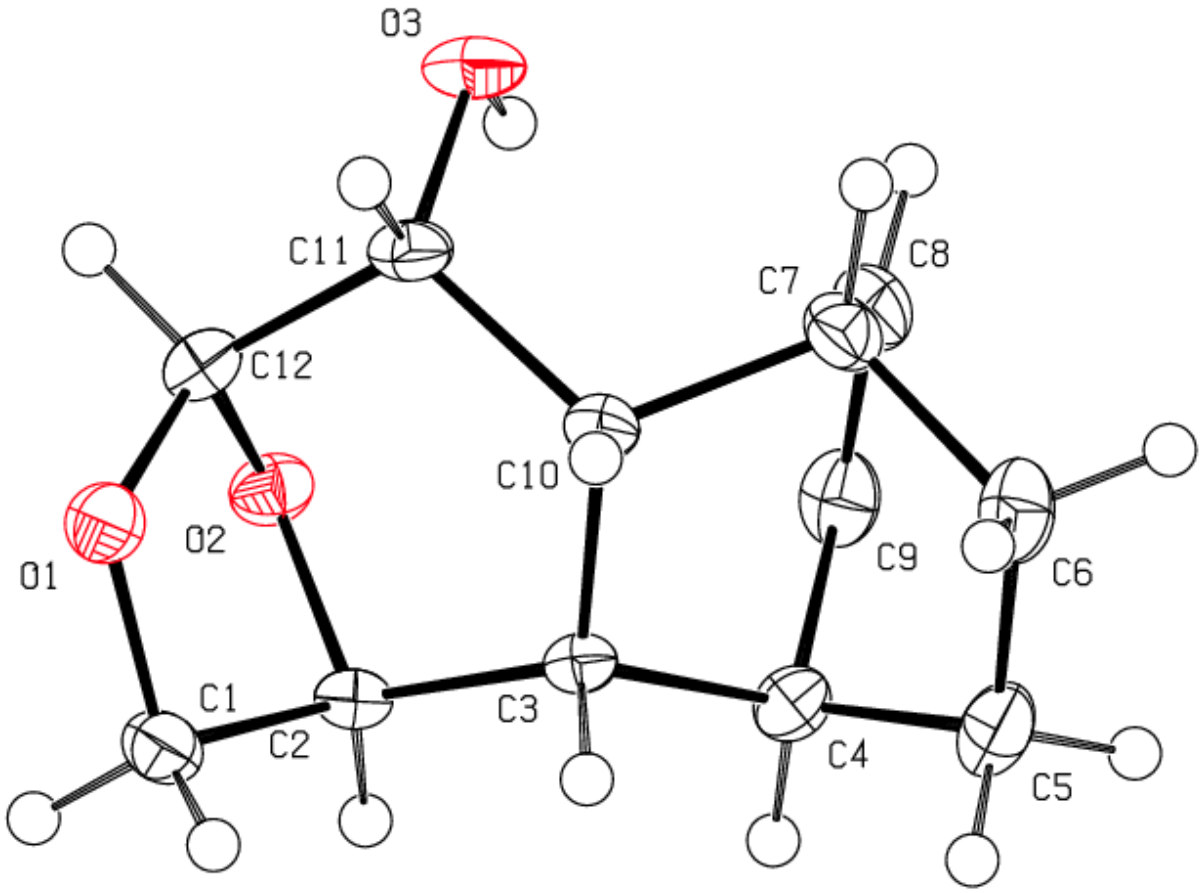

Figure S8: Molecular structure of compound **20** (CCDC 2268357). The extended structure arising from hydrogen bonding is not shown. Atomic displacement parameters shown at 50% probability level (crystal grown from diethyl ether–hexane).

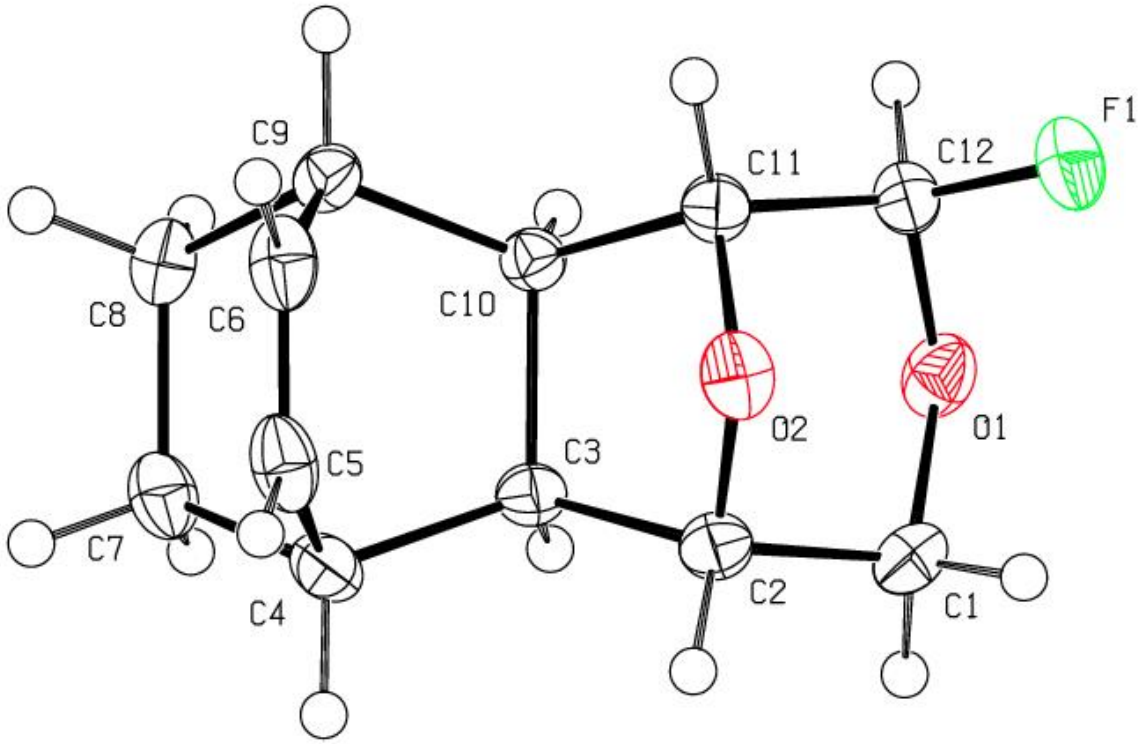

Figure S9: Molecular structure of compound **22** (CCDC 2268358). Atomic displacement parameters shown at 50% probability level (crystal grown from dichloromethane).

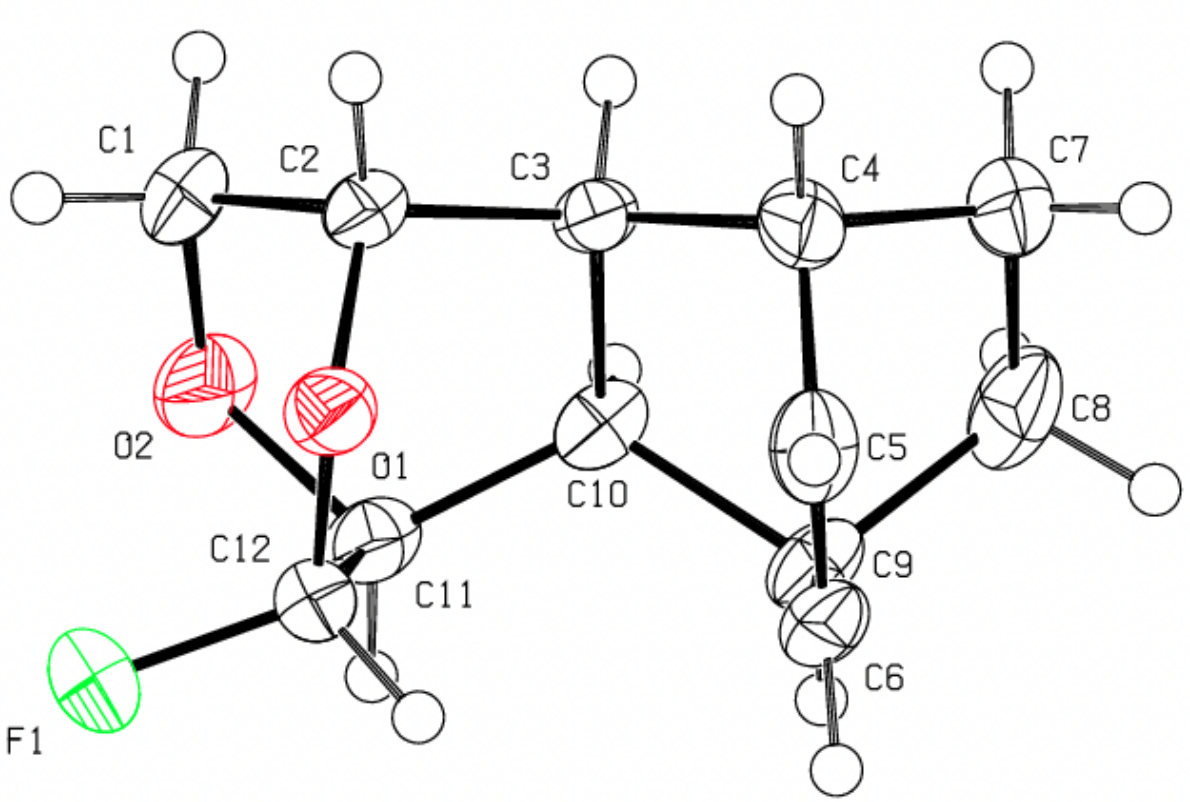

Figure S10: Molecular structure of compound **23** (CCDC 2268359). Atomic displacement parameters shown at 50% probability level (crystal grown from dichloromethane–methanol).

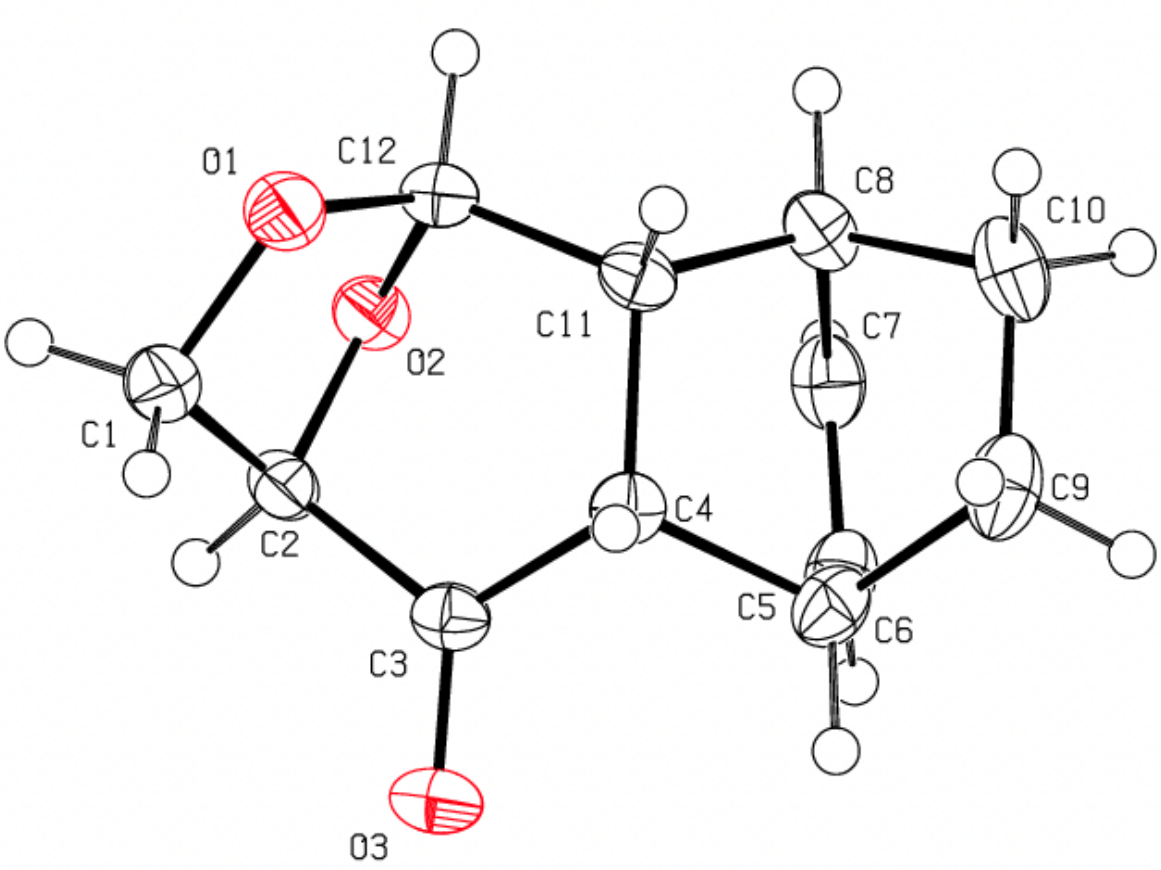

Figure S11: Molecular structure of compound **24** (CCDC 2268360). Atomic displacement parameters shown at 50% probability level (crystal grown from diethyl ether–hexane).

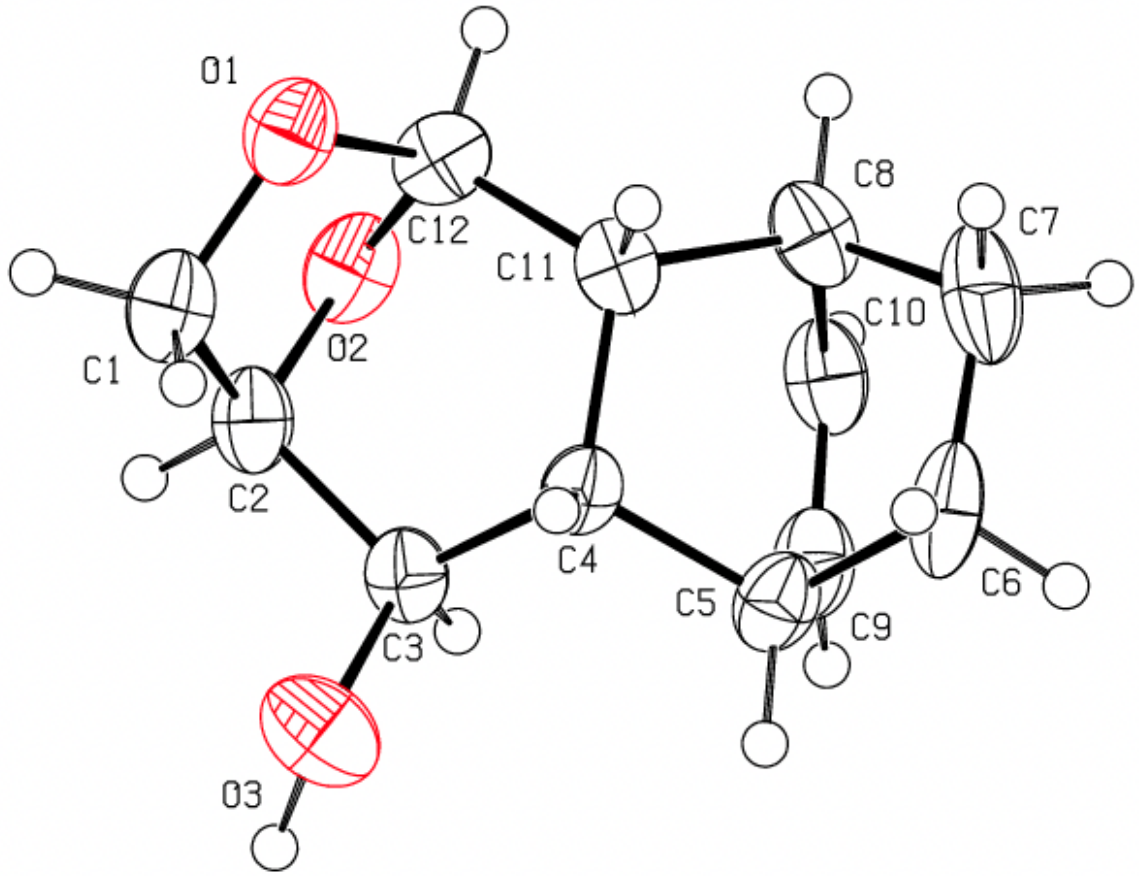

Figure S12: Molecular structure of compound **25** (CCDC 2268361). The extended structure arising from hydrogen bonding is not shown. Atomic displacement parameters shown at 50% probability level (crystal grown from dichloromethane).

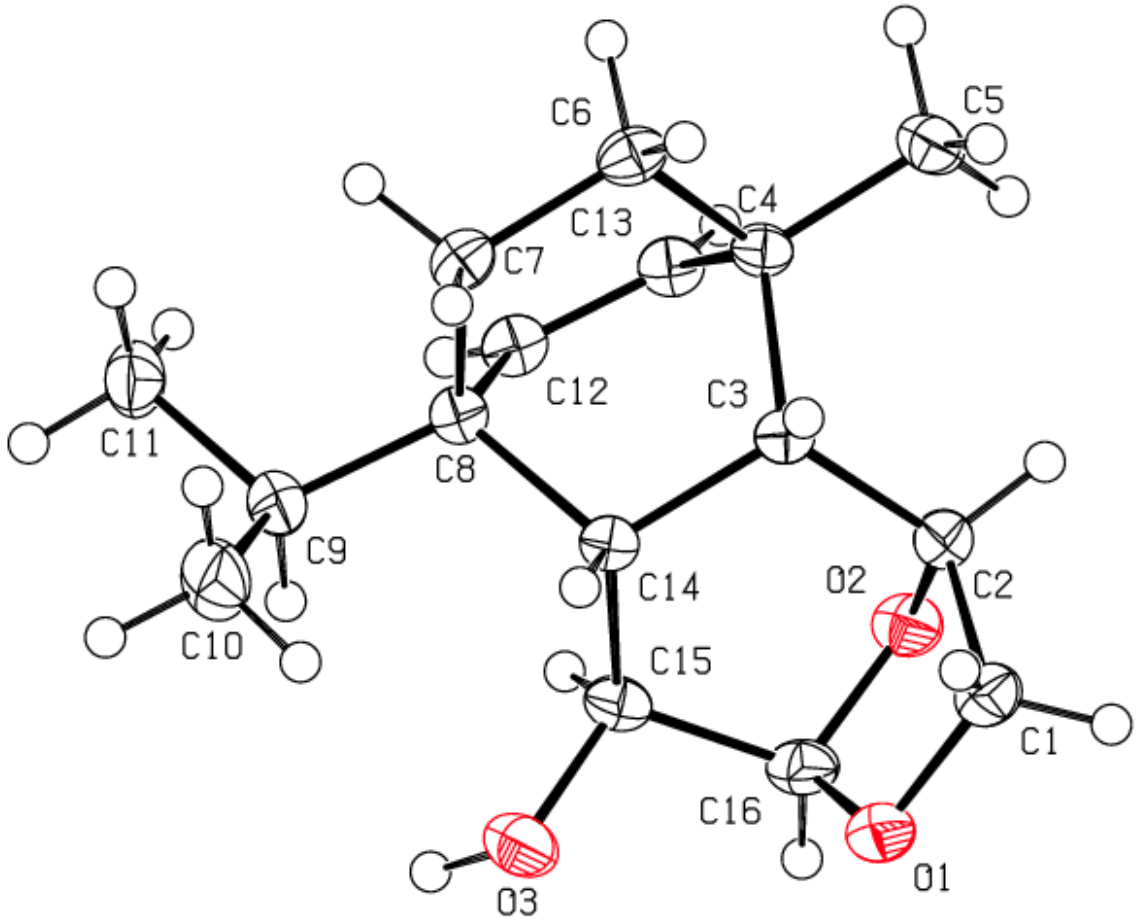

Figure S13: Molecular structure of compound **29** (CCDC 2268362). The extended structure arising from hydrogen bonding is not shown. Atomic displacement parameters shown at 50% probability level (crystal grown from dichloromethane–methanol).

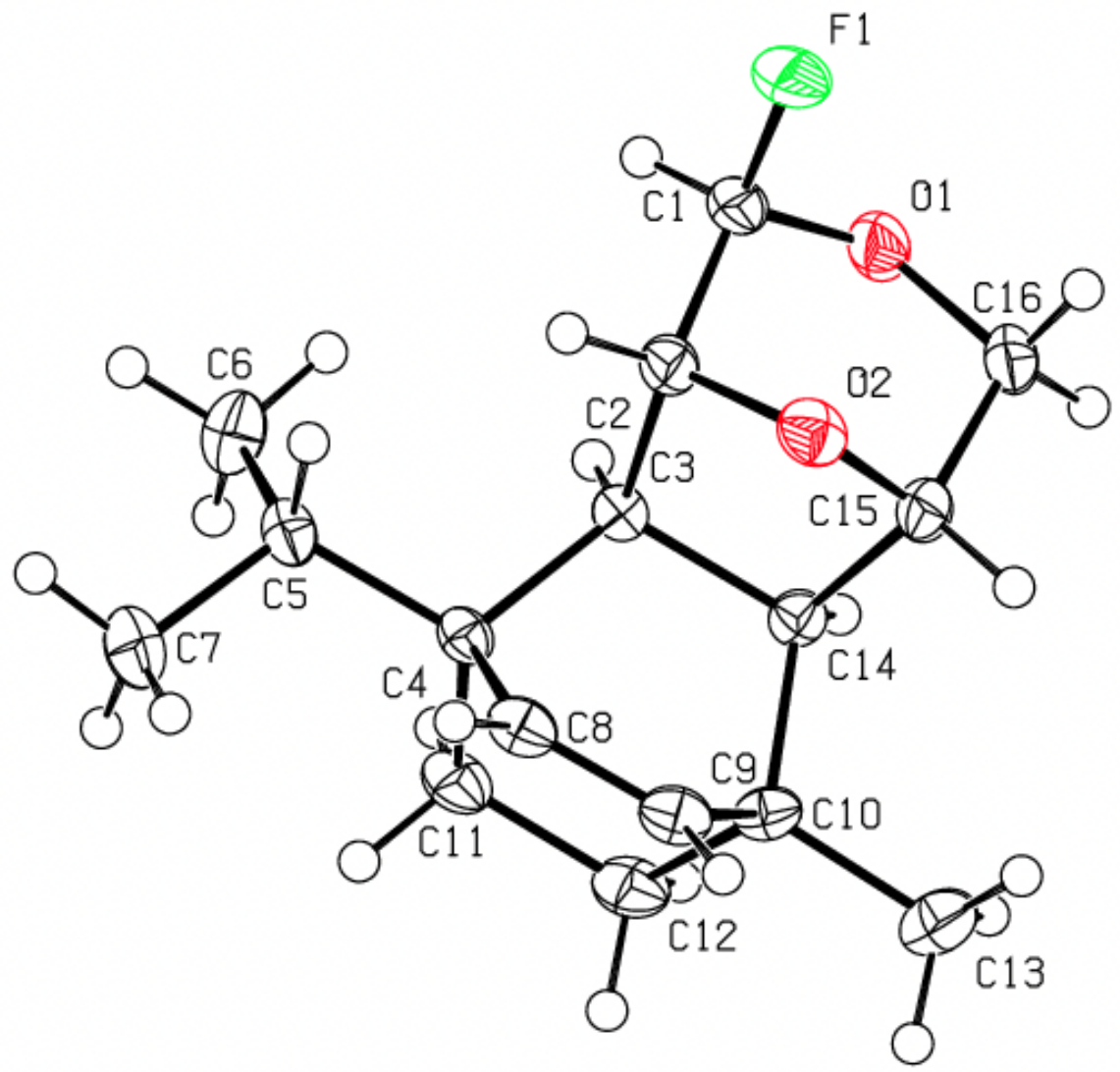

Figure S14: Molecular structure of compound **30** (CCDC 2268363). Atomic displacement parameters shown at 50% probability level (crystal grown from dichloromethane–methanol).

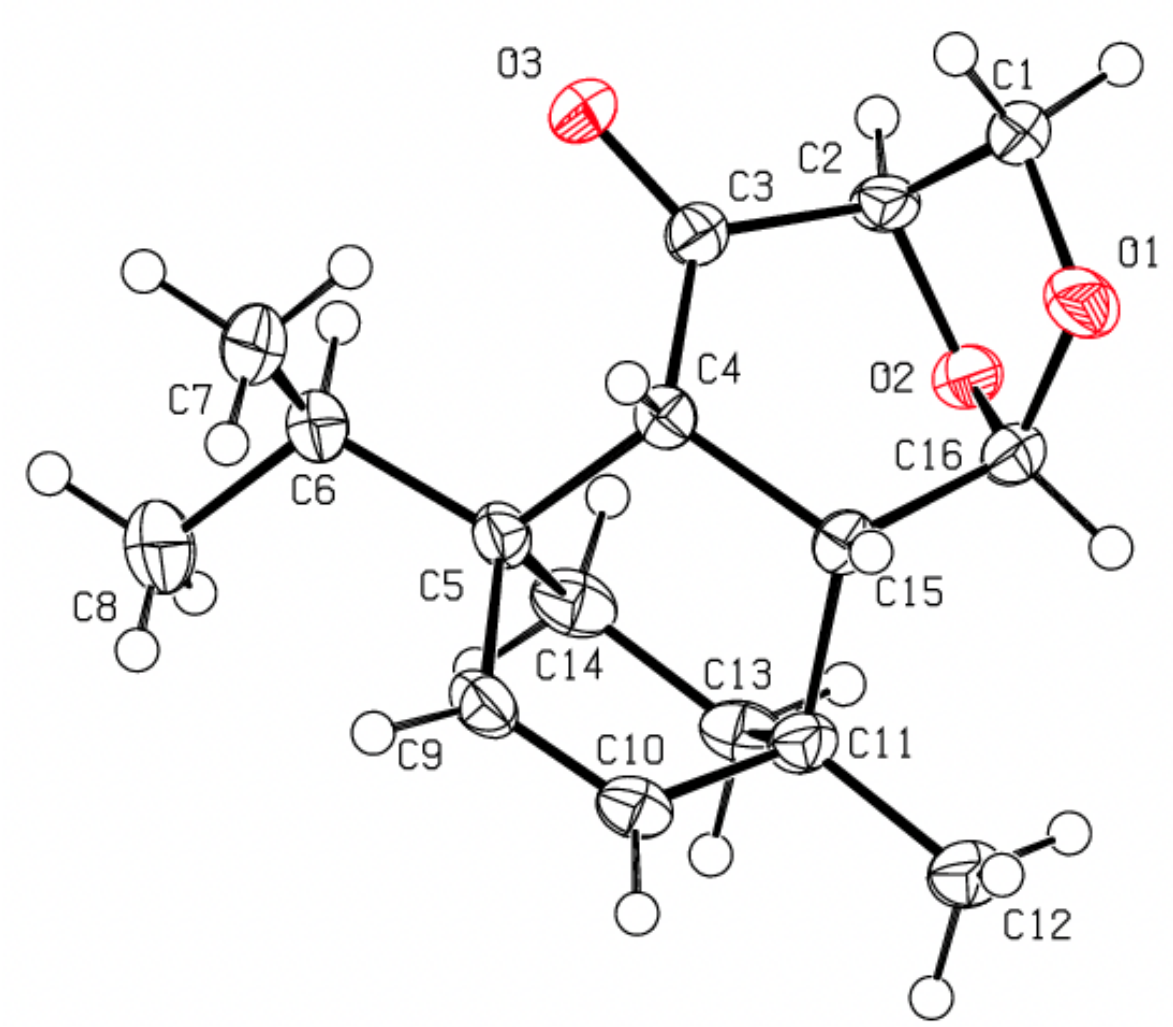

Figure S15: Molecular structure of compound **32** (CCDC 2268364). Atomic displacement parameters shown at 50% probability level (crystal grown from diethyl ether–hexane).

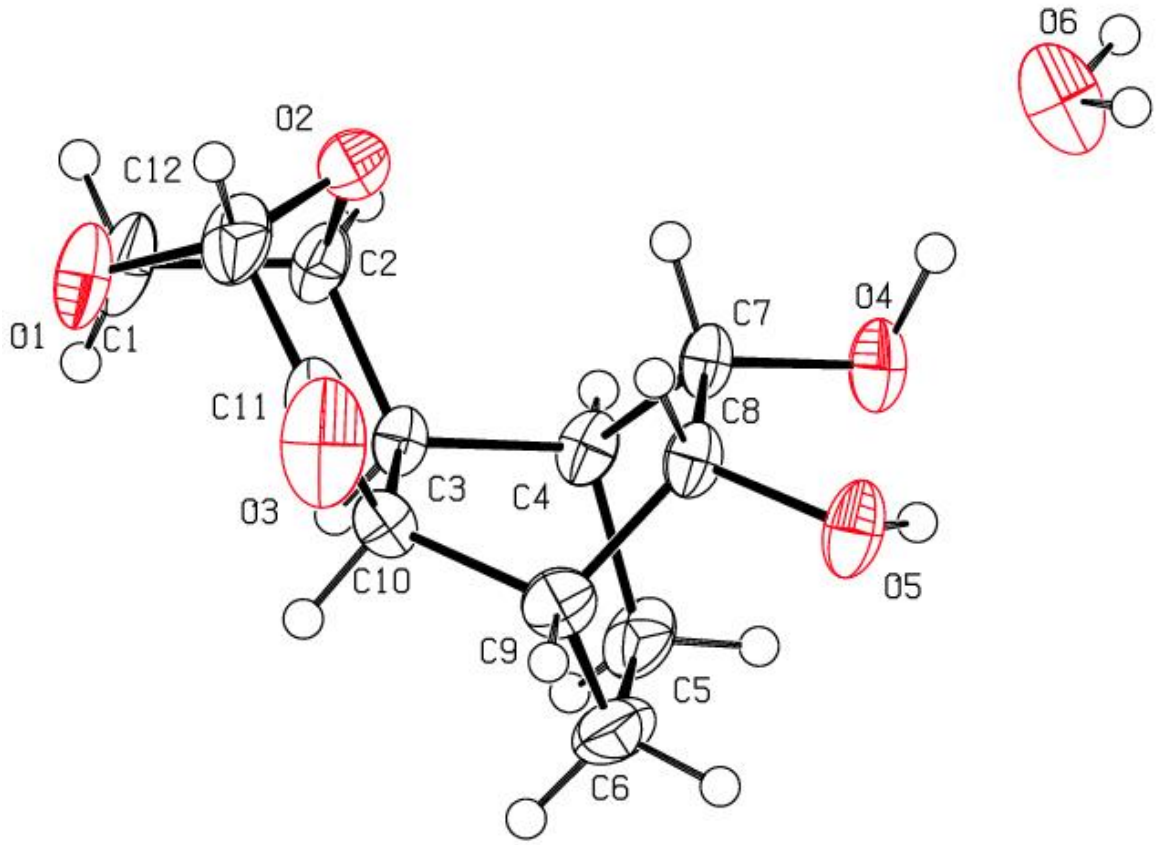

Figure S16: Molecular structure of compound **33** (CCDC 2268365) showing the water molecule in the asymmetric unit for the monohydrate (hydrogen bonding is not shown and the extended structure arising from the hydrogen bonding is also not shown). Atomic displacement parameters shown at 50% probability level (crystal grown from dichloromethane).

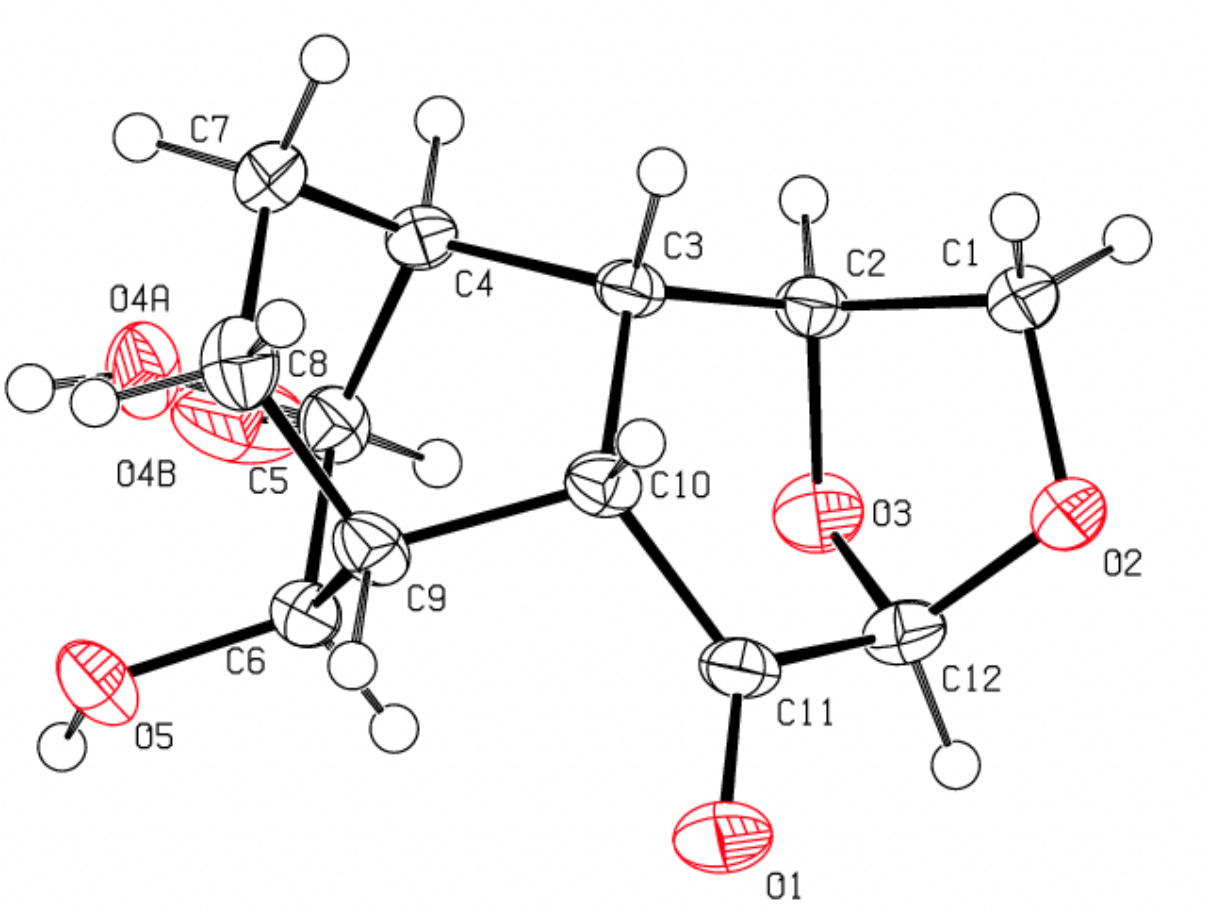

Figure S17: Molecular structure of compounds **33** and **34** (CCDC 2268366) present in the non-hydrated form of compoound **33** that was found to contain a minor co-crystallised impurity of compound **34**. The extended structure arising from hydrogen bonding is not shown for compound **33**. Atomic displacement parameters shown at 50% probability level (crystal grown from chloroform)

Tabular comparisons of the $^{13}C\{^{1}H\}$ NMR spectral data recorded on compounds 14 and 15 with those reported by Horton *et al.*[1]

Table S1: Comparison of the $^{13}C\{^{1}H\}$NMR spectral data reported by Horton *et al.*[1] for the chromatographically more mobile alcohol derived from reduction of the Diels–Alder adduct of LGO and cyclopentadiene (compound **14**) with those derived from compound **15** prepared during the course of the present study.

Compound **14** reported by Horton *et al.* δ_C	Compound **15** δ_C	$\Delta\delta$
135.8	136.1	+0.3
135.5	135.7	+0.2
101.7	101.8	+0.1
73.2	73.3	+0.1
68.4	68.6	+0.2
61.4	61.6	+0.2
50.6	50.8	+0.2
48.6	48.6	0
46.5	46.2	–0.3
45.8	46.0	+0.2
43.9	44.1	+0.2

Compound **14** data are obtained from Horton *et al.*[1] and are recorded in $CDCl_3$ at 125 MHz. Compound **15** data are recorded in $CDCl_3$ at 100 MHz. $\Delta\delta$ calculated by subtracting the δ_C values in the first column from those in the second.

Table S2: Comparison of the $^{13}C\{^{1}H\}$NMR spectral data reported by Horton *et al.*[1] for the chromatographically less mobile alcohol derived from reduction of the Diels–Alder adduct of LGO and cyclopentadiene (compound **15**) with those derived from compound **14** prepared during the course of the present study.

Compound **15** reported by Horton *et al.* δ_C	Compound **14** δ_C	$\Delta\delta$
137.4	137.5	+0.1
133.0	133.2	+0.2
102.6	102.7	+0.1
76.4	76.6	+0.2
69.4	69.5	+0.1
64.3	64.5	+0.2
50.7	50.9	+0.2
46.8	47.0	+0.2
46.1	46.3	+0.2
44.3	44.5	+0.2
40.3	40.5	+0.2

Compound **15** data are obtained from Horton *et al.*[1] and are recorded in $CDCl_3$ at 125 MHz. Compound **14** data are recorded in $CDCl_3$ at 100 MHz. $\Delta\delta$ calculated by subtracting the δ_C values in the first column from those in the second.

Tabular comparisons of the $^{13}C\{^{1}H\}$ NMR spectral data recorded on compounds 20 and 21 with those reported by Zurita *et al.*[2]

Table S3: Comparison of the $^{13}C\{^{1}H\}$NMR spectral data reported by Zurita *et al.*[2] for the major alcohol derived from reduction of the Diels–Alder adduct of LGO and cyclohexadiene (compound **10**) with those derived from compound **20** prepared during the course of the present study.

Compound **10** reported by Zurita *et al.* δ_C	Compound **20** δ_C	$\Delta\delta$
134.5	134.6	+0.1
133.3	133.4	+0.1
102.5	102.5	0
77.0	77.0	0
71.7	71.7	0
68.6	68.6	0
44.5	44.5	0
39.7	39.7	0
36.7	36.7	0
33.2	33.2	0
29.1	29.1	0
23.3	23.4	+0.1

Compound **10** data are obtained from Zurita *et al*.[2] and are recorded in $CDCl_3$ at 75 MHz. Compound **20** data are recorded in $CDCl_3$ at 100 MHz. $\Delta\delta$ calculated by subtracting the δ_C values in the first column from those in the second.

Table S4: Comparison of the $^{13}C\{^{1}H\}$NMR spectral data reported by Zurita *et al.*[2] for the minor alcohol derived from reduction of the Diels–Alder adduct of LGO and cyclohexadiene (compound **17**) with those derived from compound **21** prepared during the course of the present study.

Compound **17** reported by Zurita *et al.* δ_C	Compound **21** δ_C	$\Delta\delta$
135.3	135.3	0
132.4	132.4	0
100.9	100.9	0
77.2	77.2	0
71.2	71.2	0
70.2	70.2	0
46.3	46.3	0
45.3	45.4	+0.1
36.1	36.2	+0.1
33.9	34.0	+0.1
28.7	28.7	0
22.3	22.4	+0.1

Compound **17** data are obtained from Zurita *et al.*[2] and are recorded in $CDCl_3$ at 75 MHz. Compound **21** data are recorded in $CDCl_3$ at 100 MHz. $\Delta\delta$ calculated by subtracting the δ_C values in the first column from those in the second.

Tabular comparisons of the $^{13}C\{^1H\}$ NMR spectral data recorded on compounds 27 and 28 with those reported by Galimova *et al.*[3]

Table S5: Comparison of the $^{13}C\{^1H\}$NMR spectral data reported by Galimova *et al.*[3] for the Diels–Alder adduct of LGO and *in situ*-generated α-terpinene (Compound V) with those derived from compound **27** prepared during the course of the present study.

Compound V reported by Galimova *et al.* δ_C	Compound **27** δ_C	$\Delta\delta$
200.96	201.0	0
138.26	138.4	+0.1
135.53	135.7	+0.2
100.61	100.8	+0.2
73.12	73.3	+0.2
68.29	68.5	+0.2
49.29	49.5	+0.2
48.58	48.8	+0.2
44.98	45.1	+0.1
38.13	38.3	+0.2
35.59	35.8	+0.2
29.97	30.1	+0.1
22.76	22.9	+0.1
20.80	21.0	+0.2
18.70	18.8	+0.1
16.76	16.9	+0.1

Compound V data are obtained from Galimova *et al.*[3] and are recorded in $CDCl_3$ at 75.47 MHz. Compound **27** data are recorded in $CDCl_3$ at 100 MHz. $\Delta\delta$ calculated by rounding the δ_C values for compound V to the first decimal place and then subtracting these from the corresponding value for compound **27**.

Table S6: Comparison of the $^{13}C\{^{1}H\}$NMR spectral data reported by Galimova *et al.*[3] for the Diels–Alder adduct of LGO and *in situ*-generated α-terpinene (Compound V) with those derived from compound **28** prepared during the course of the present study

Compound V reported by Galimova *et al.* δ_C	Compound **28** δ_C	$\Delta\delta$
200.96	200.9	–0.1
138.26	138.2	–0.1
135.53	135.5	0
100.61	100.6	0
73.12	73.1	0
68.29	68.3	0
49.29	49.3	0
48.58	48.6	0
44.98	45.0	0
38.13	38.1	0
35.59	35.6	0
29.97	30.0	0
22.76	22.8	0
20.80	20.8	0
18.70	18.7	0
16.76	16.8	0

Compound V data are obtained from Galimova *et al*.[3] and are recorded in $CDCl_3$ at 75.47 MHz. Compound **28** data are recorded in $CDCl_3$ at 100 MHz. $\Delta\delta$ calculated by rounding the δ_C values for compound V to the first decimal place and then subtracting these from the corresponding value for compound **28**.

^{1}H and ^{13}C{^{1}H} NMR spectra derived from compounds 10-16, 18-25, 27-30, 32 and 33

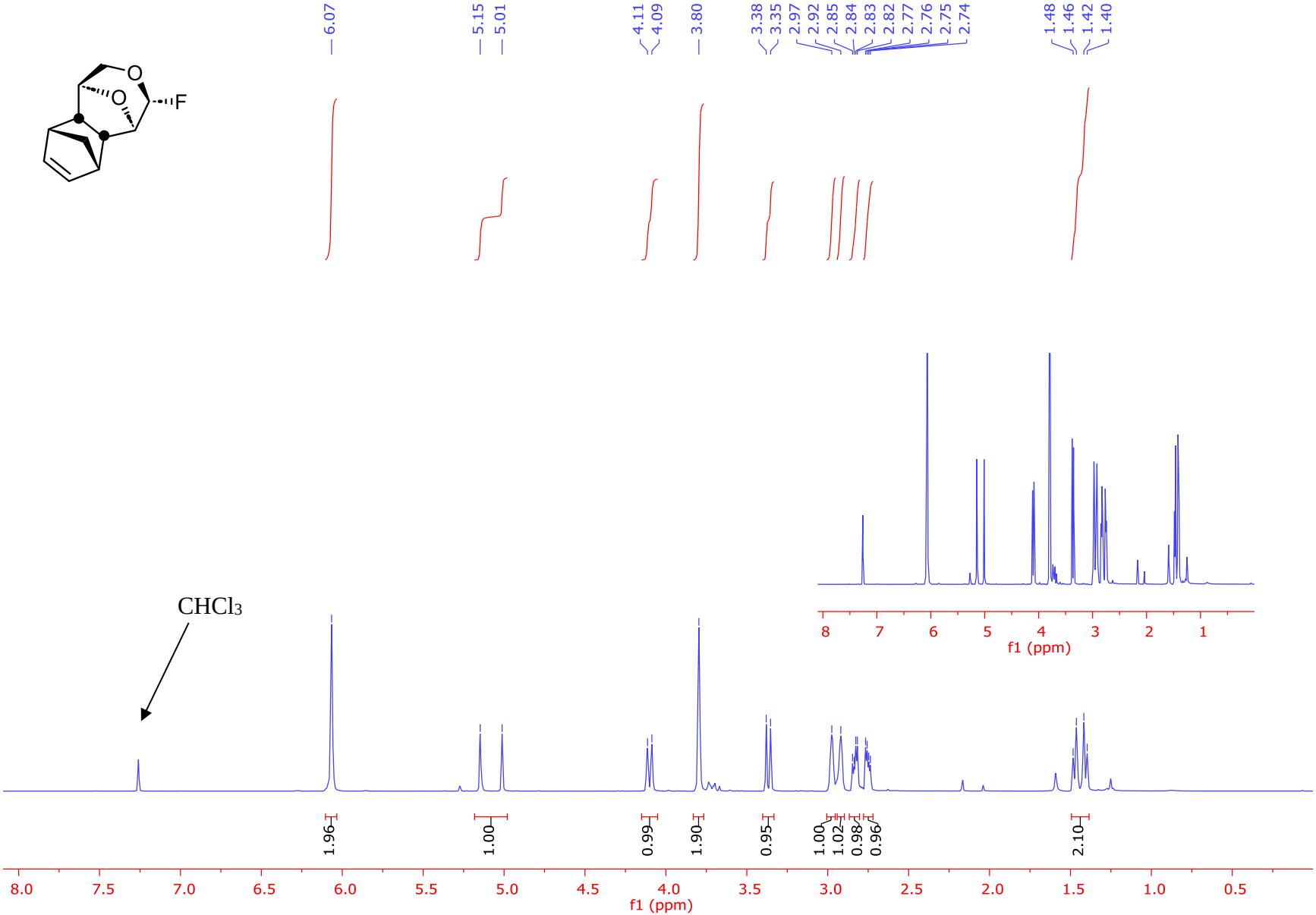

Figure S18: 400 MHz ^{1}H NMR Spectrum of Compound **10** (Recorded in $CDCl_3$)

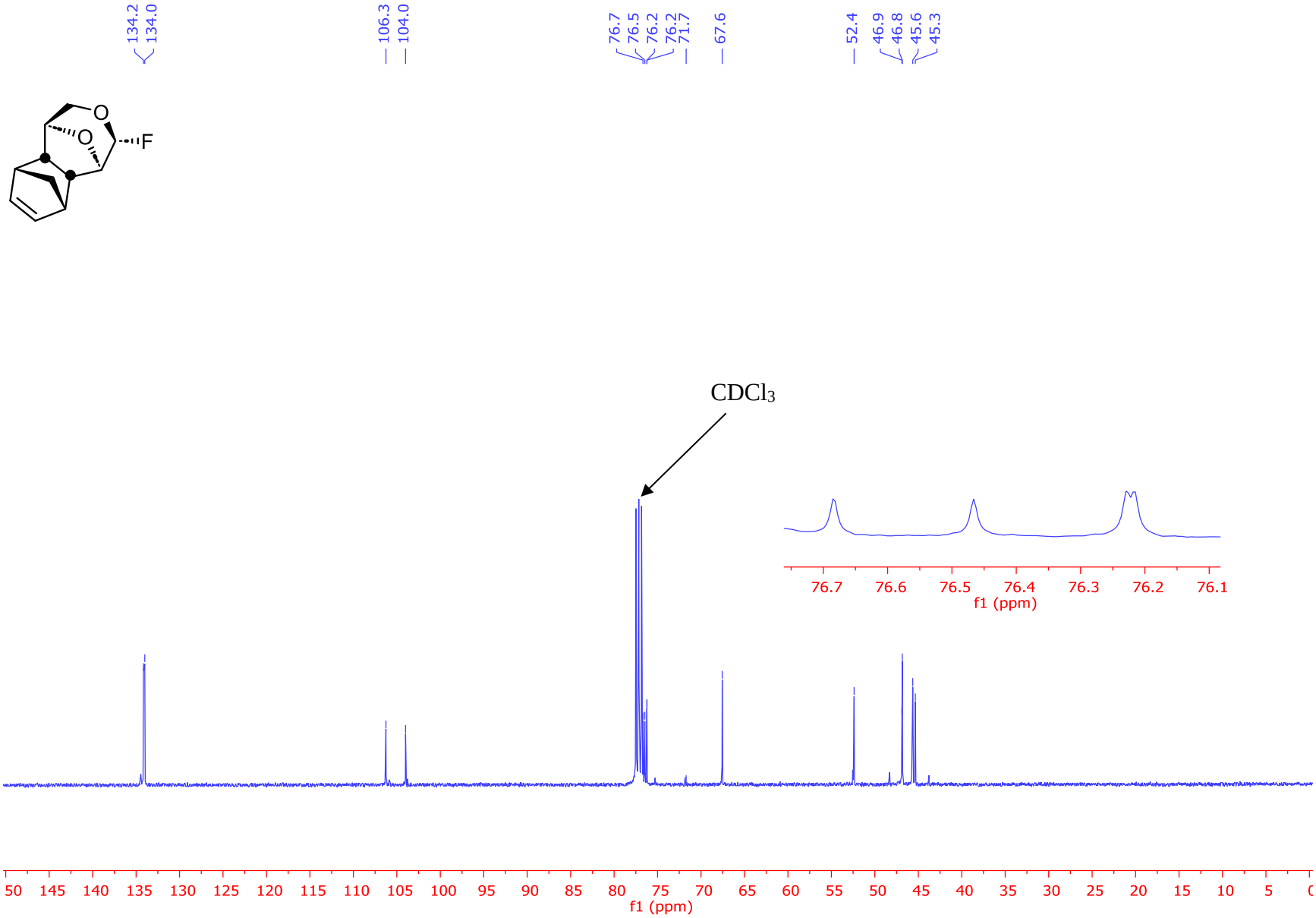

Figure S19: 101 MHz $^{13}C\{^{1}H\}$ NMR Spectrum of Compound **10** (Recorded in $CDCl_3$)

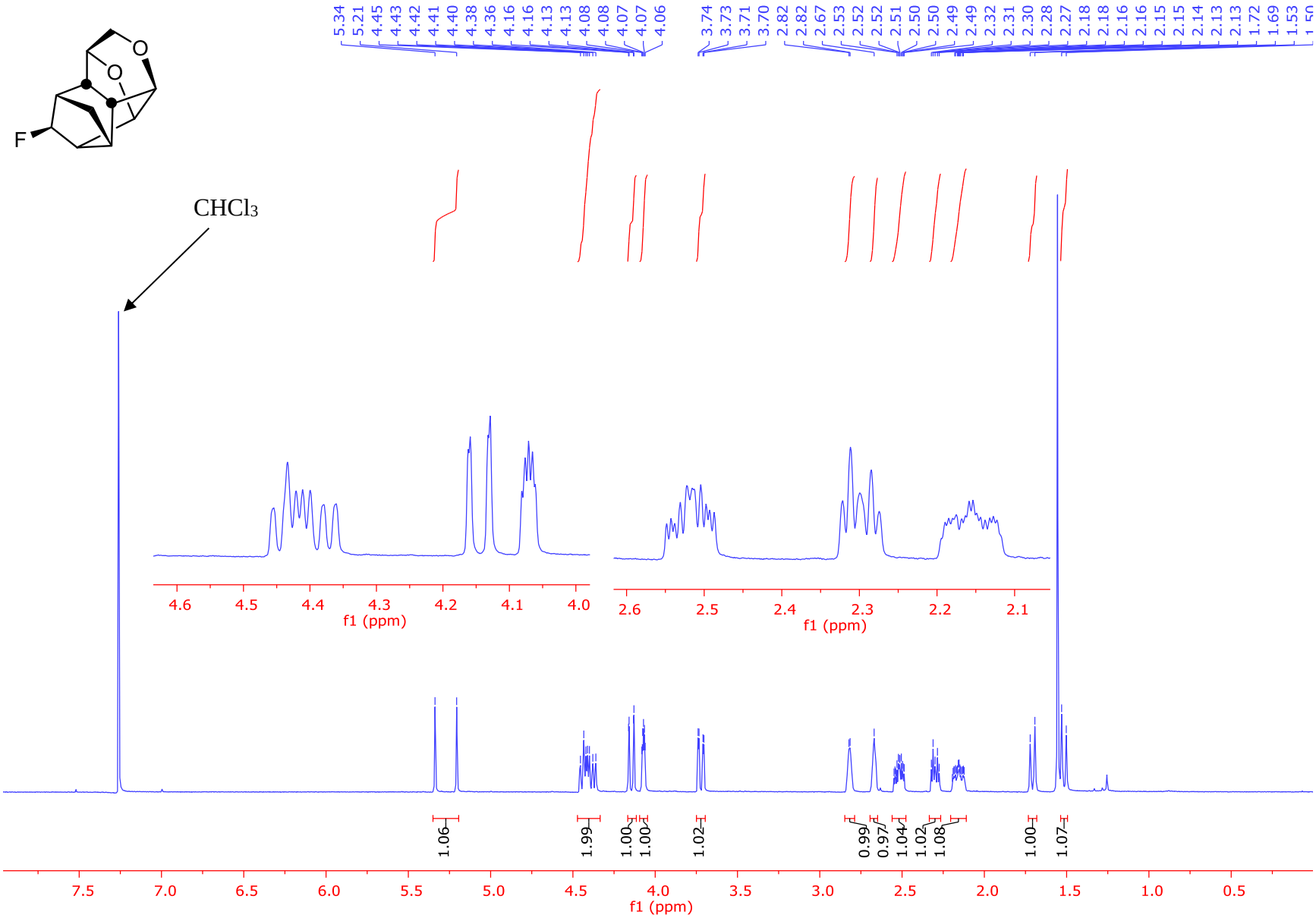

Figure S20: 400 MHz ^{1}H NMR Spectrum of Compound **11** (Recorded in $CDCl_3$)

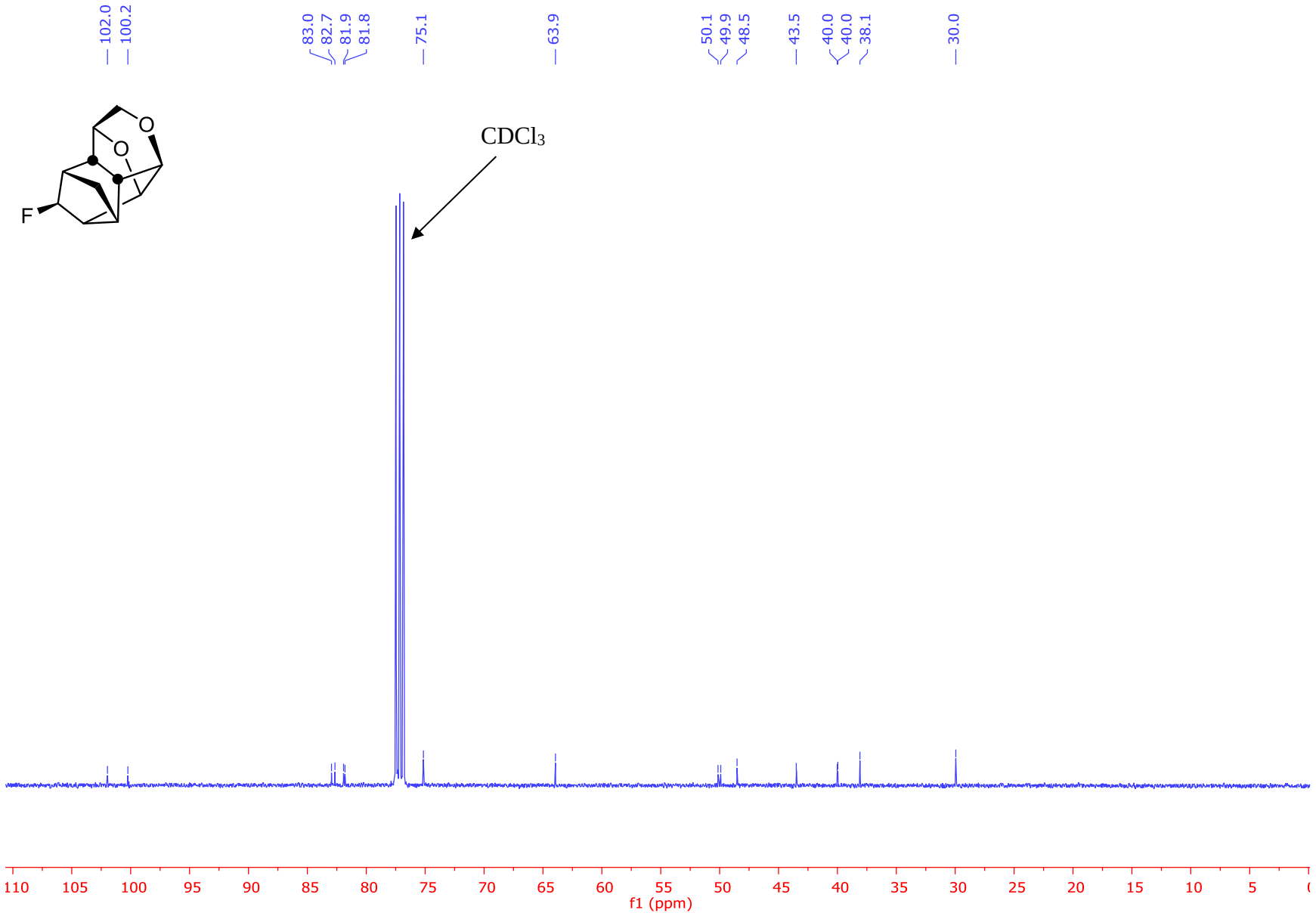

Figure S21: 101 MHz $^{13}C\{^{1}H\}$ NMR Spectrum of Compound **11** (Recorded in $CDCl_3$)

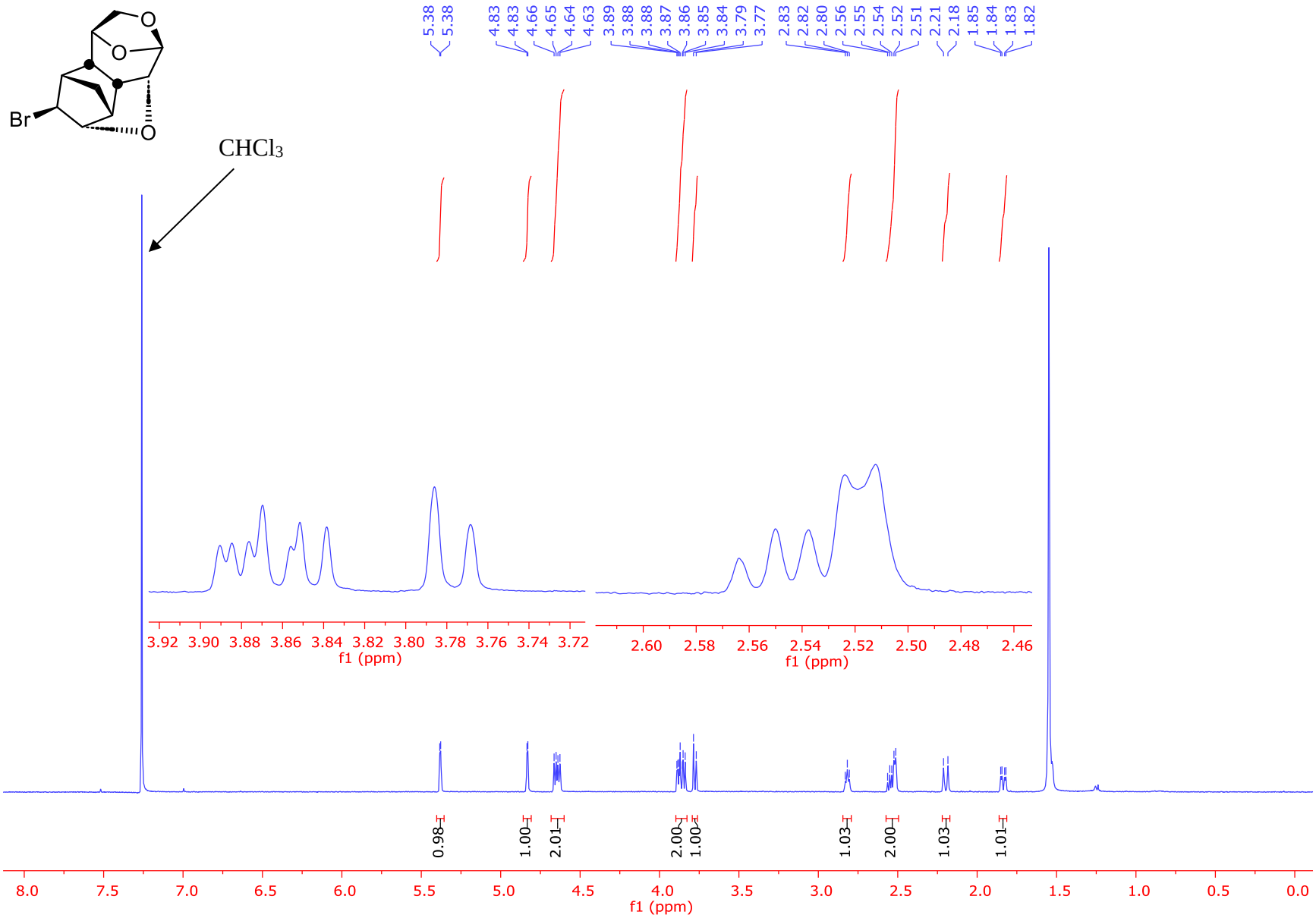

Figure S22: 400 MHz ^{1}H NMR Spectrum of Compound **12** (Recorded in $CDCl_3$)

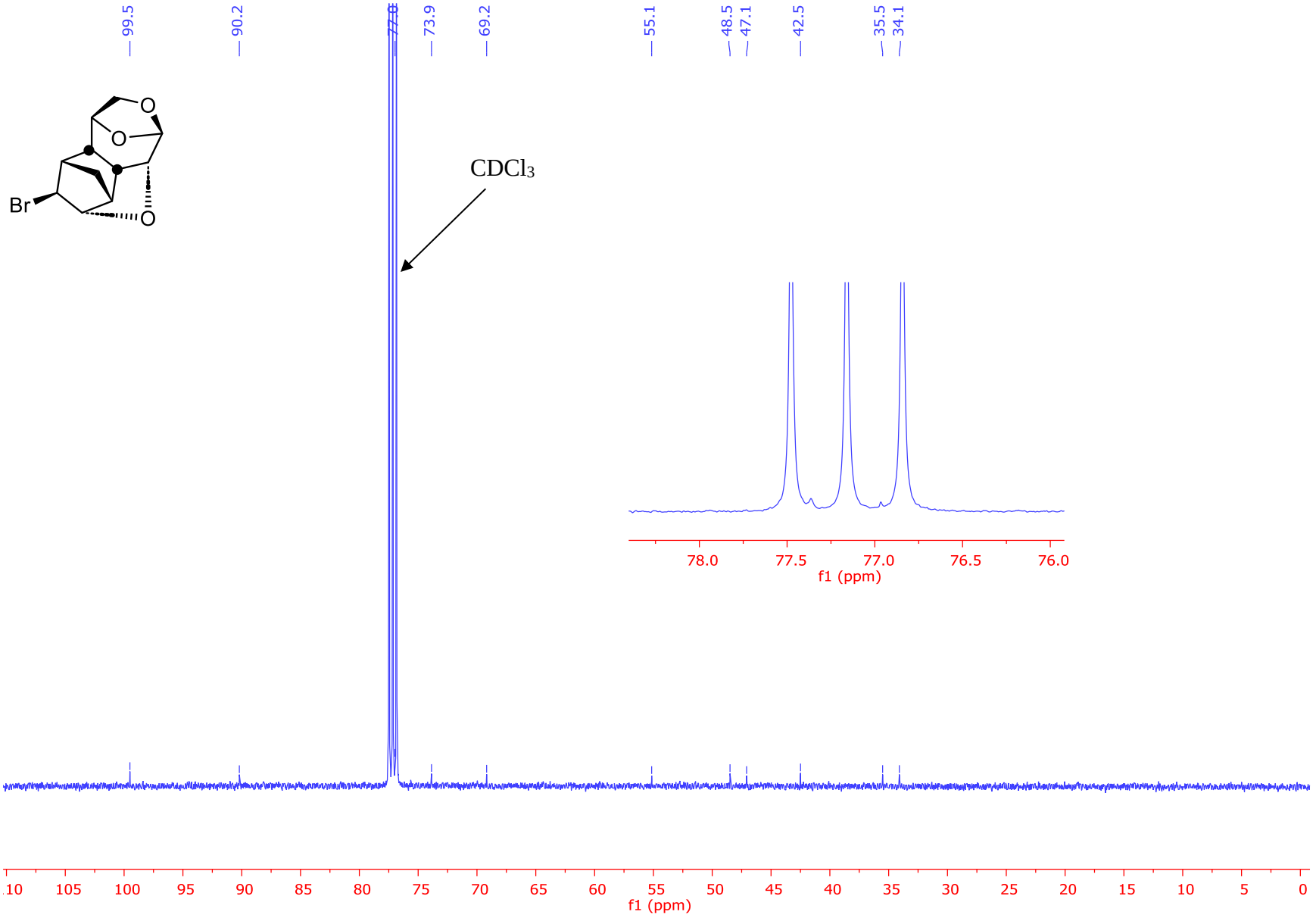

Figure S23: 101 MHz $^{13}C\{^{1}H\}$ NMR Spectrum of Compound **12** (Recorded in $CDCl_3$)

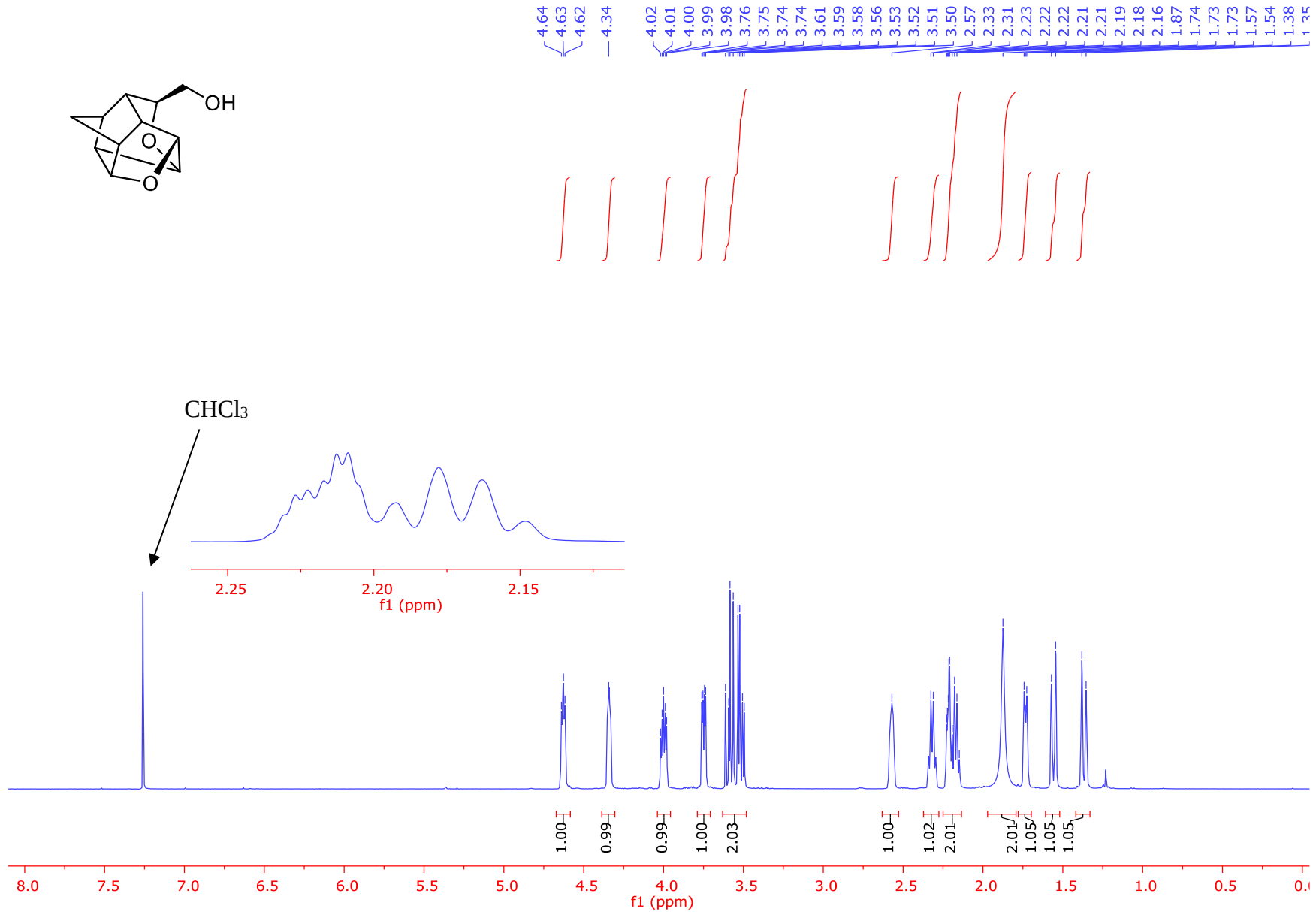

Figure S24: 400 MHz ^{1}H NMR Spectrum of Compound **13** (Recorded in $CDCl_3$)

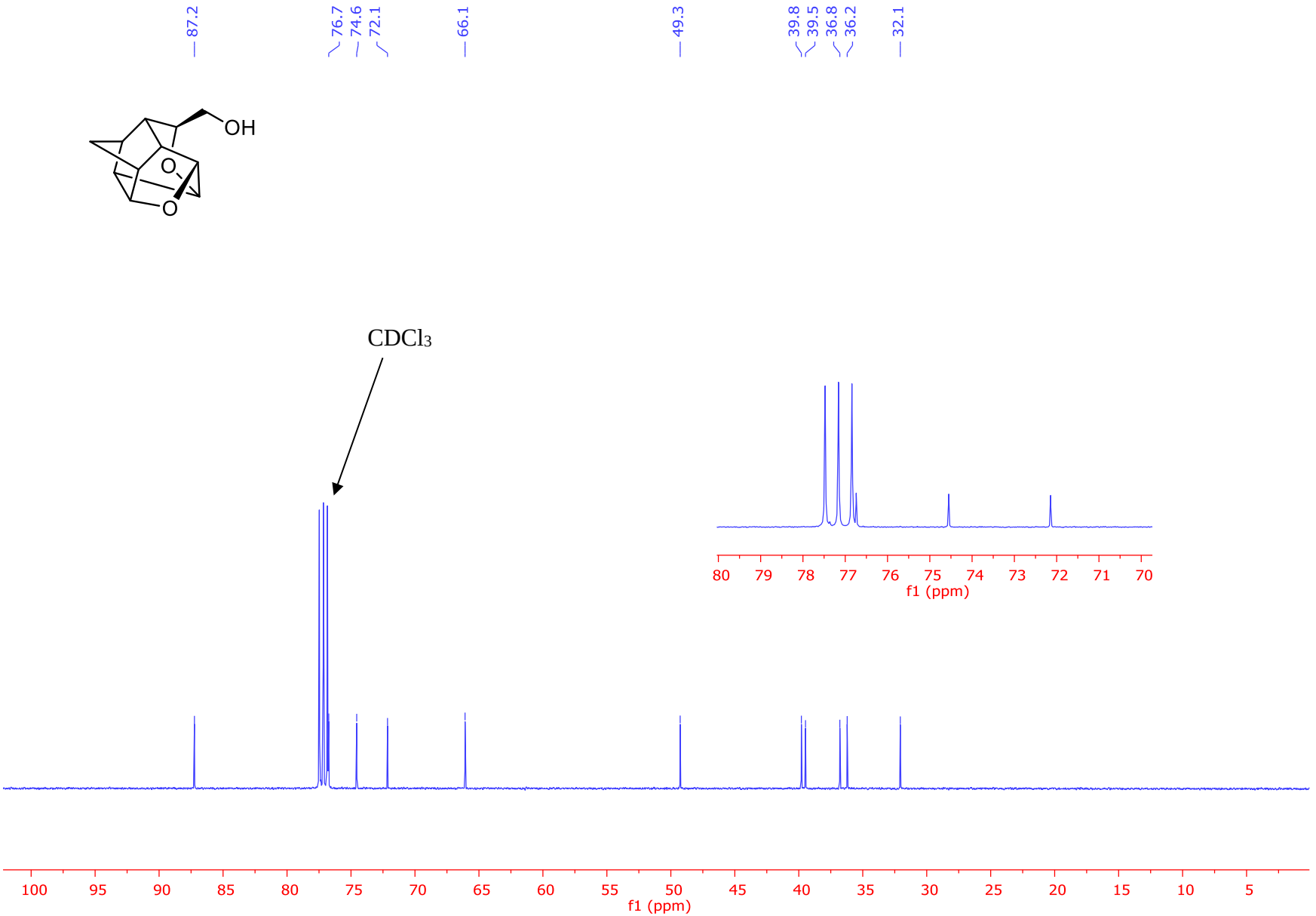

Figure S25: 101 MHz $^{13}C\{^{1}H\}$ NMR Spectrum of Compound **13** (Recorded in $CDCl_3$)

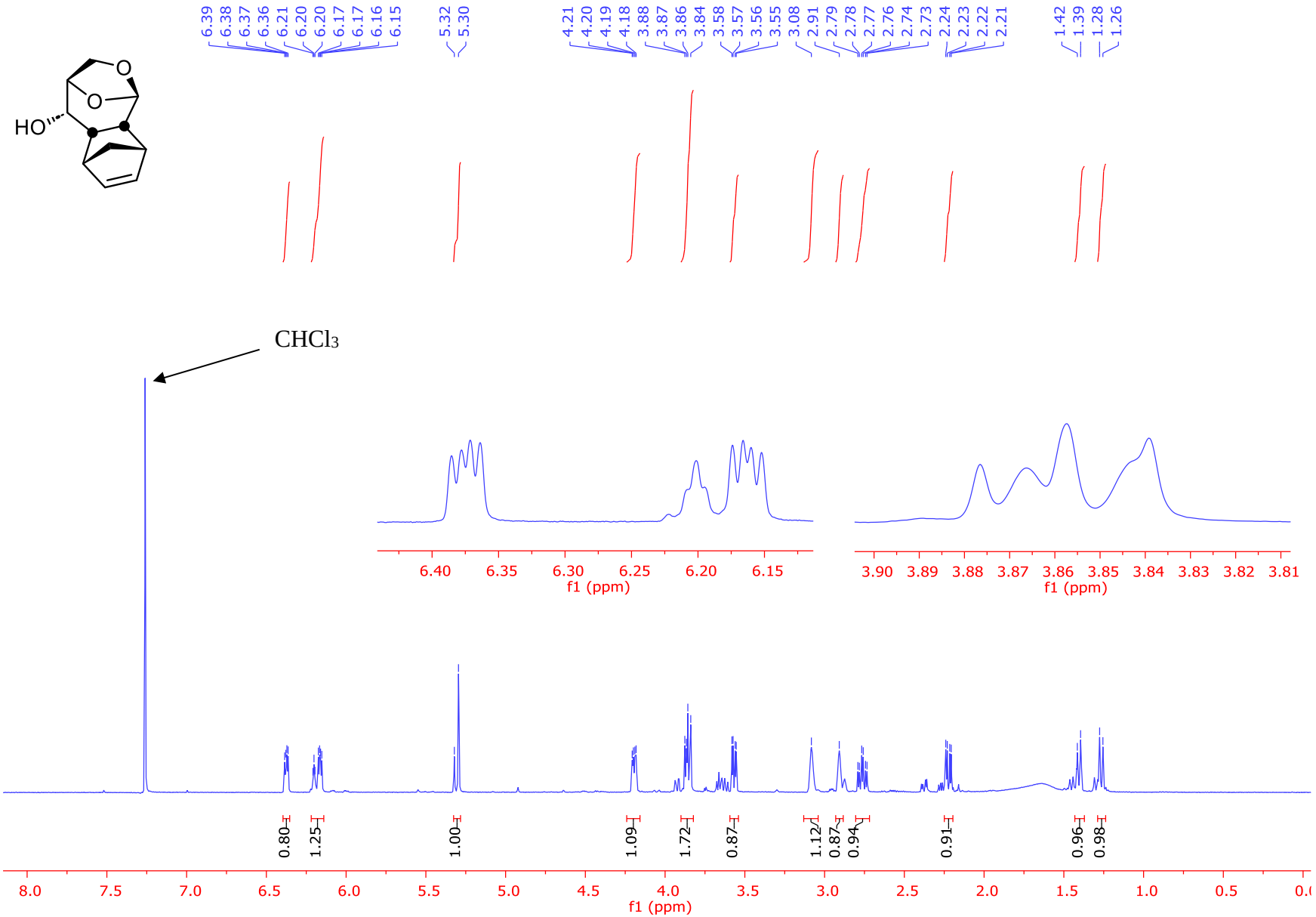

Figure S26: 400 MHz ^{1}H NMR Spectrum of Compound **14** (Recorded in $CDCl_3$)

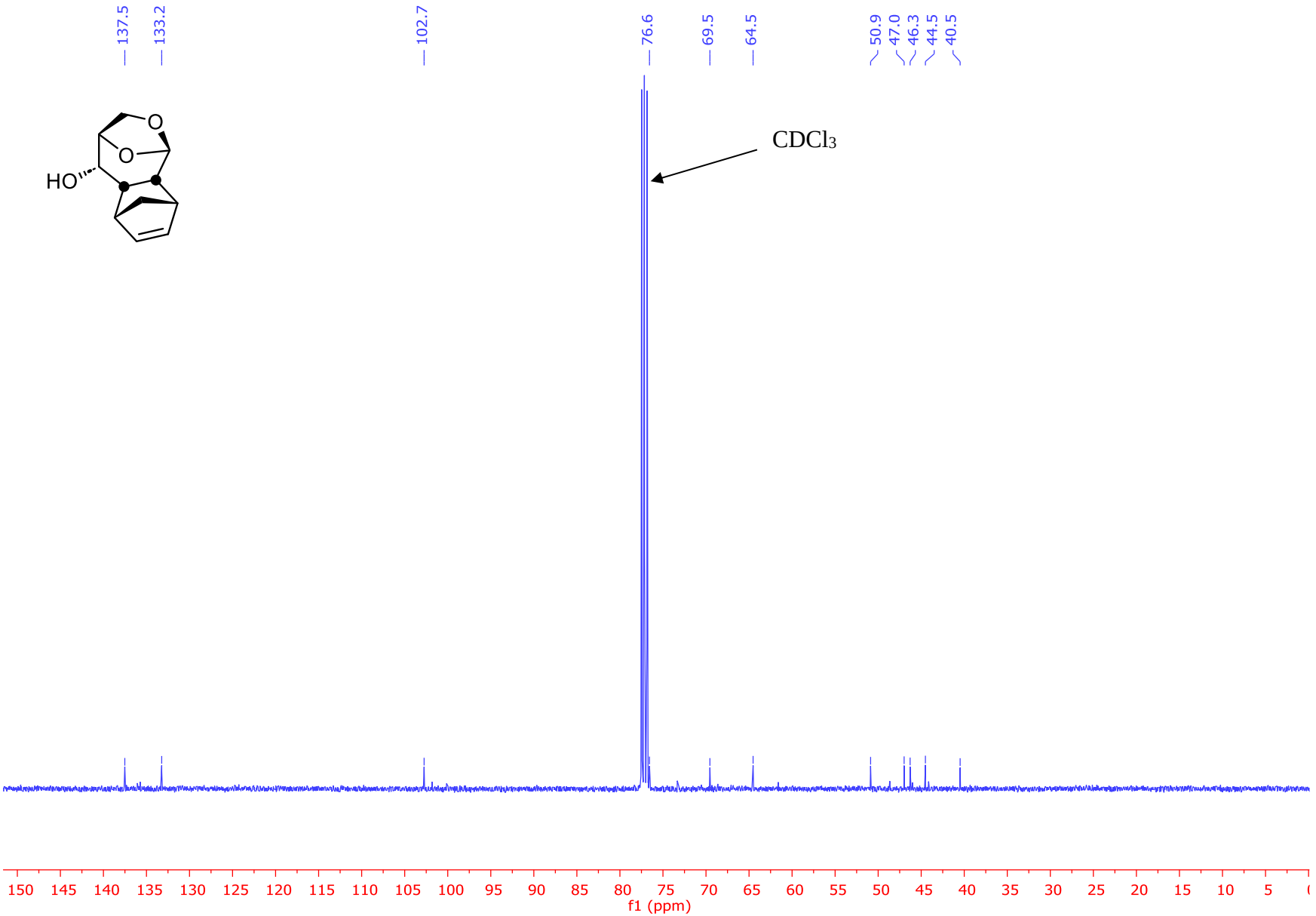

Figure S27: 101 MHz $^{13}C\{^{1}H\}$ NMR Spectrum of Compound **14** (Recorded in $CDCl_3$)

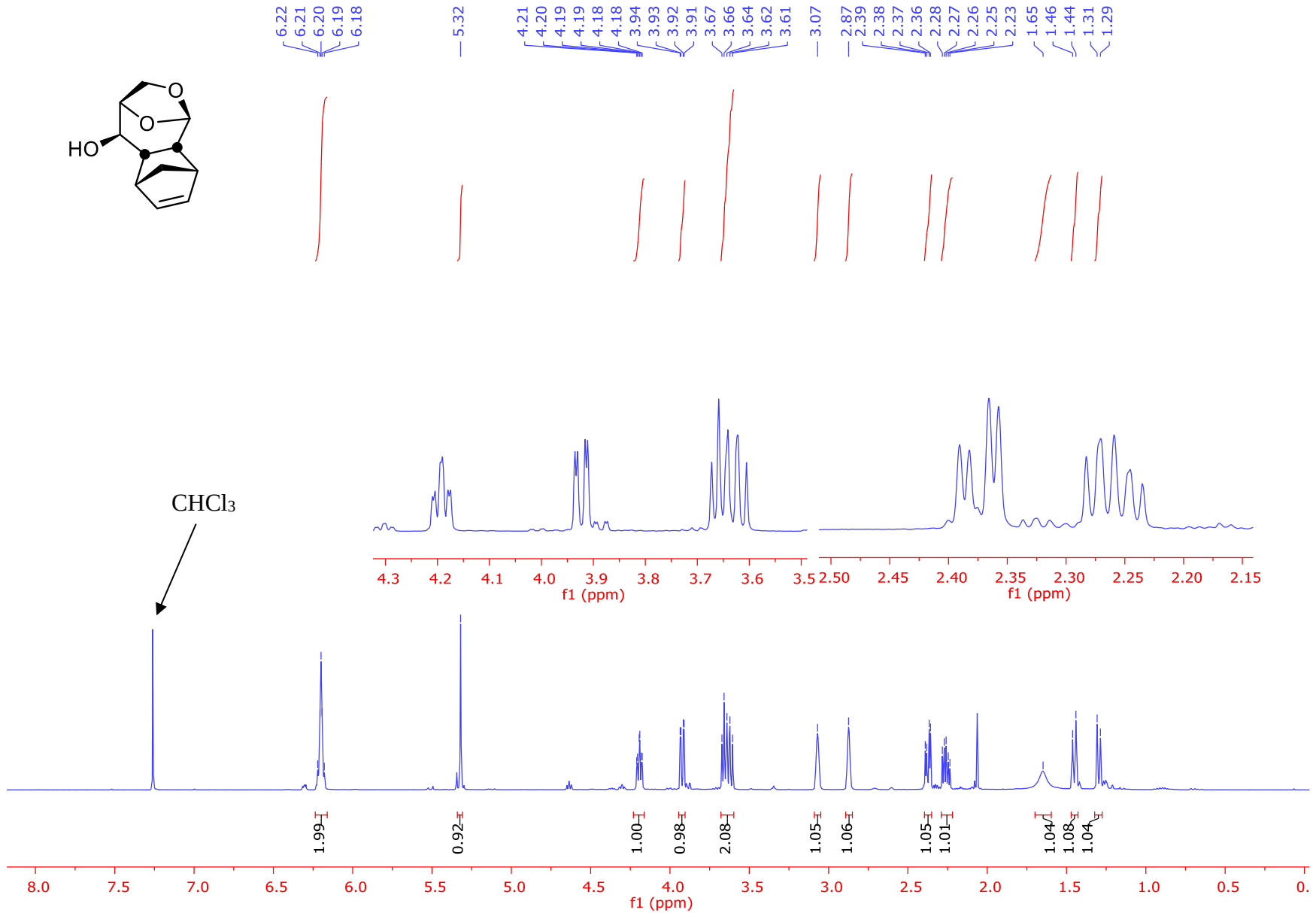

Figure S28: 400 MHz ^{1}H NMR Spectrum of Compound **15** (Recorded in $CDCl_3$)

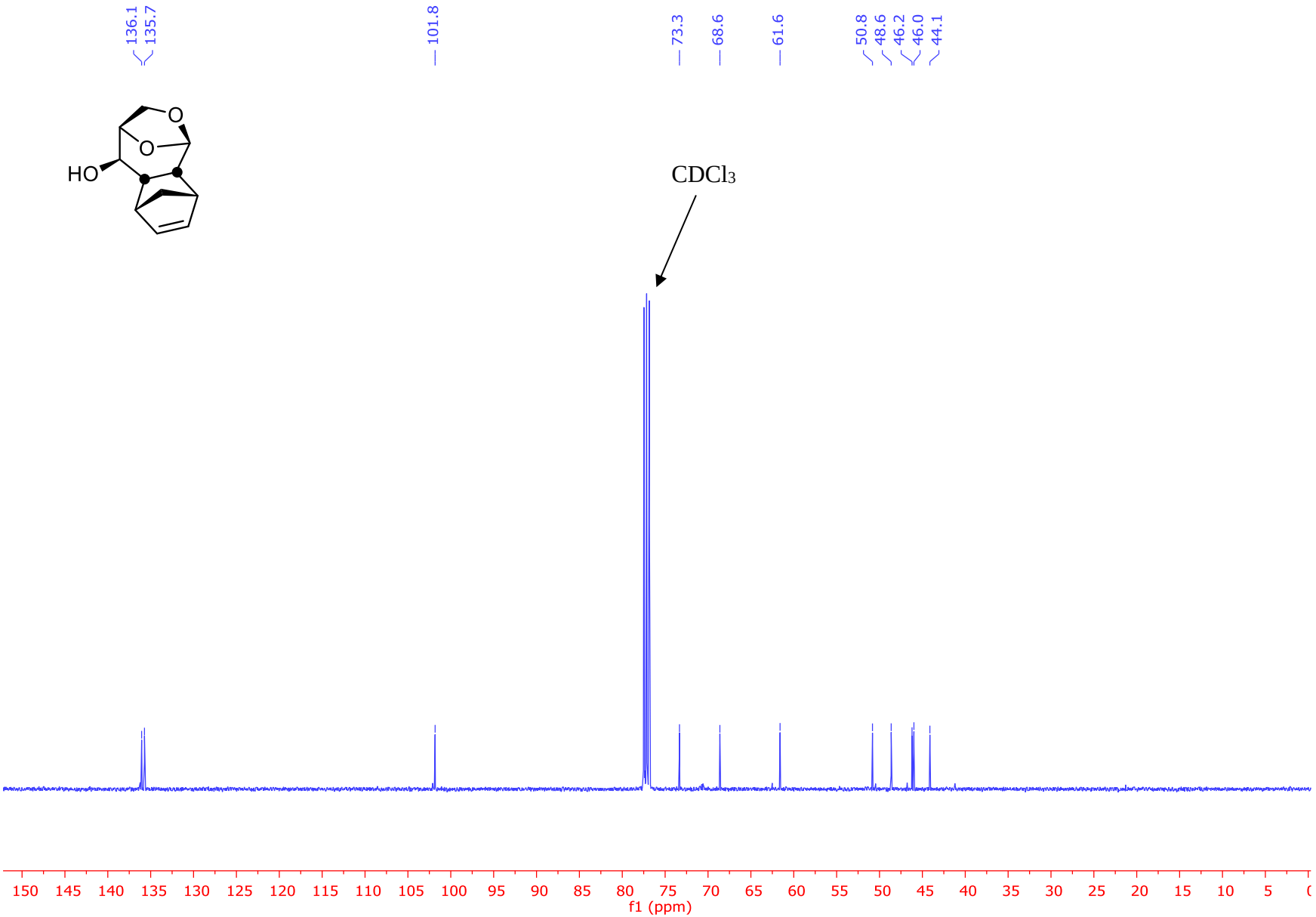

Figure S29: 101 MHz $^{13}C\{^{1}H\}$ NMR Spectrum of Compound **15** (Recorded in $CDCl_3$)

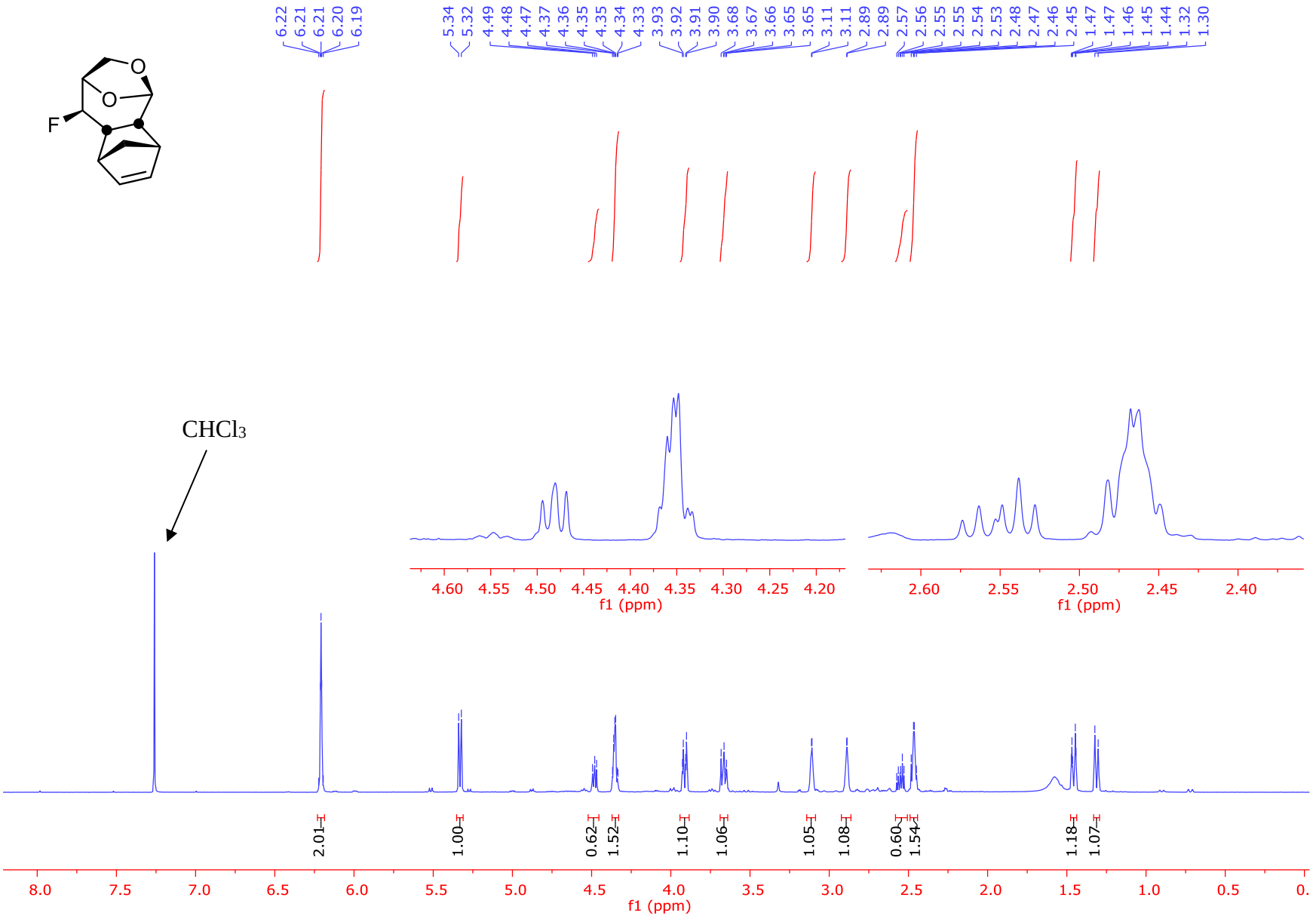

Figure S30: 400 MHz ^{1}H NMR Spectrum of Compound **16** (Recorded in $CDCl_3$)

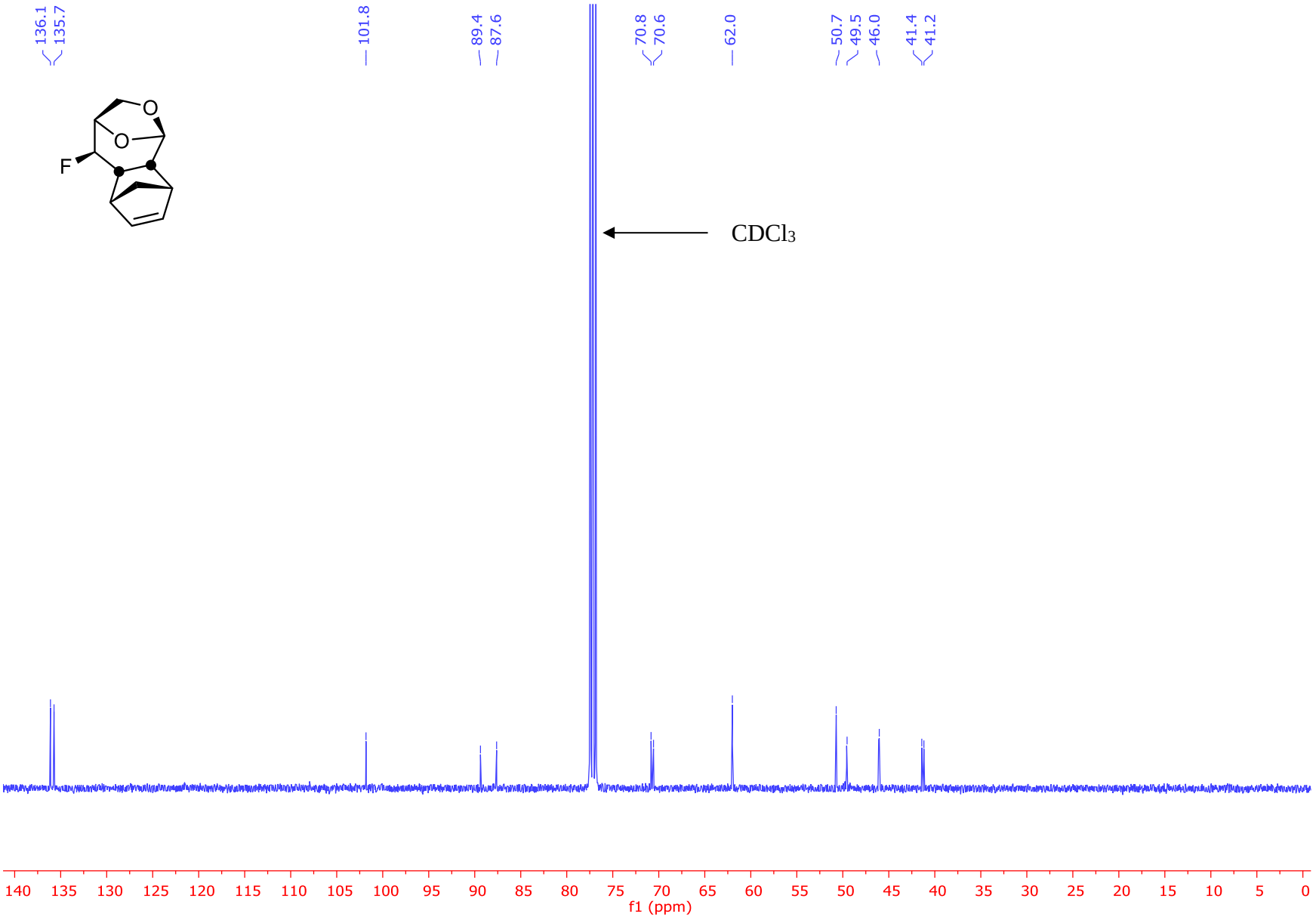

Figure S31: 101 MHz $^{13}C\{^{1}H\}$ NMR Spectrum of Compound **16** (Recorded in $CDCl_3$)

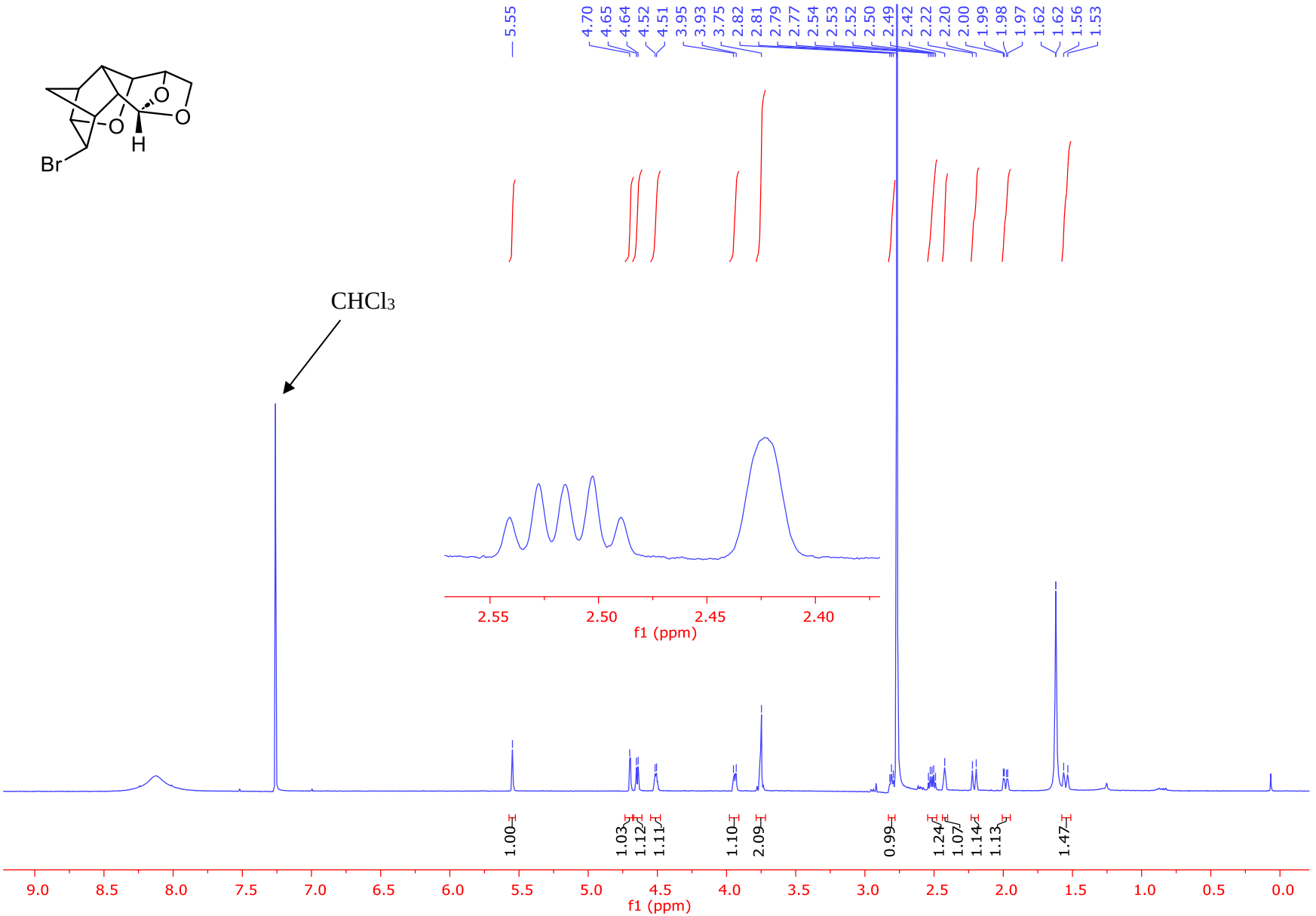

Figure S32: 400 MHz ^{1}H NMR Spectrum of Compound **18** (Recorded in $CDCl_3$)

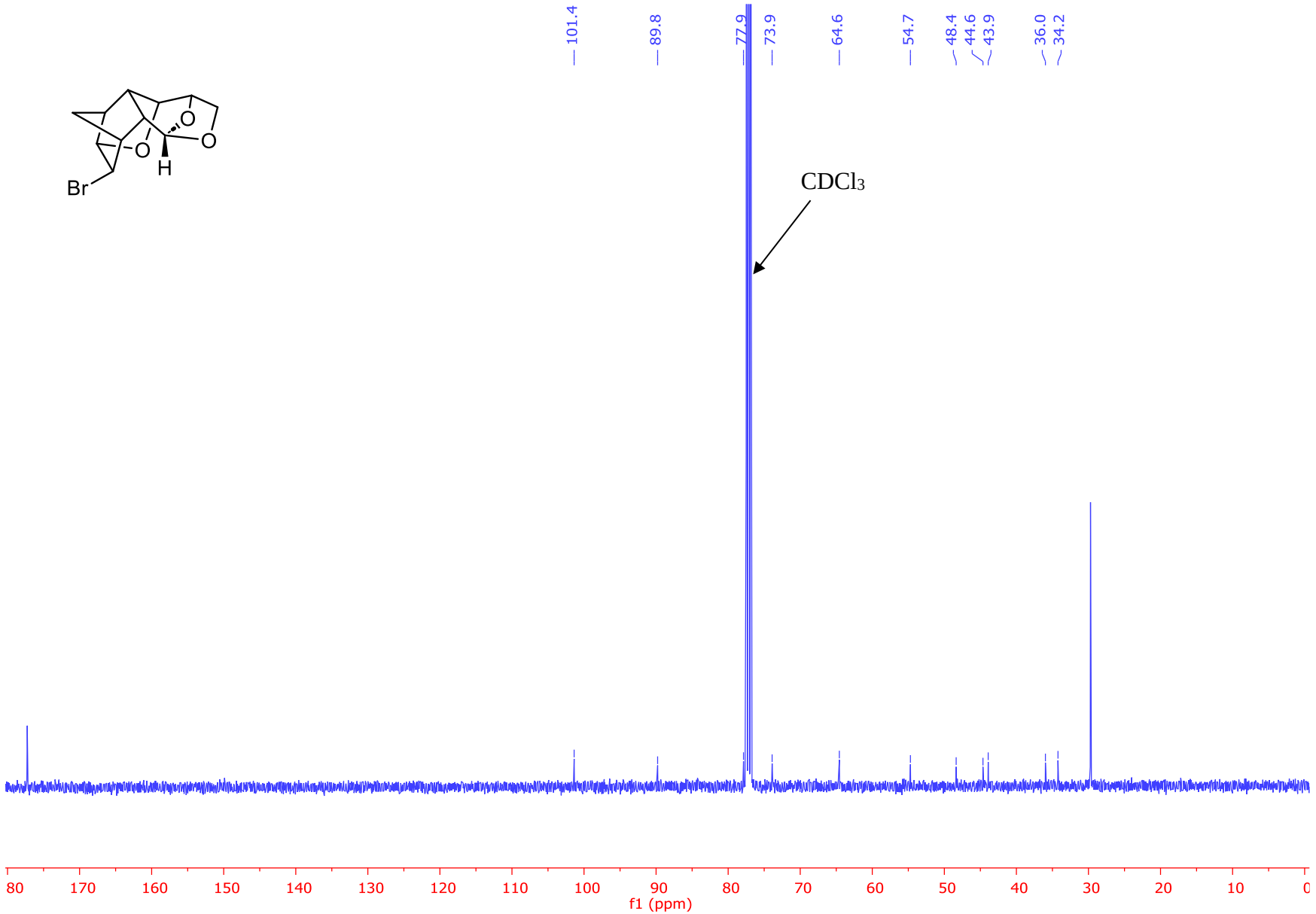

Figure S33: 101 MHz $^{13}C\{^{1}H\}$ NMR Spectrum of Compound **18** (Recorded in $CDCl_3$)

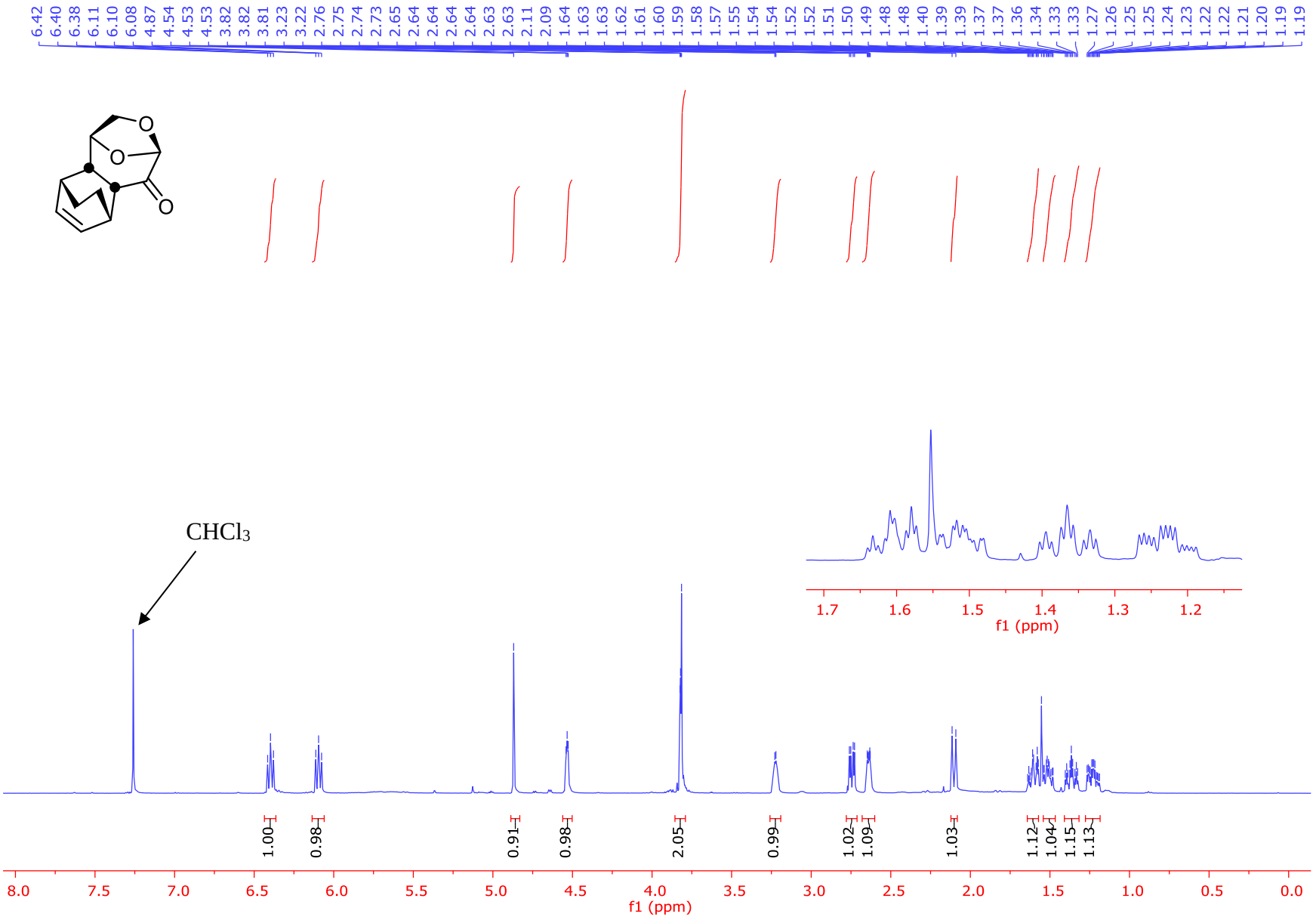

Figure S34: 400 MHz ^{1}H NMR Spectrum of Compound **19** (Recorded in $CDCl_3$)

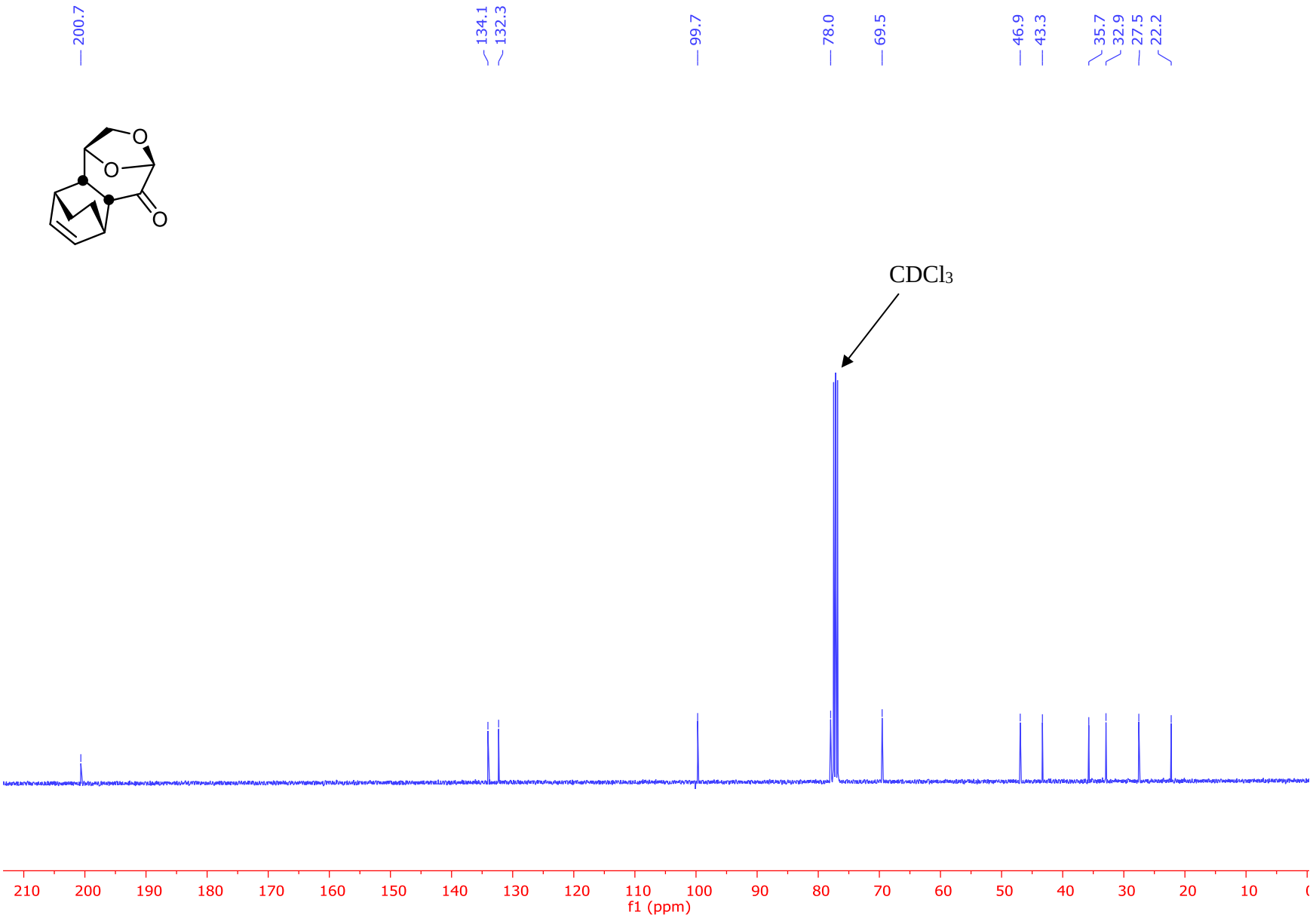

Figure S35: 101 MHz $^{13}C\{^{1}H\}$ NMR Spectrum of Compound **19** (Recorded in $CDCl_3$)

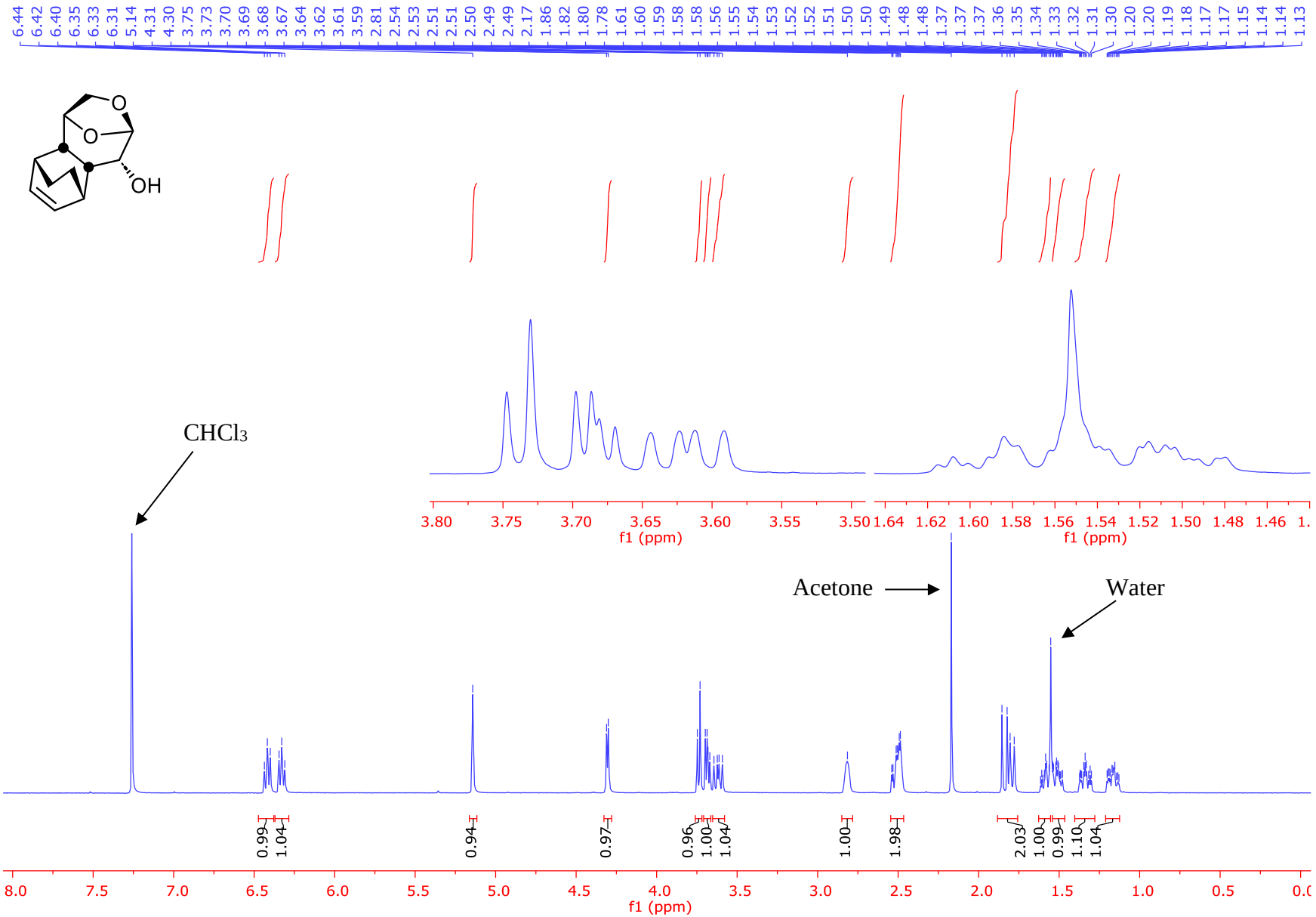

Figure S36: 400 MHz ^{1}H NMR Spectrum of Compound **20** (Recorded in $CDCl_3$)

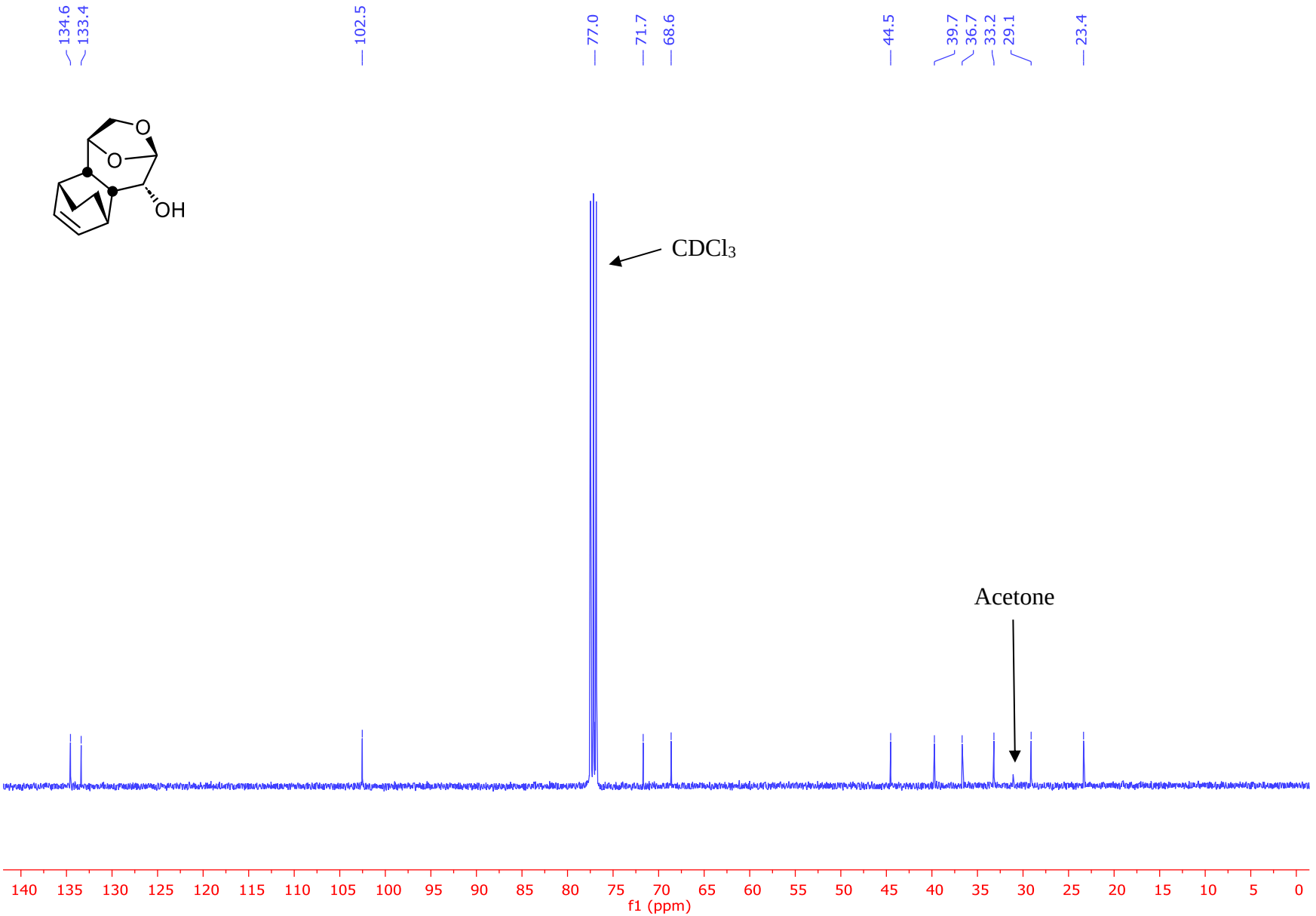

Figure S37: 101 MHz $^{13}C\{^{1}H\}$ NMR Spectrum of Compound **20** (Recorded in $CDCl_3$)

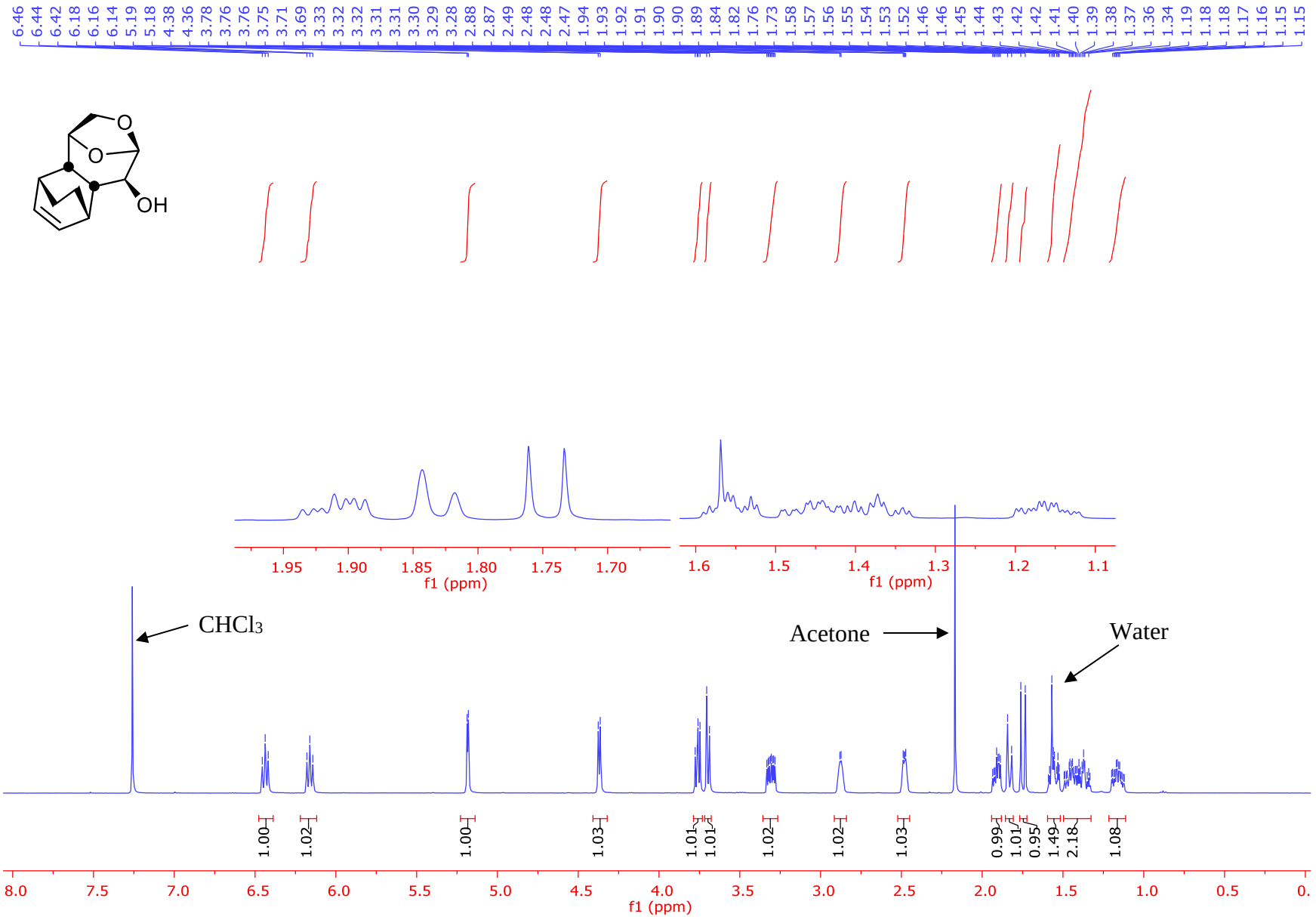

Figure S38: 400 MHz ^{1}H NMR Spectrum of Compound **21** (Recorded in $CDCl_3$)

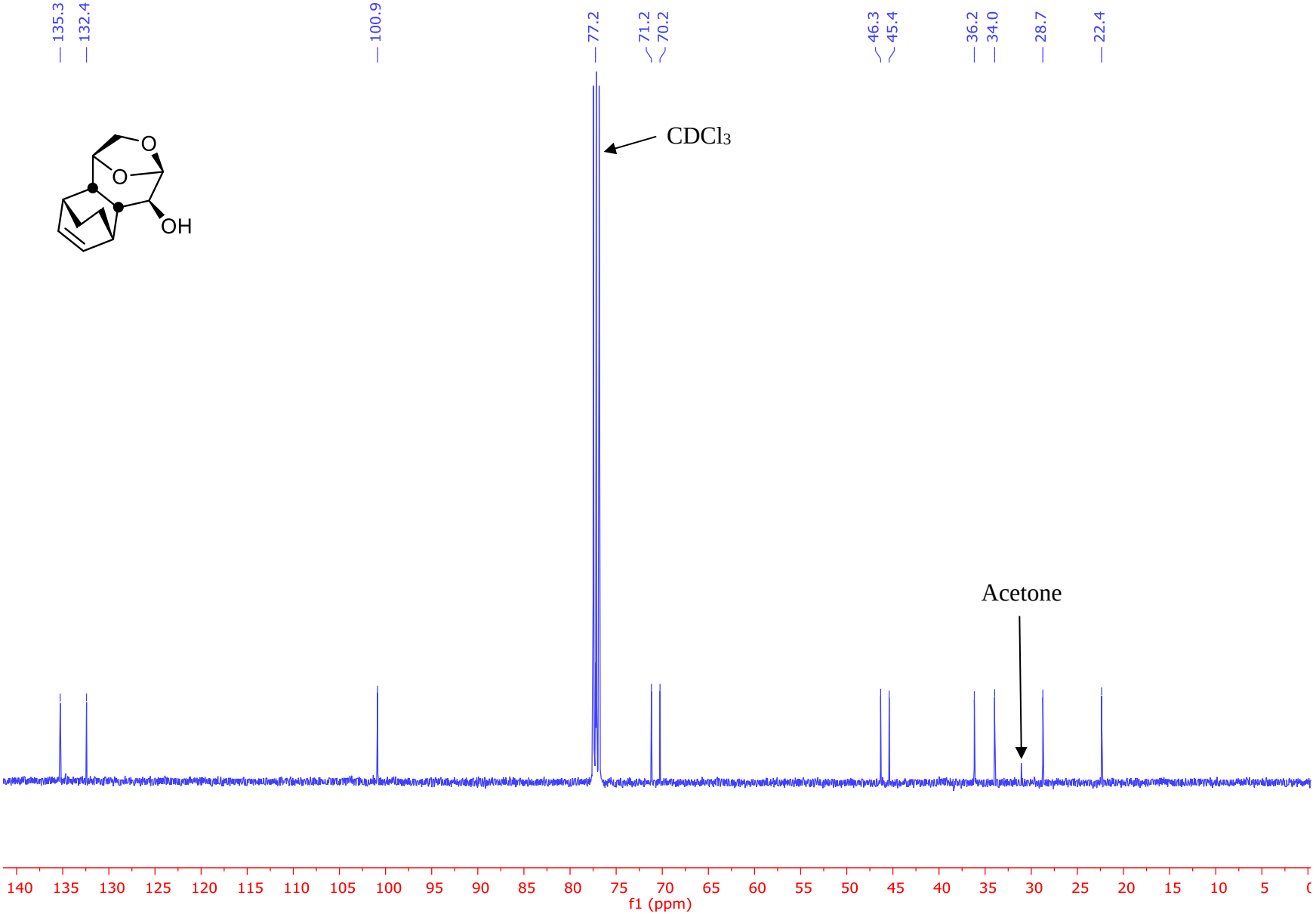

Figure S39: 101 MHz $^{13}C\{^{1}H\}$ NMR Spectrum of Compound **21** (Recorded in $CDCl_3$)

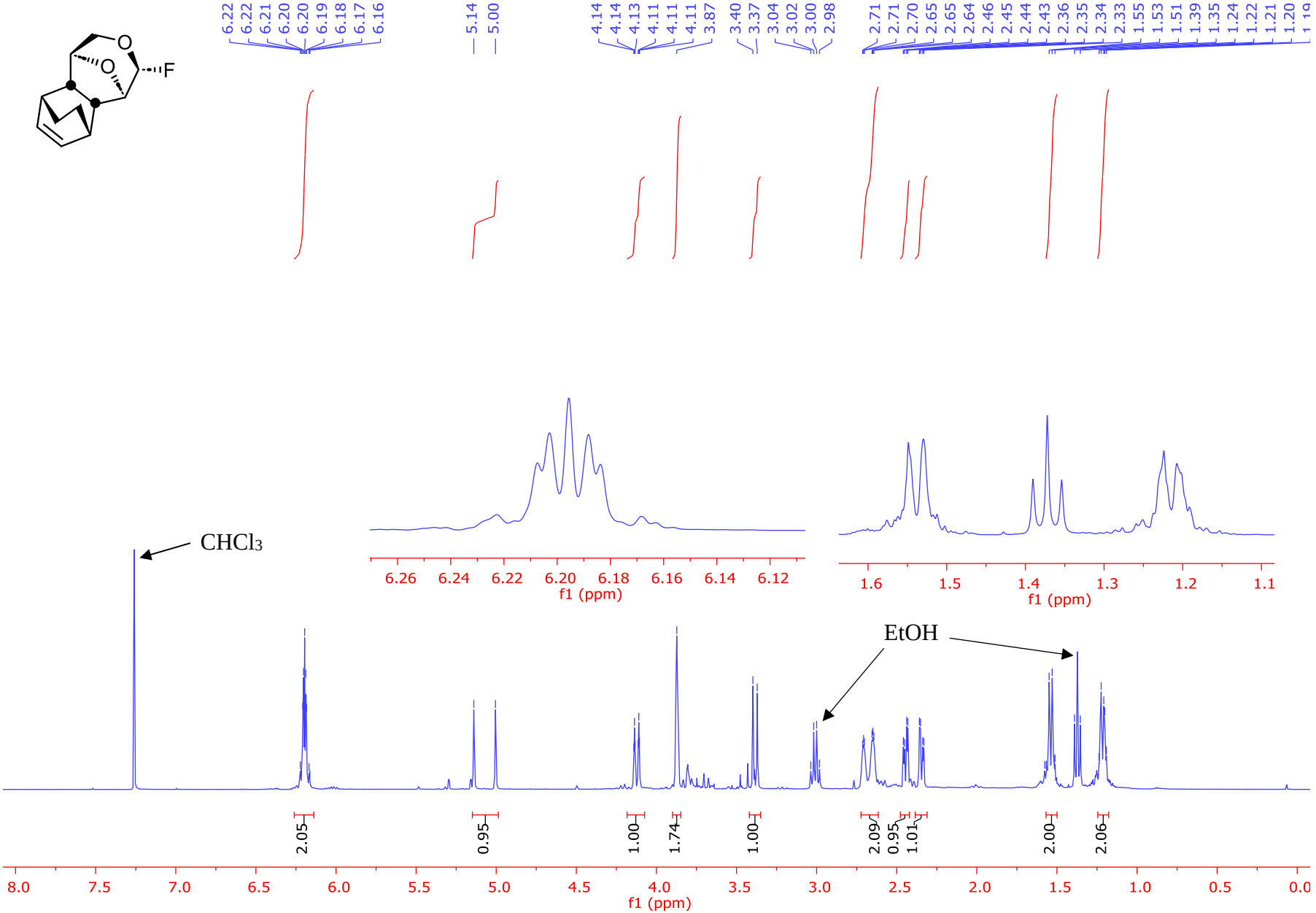

Figure S40: 400 MHz ^{1}H NMR Spectrum of Compound **22** (Recorded in $CDCl_3$)

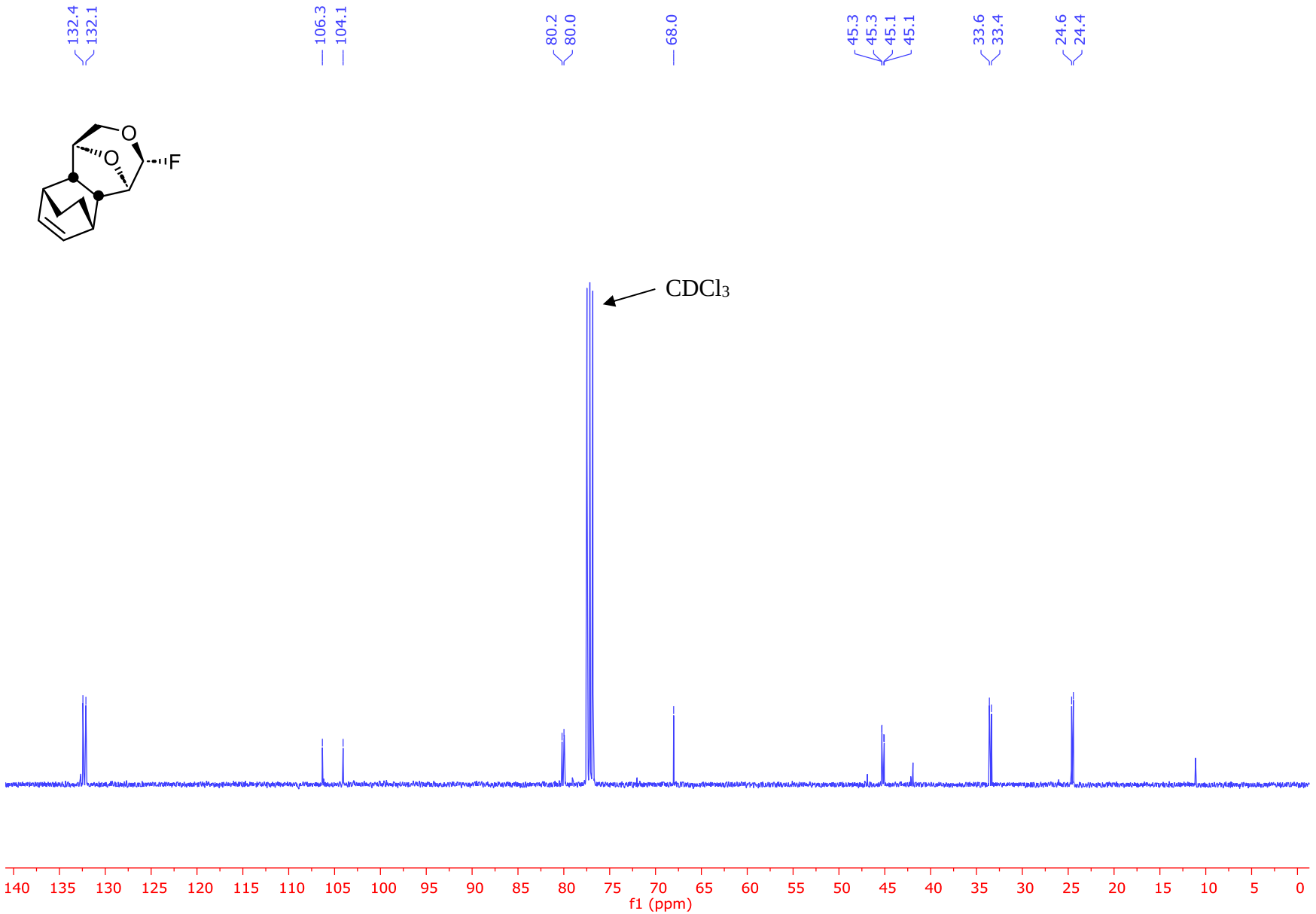

Figure S41: 101 MHz $^{13}C\{^{1}H\}$ NMR Spectrum of Compound **22** (Recorded in $CDCl_3$)

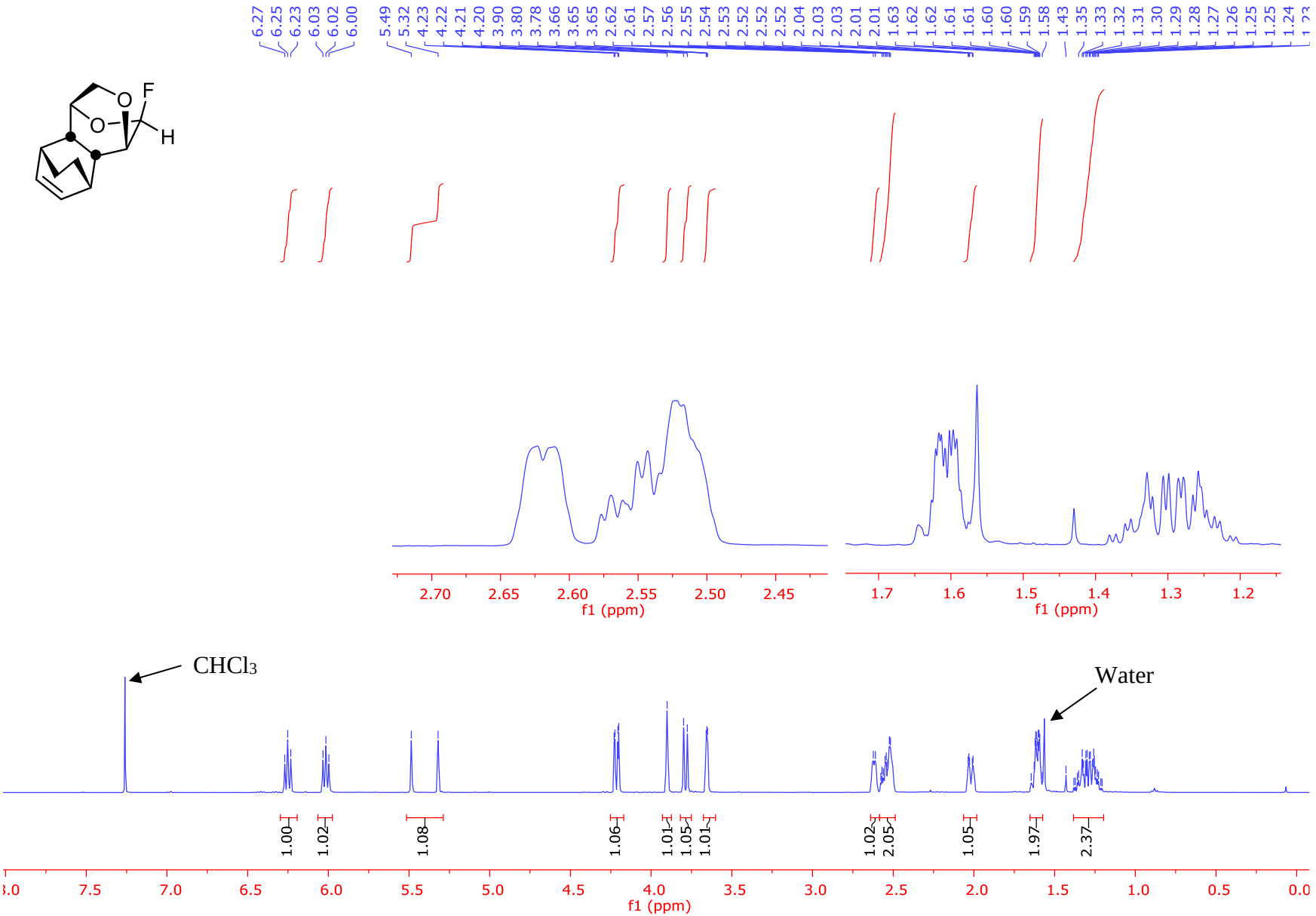

Figure S42: 400 MHz ^{1}H NMR Spectrum of Compound **23** (Recorded in $CDCl_3$)

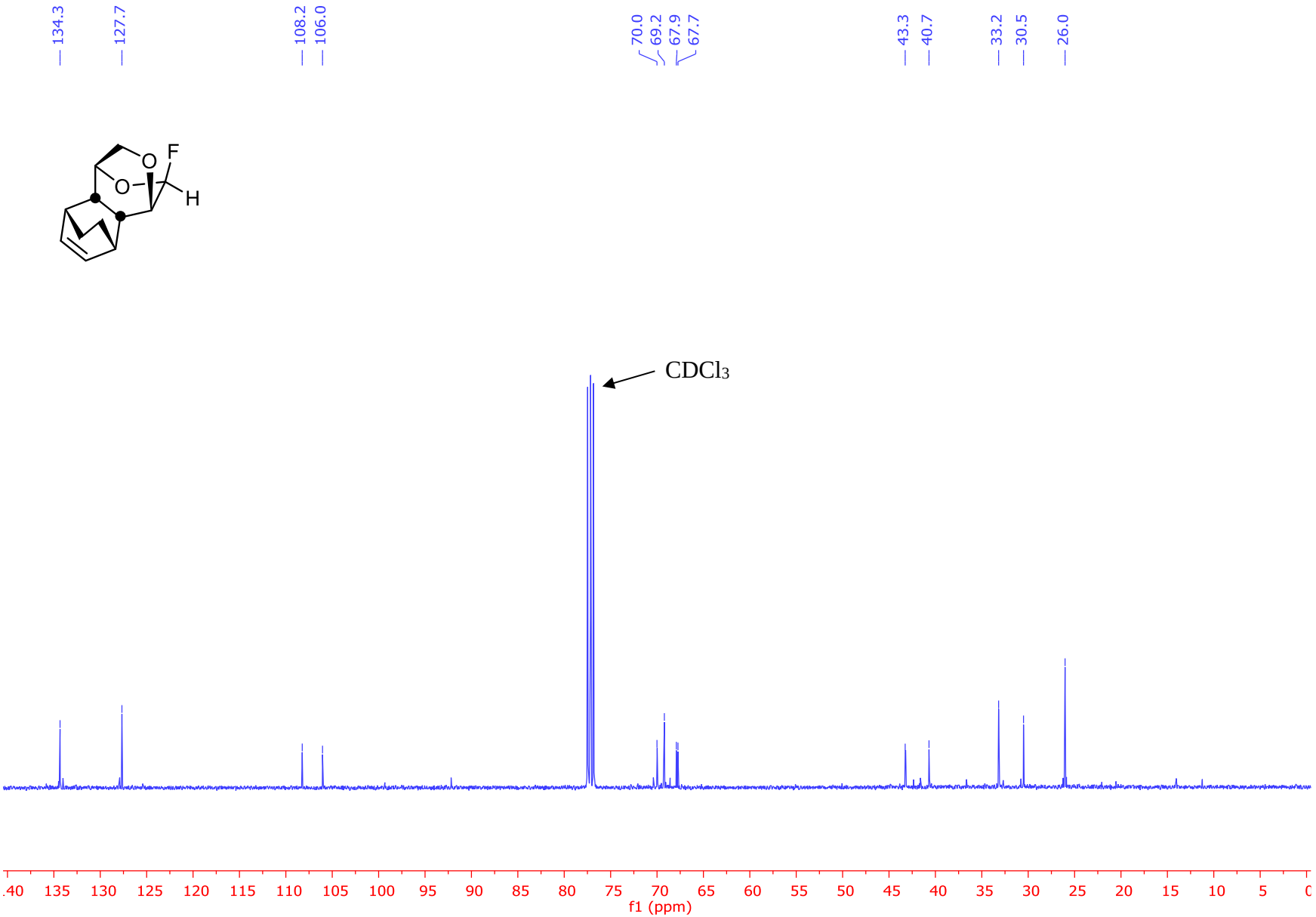

Figure S43: 101 MHz $^{13}C\{^{1}H\}$ NMR Spectrum of Compound **23** (Recorded in $CDCl_3$)

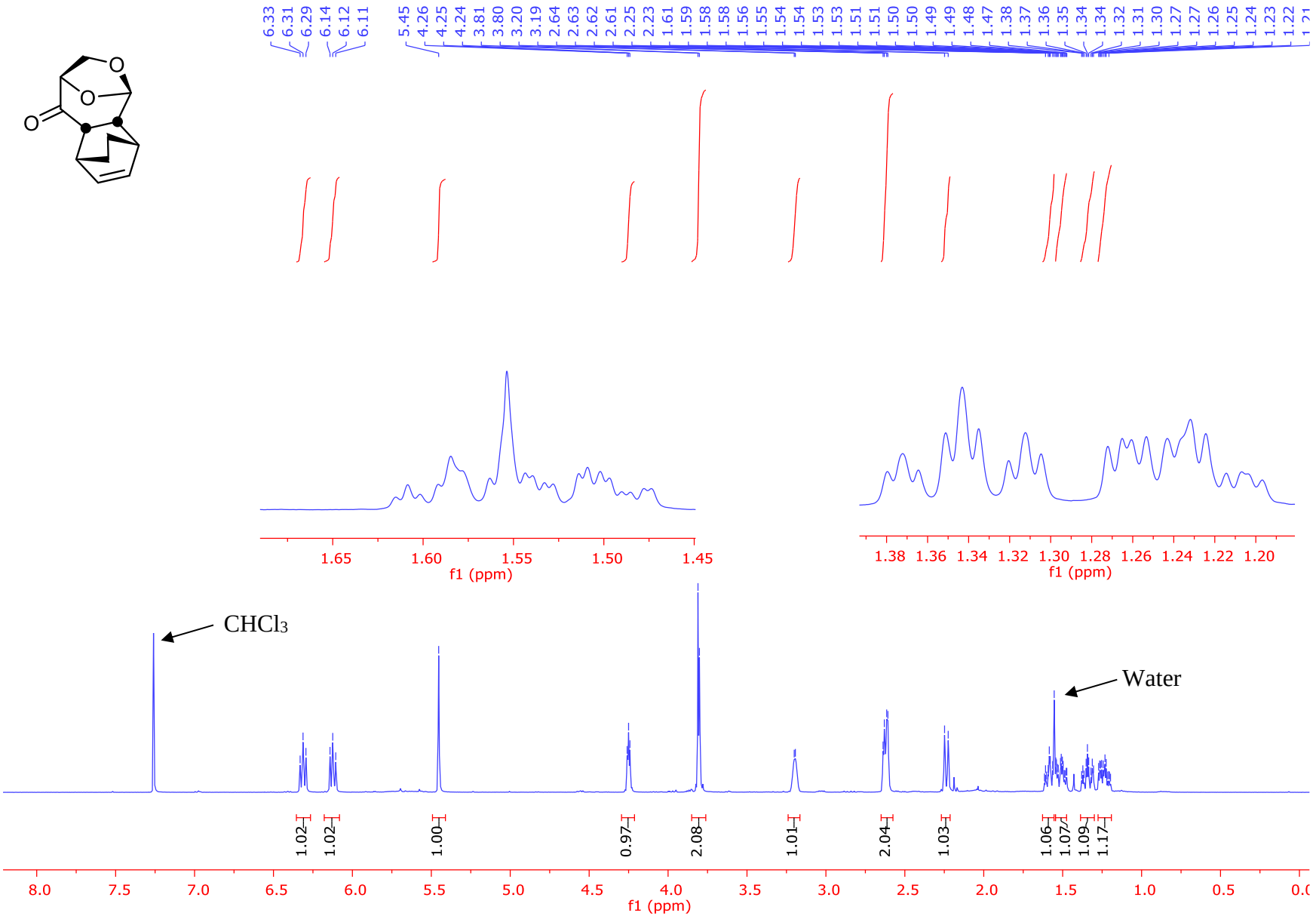

Figure S44: 400 MHz ^{1}H NMR Spectrum of Compound **24** (Recorded in $CDCl_3$)

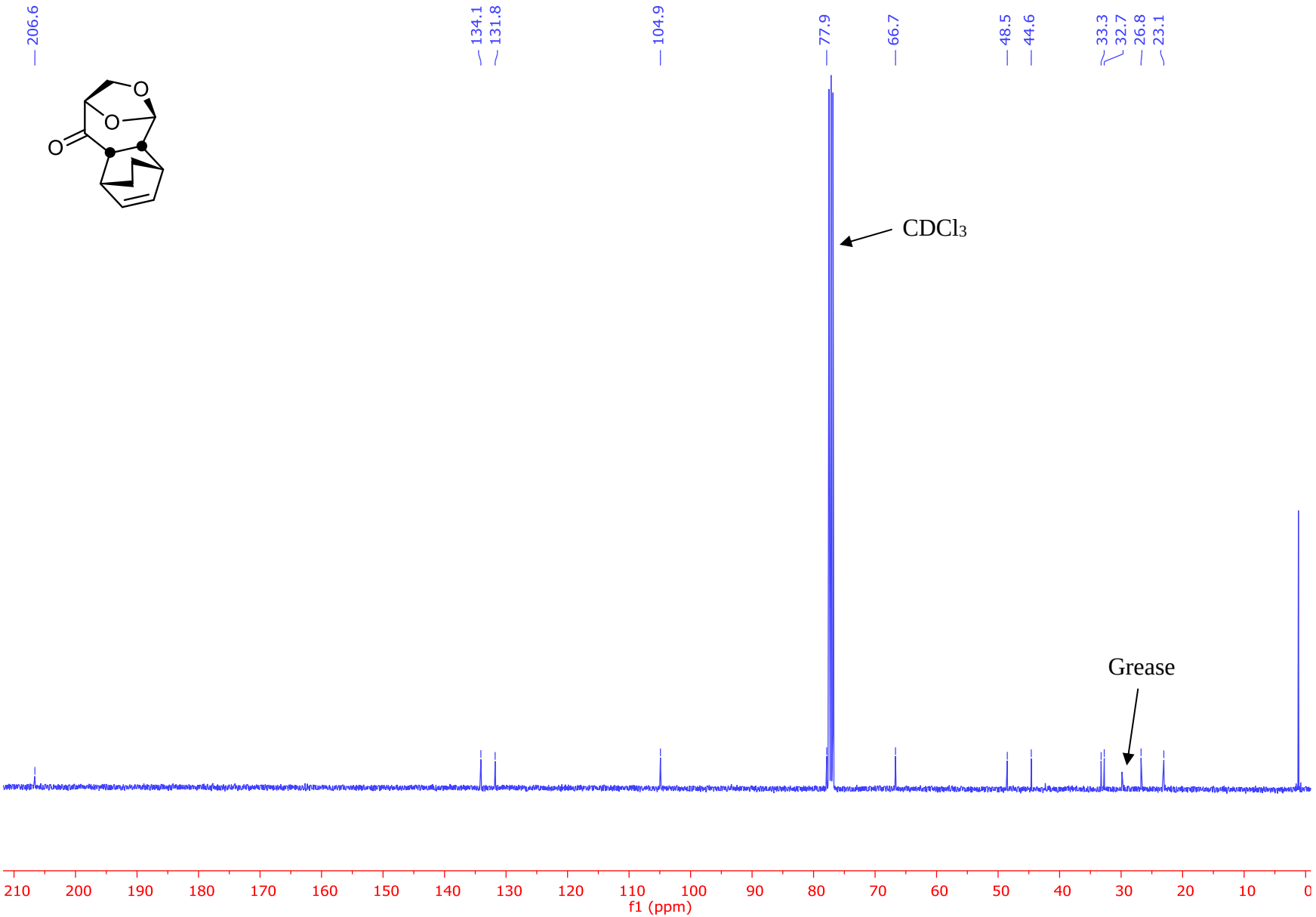

Figure S45: 101 MHz $^{13}C\{^{1}H\}$ NMR Spectrum of Compound **24** (Recorded in $CDCl_3$)

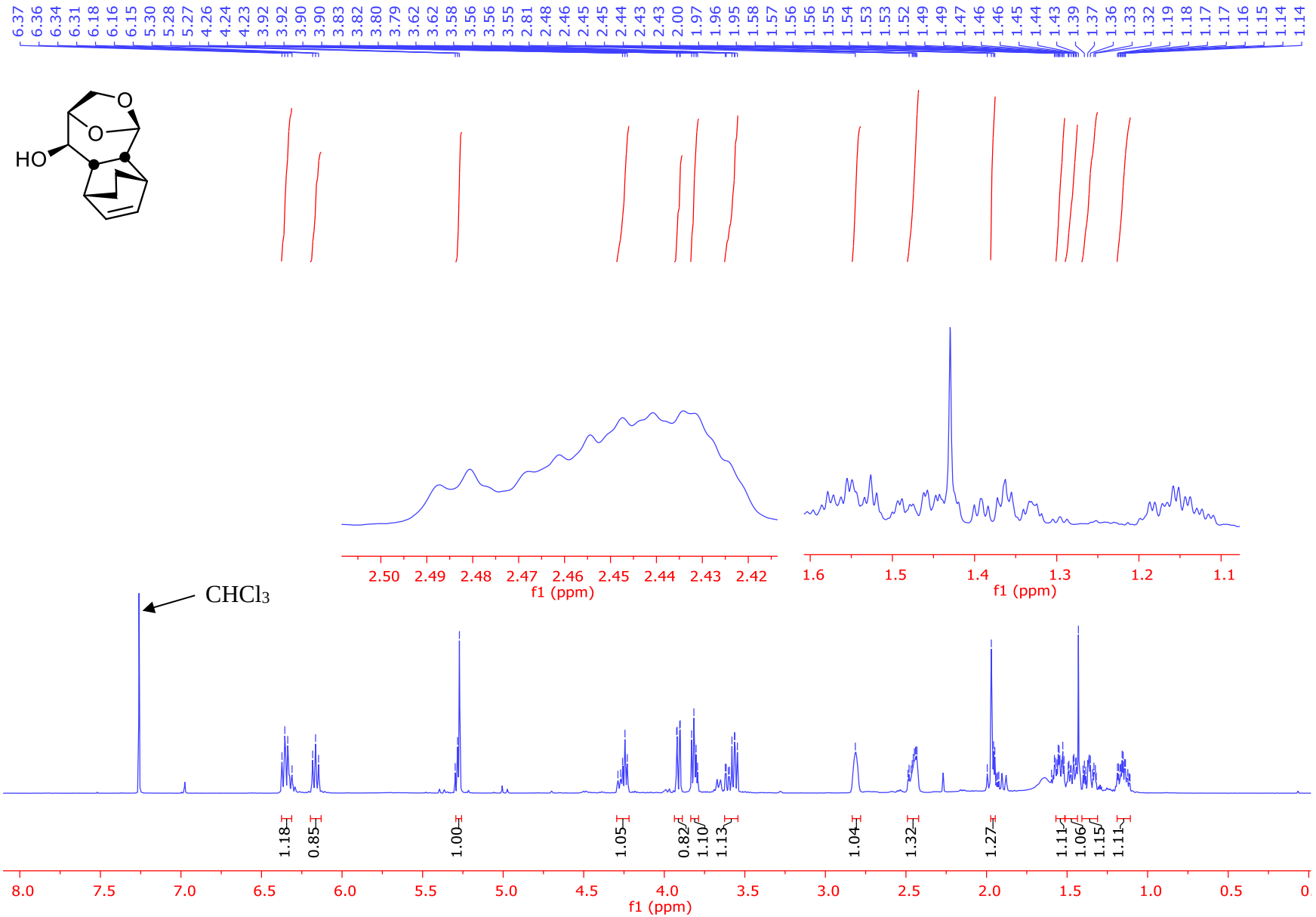

Figure S46: 400 MHz ^{1}H NMR Spectrum of Compound **25** (Recorded in $CDCl_3$)

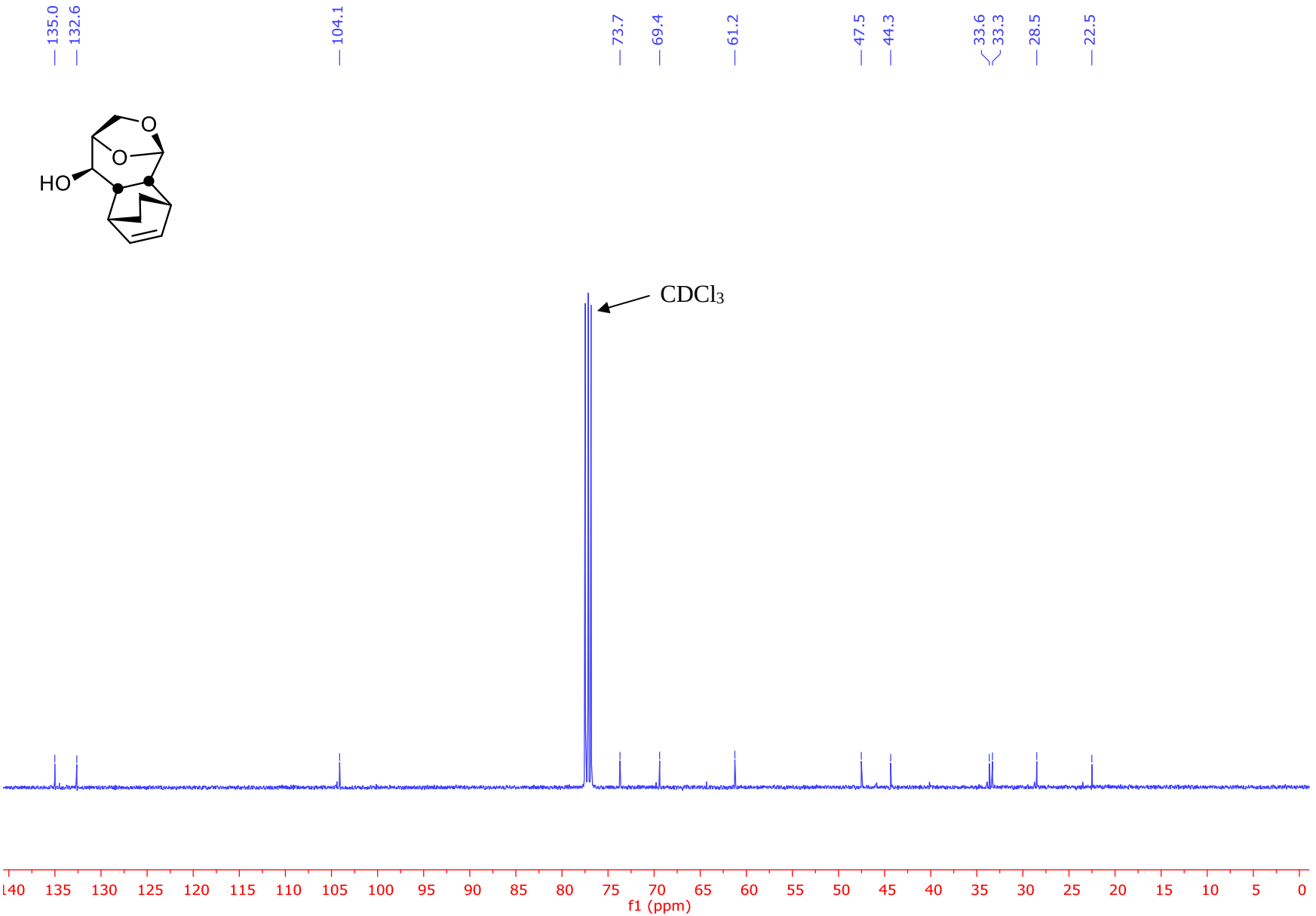

Figure S47: 101 MHz $^{13}C\{^{1}H\}$ NMR Spectrum of Compound **25** (Recorded in $CDCl_3$)

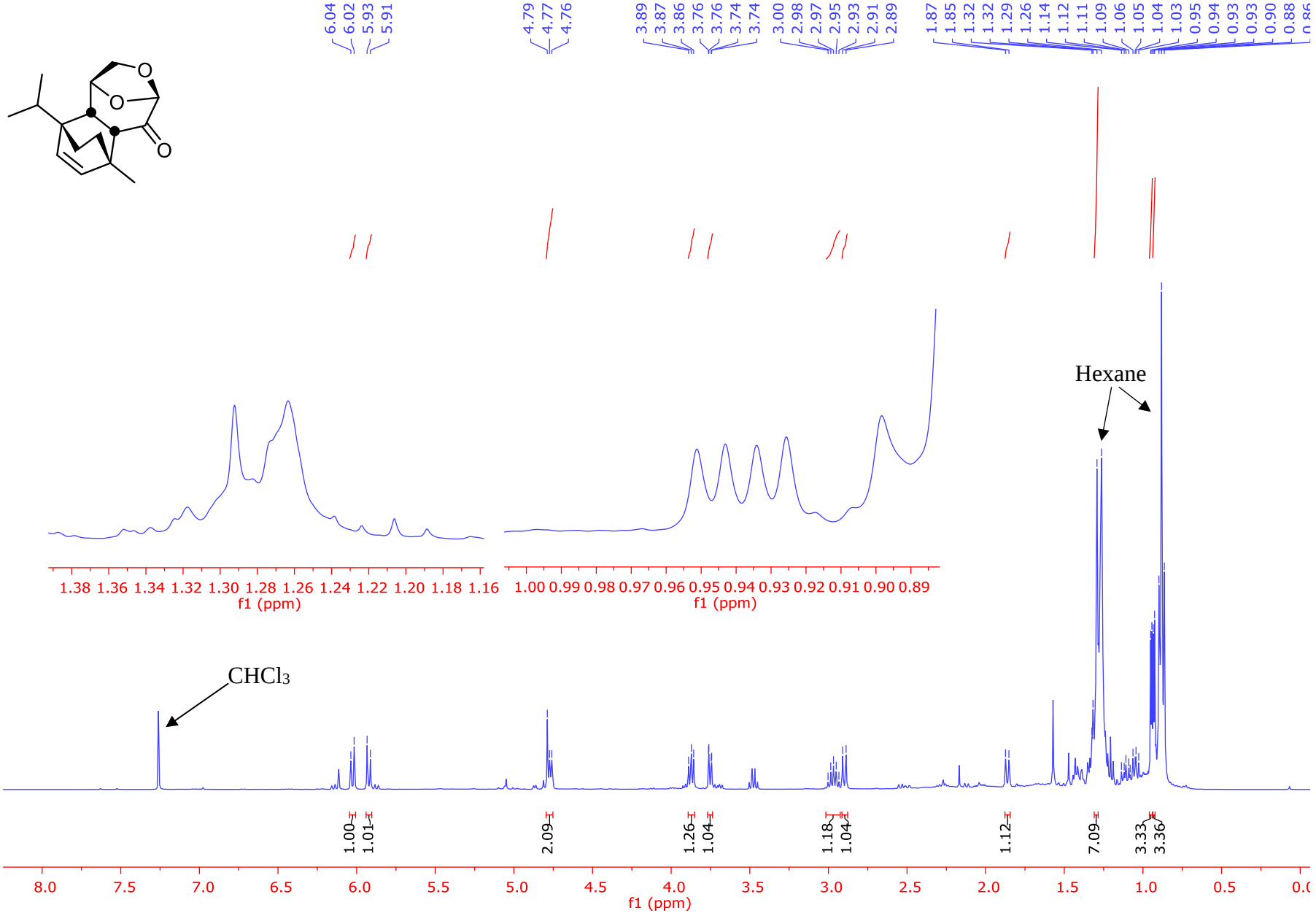

Figure S48: 400 MHz ^{1}H NMR Spectrum of Compound **27** (Recorded in $CDCl_3$)

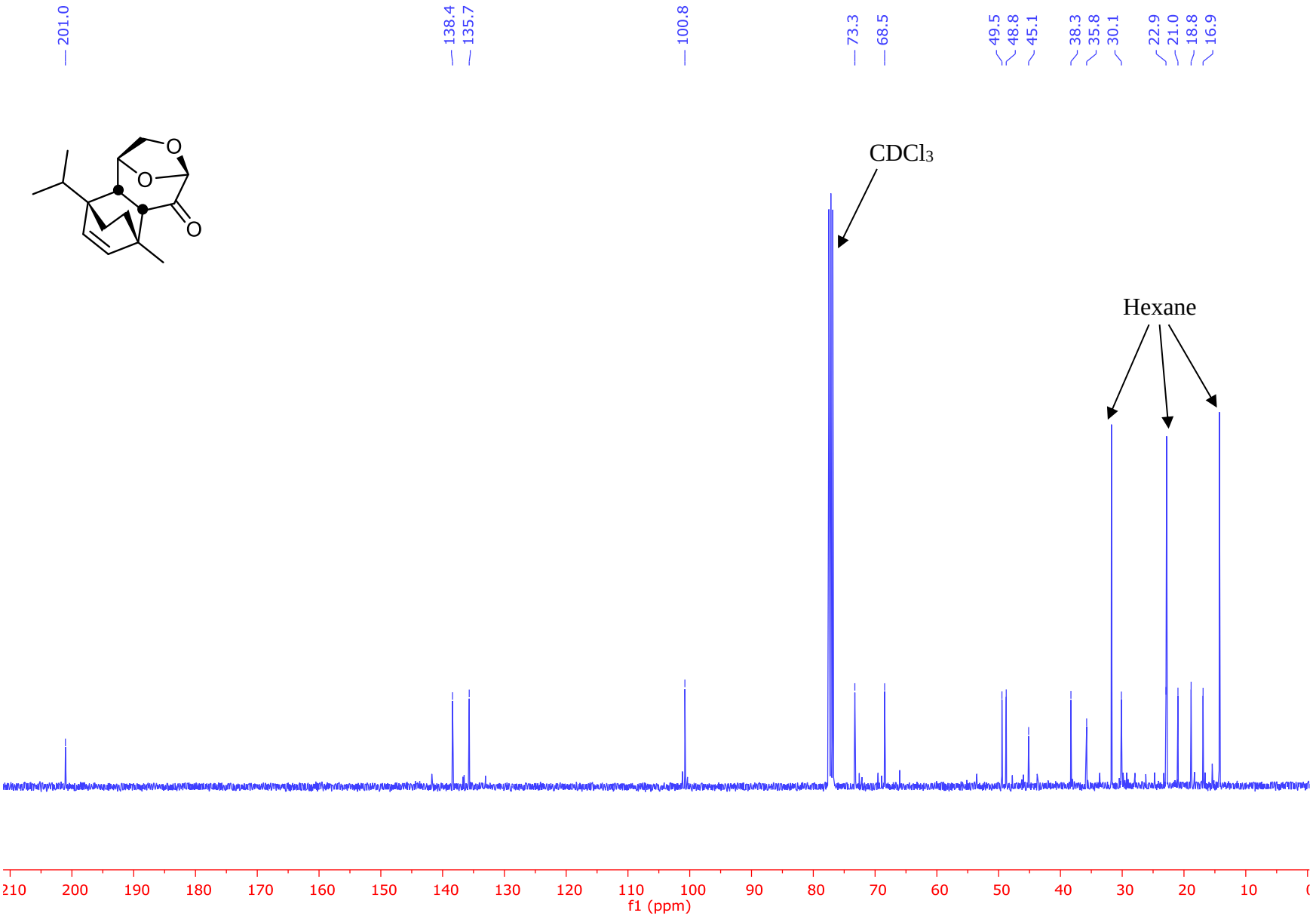

Figure S49: 101 MHz $^{13}C\{^{1}H\}$ NMR Spectrum of Compound **27** (Recorded in $CDCl_3$)

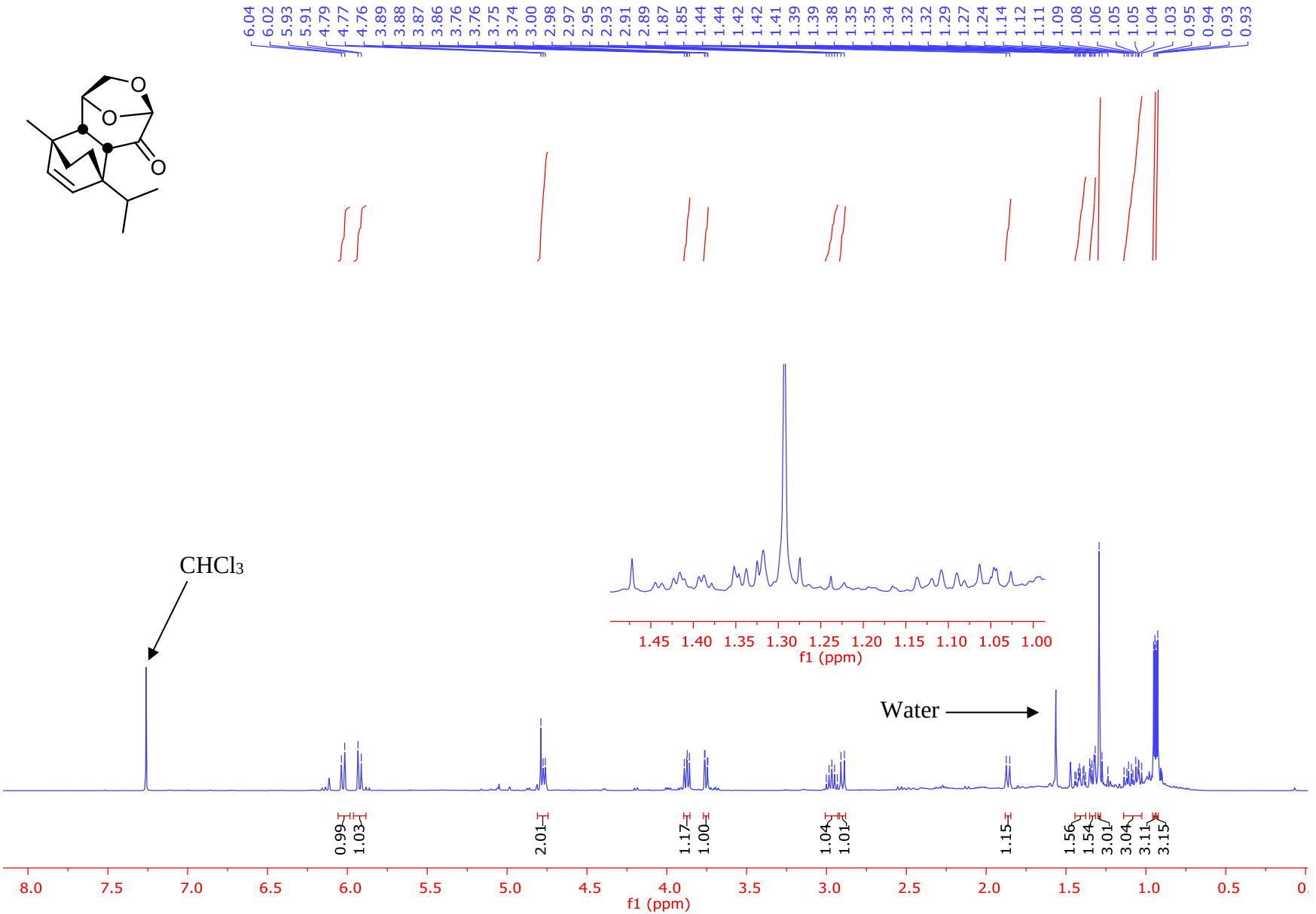

Figure S50: 400 MHz ^{1}H NMR Spectrum of Compound **28** (Recorded in $CDCl_3$)

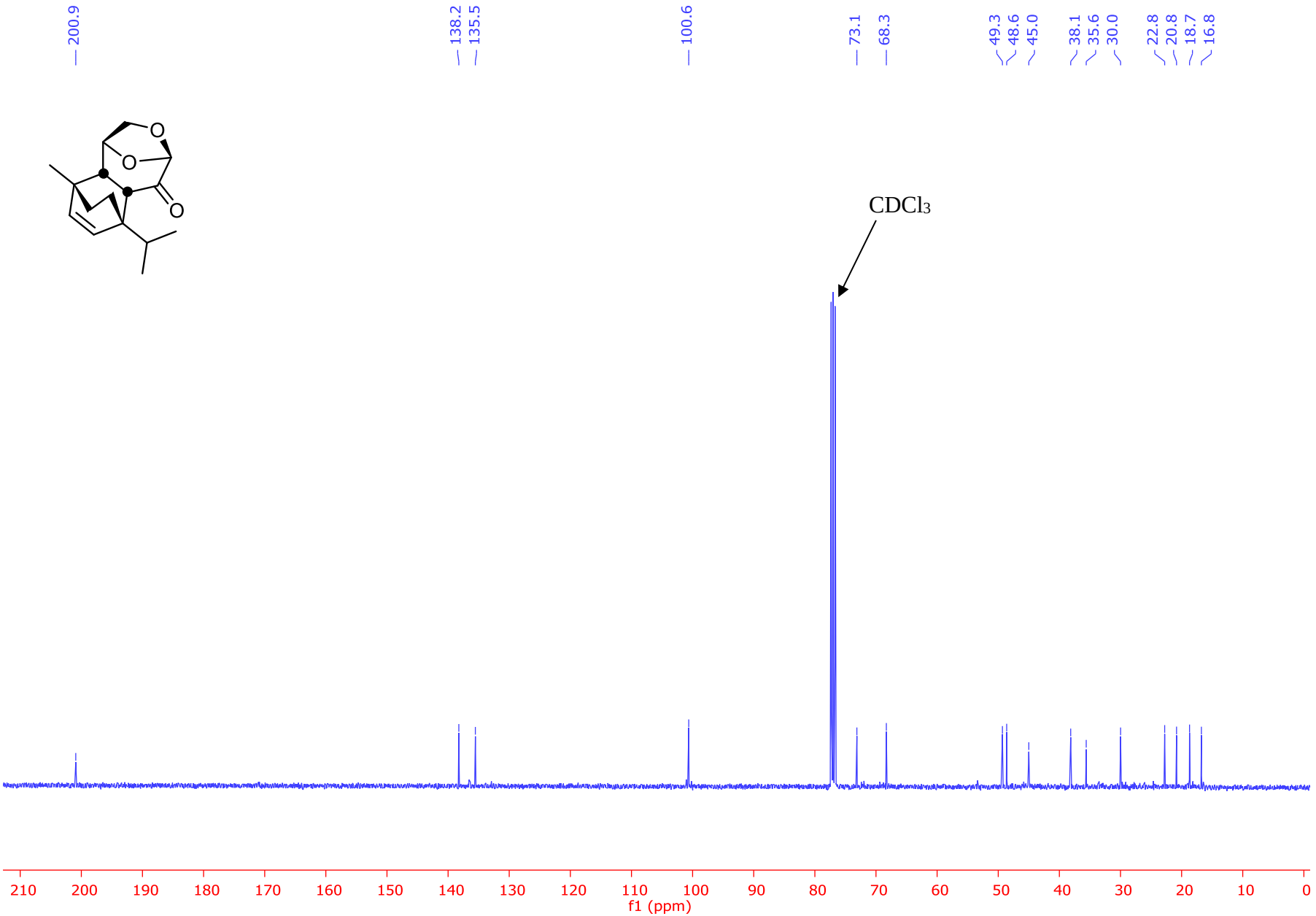

Figure S51: 101 MHz $^{13}C\{^{1}H\}$ NMR of Compound **28** (Recorded in $CDCl_3$)

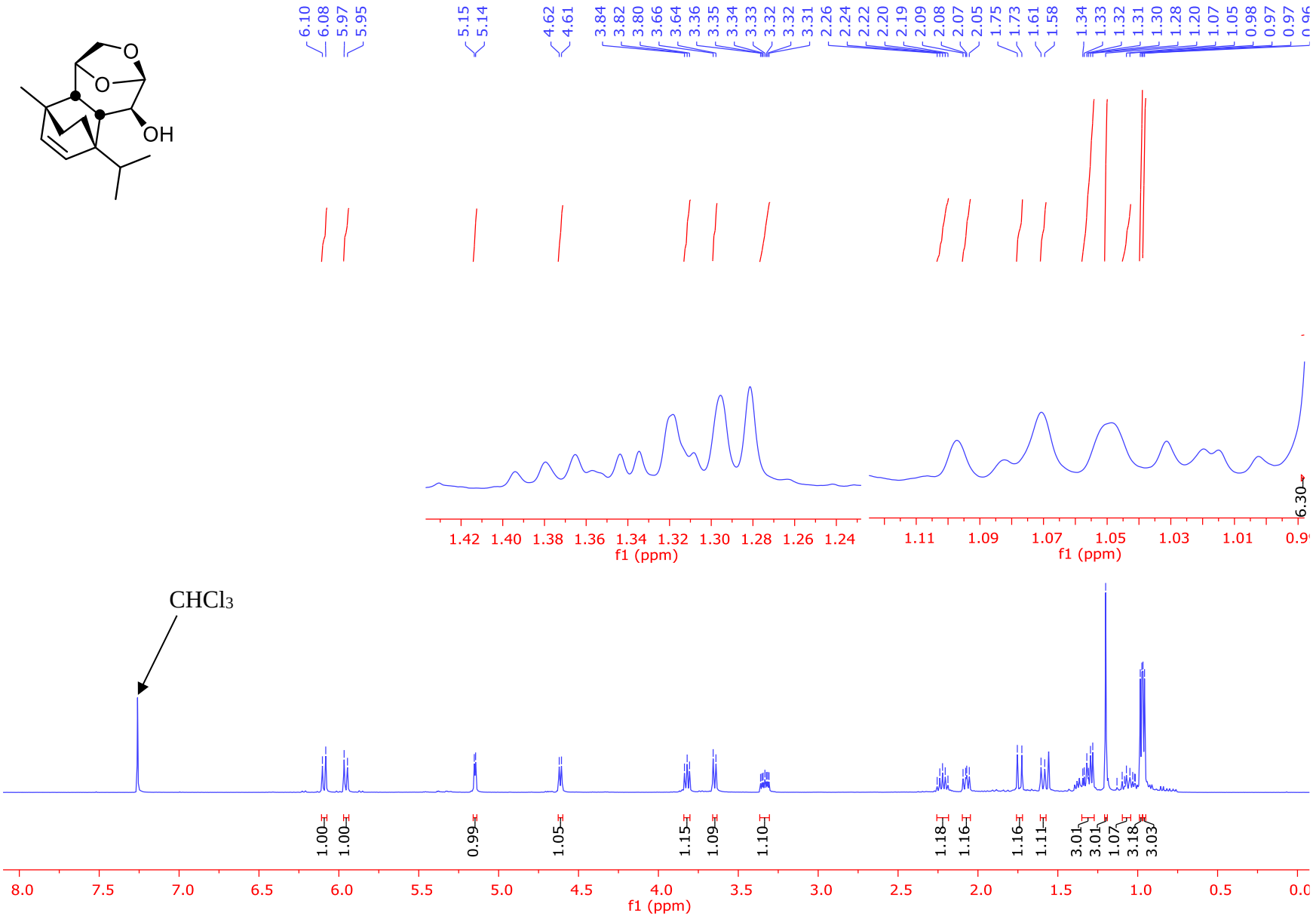

Figure S52: 400 MHz ^{1}H NMR of Compound **29** (Recorded in $CDCl_3$)

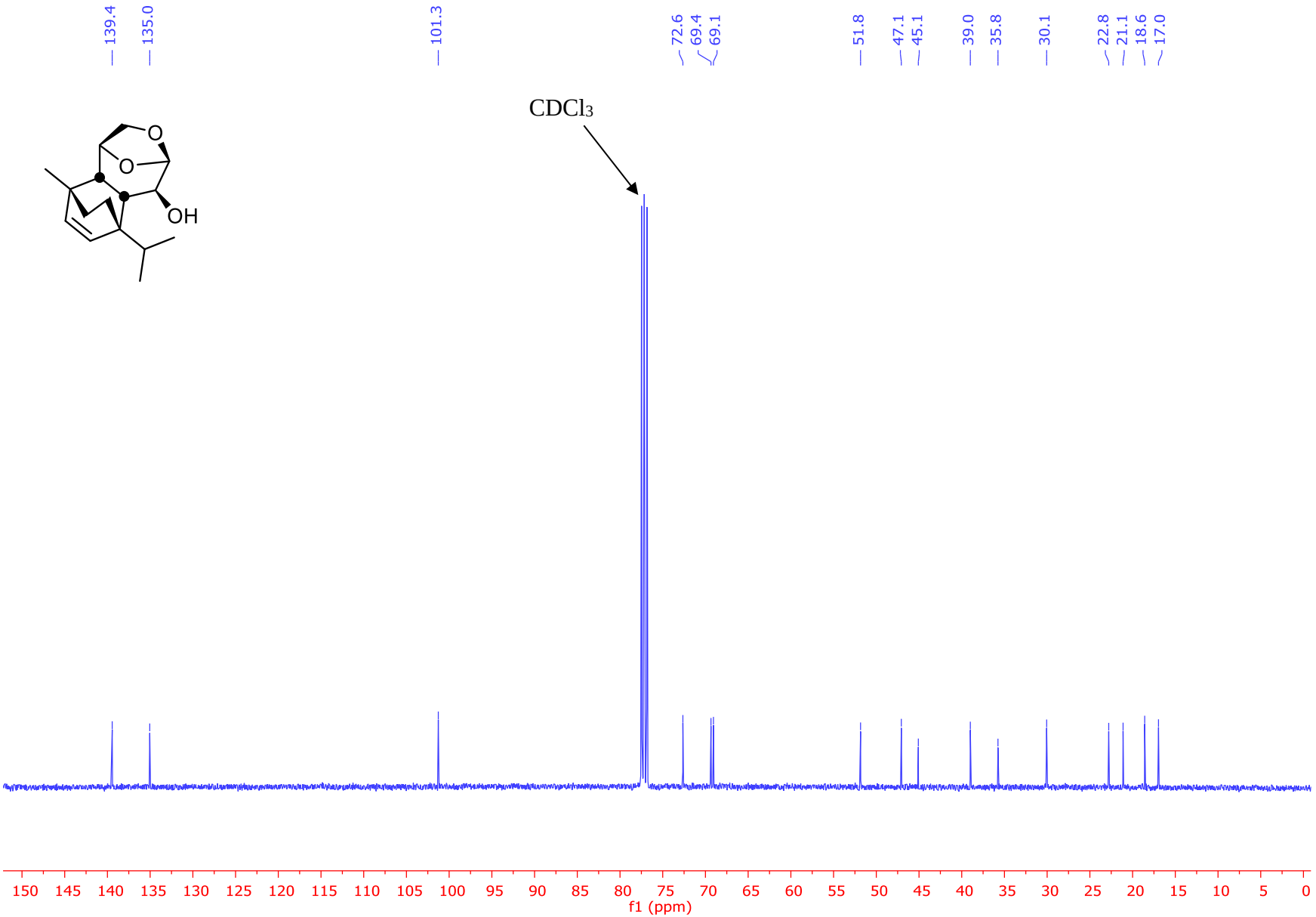

Figure S53: 101 MHz $^{13}C\{^{1}H\}$ NMR Spectrum of Compound **29** (Recorded in $CDCl_3$)

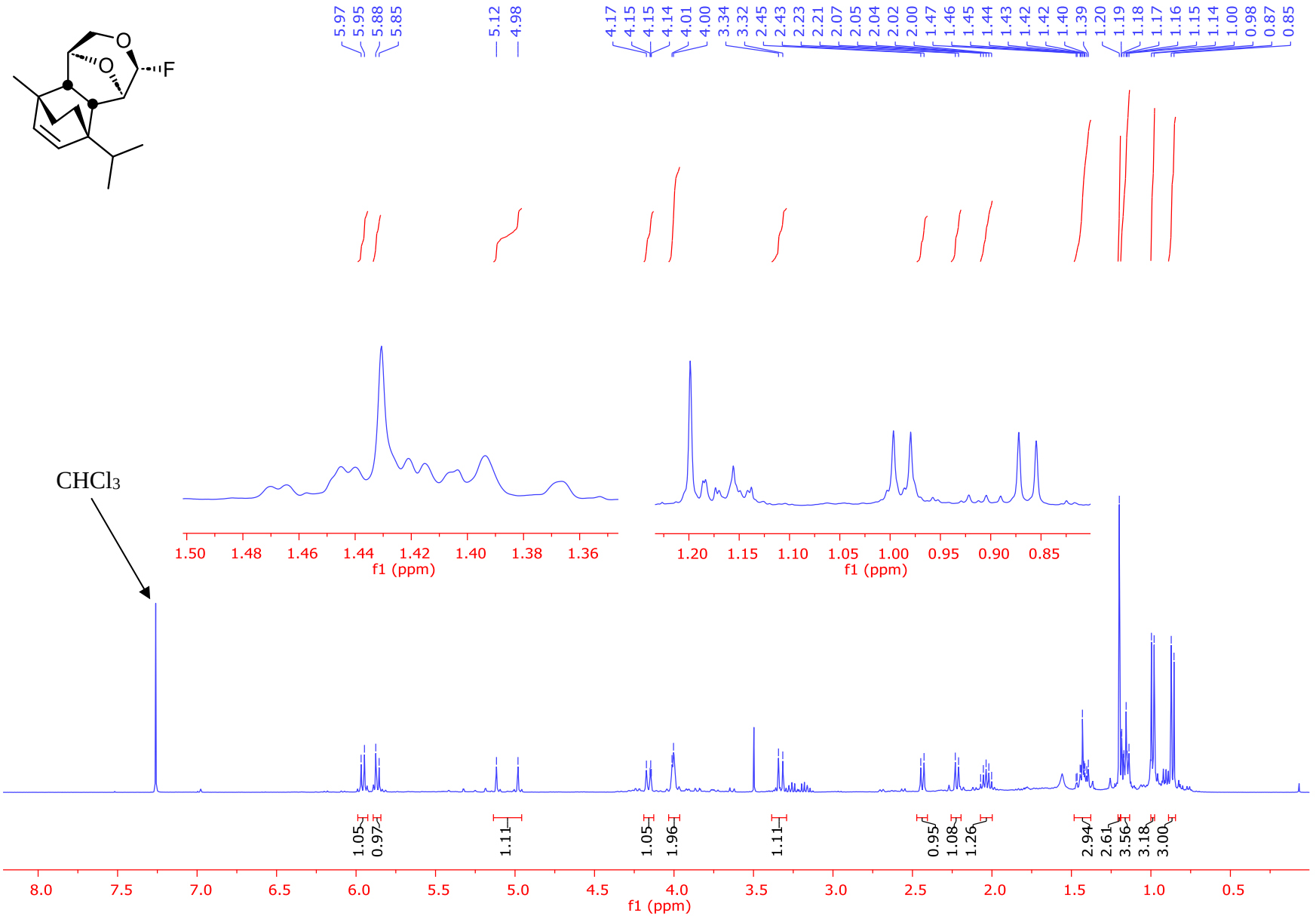

Figure S54: 400 MHz ^{1}H NMR Spectrum of Compound **30** (Recorded in $CDCl_3$)

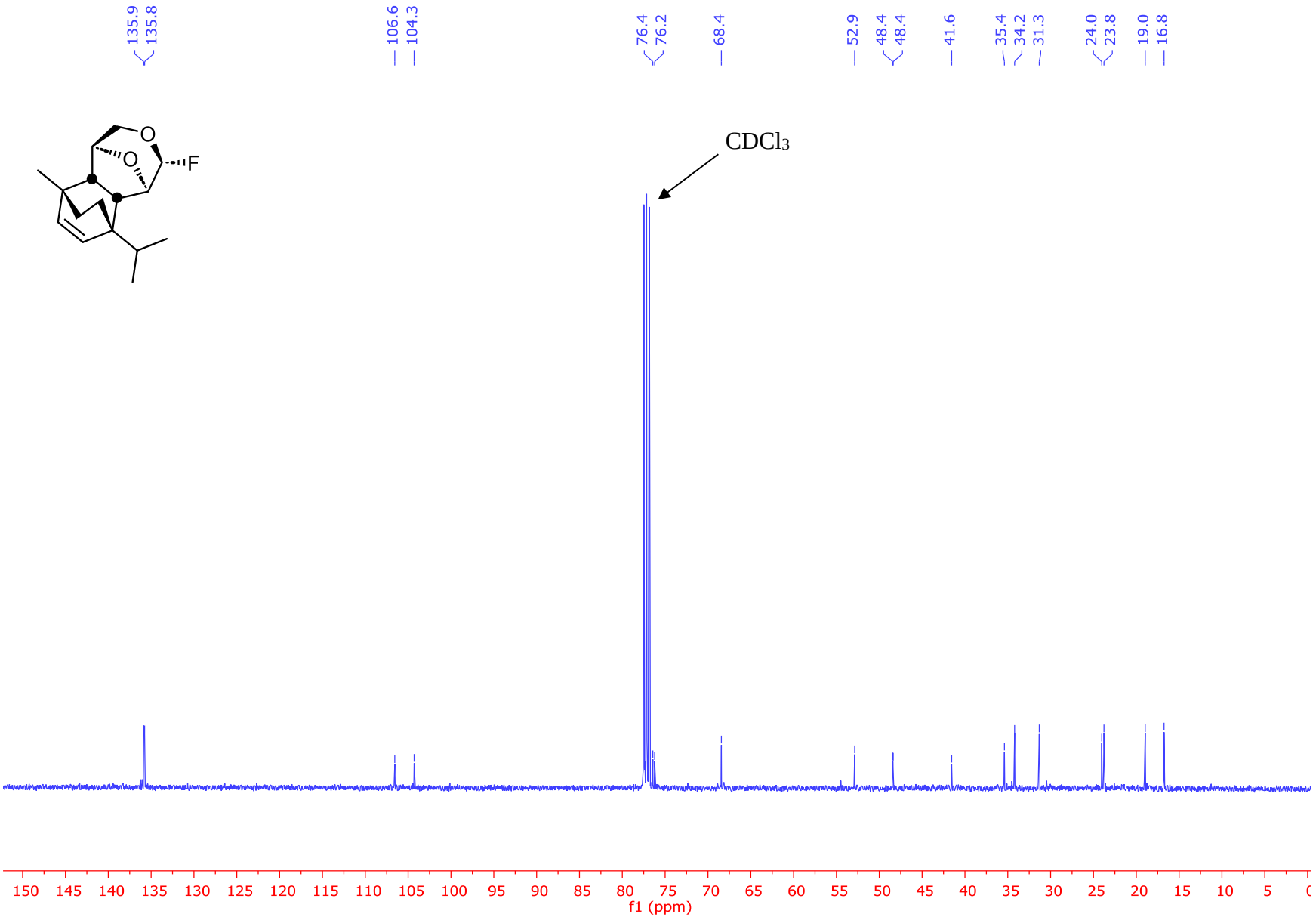

Figure S55: 101 MHz $^{13}C\{^{1}H\}$ NMR Spectrum of Compound **30** (Recorded in $CDCl_3$)

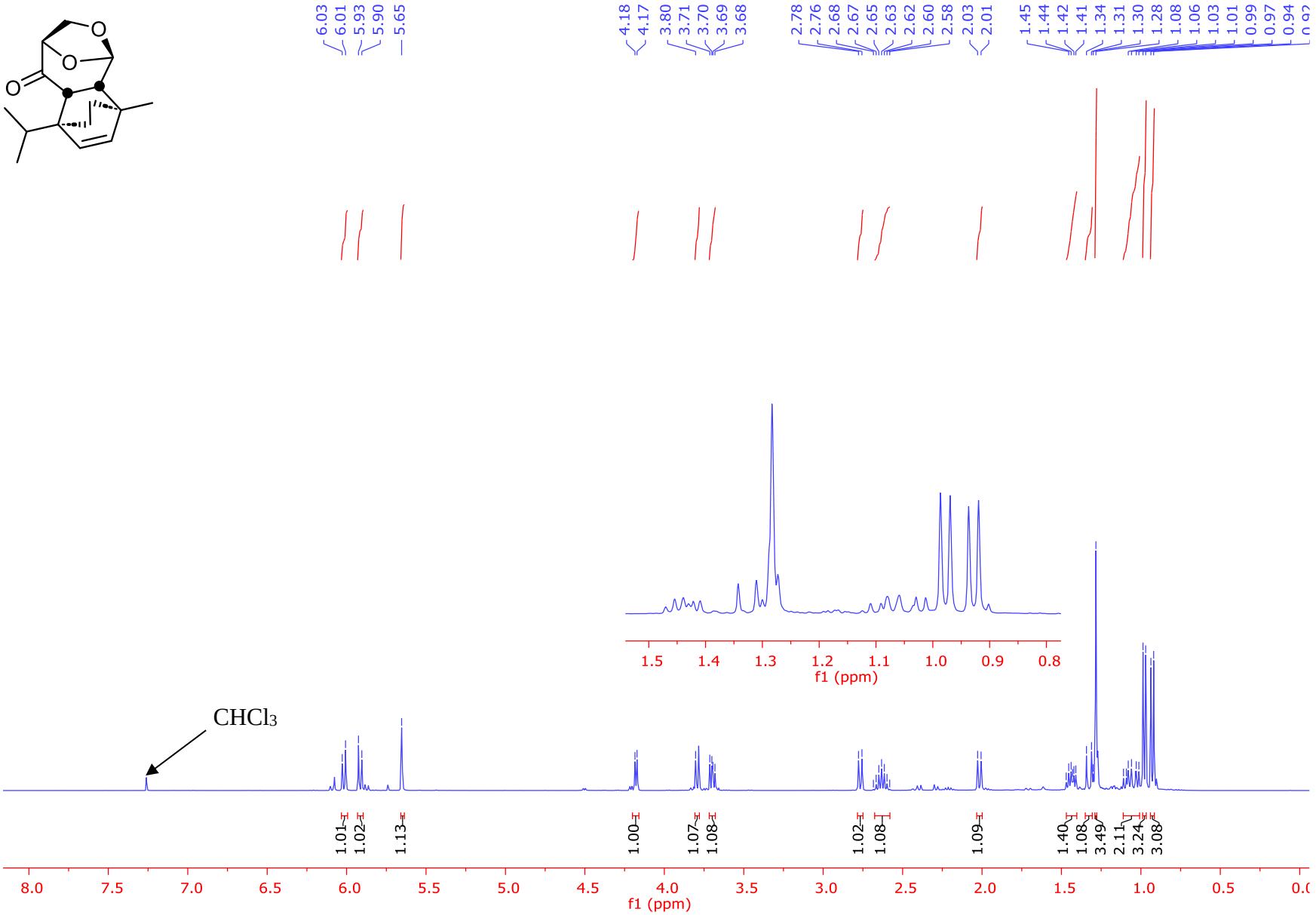

Figure S56: 400 MHz ^{1}H NMR Spectrum of Compound **32** (Recorded in $CDCl_3$)

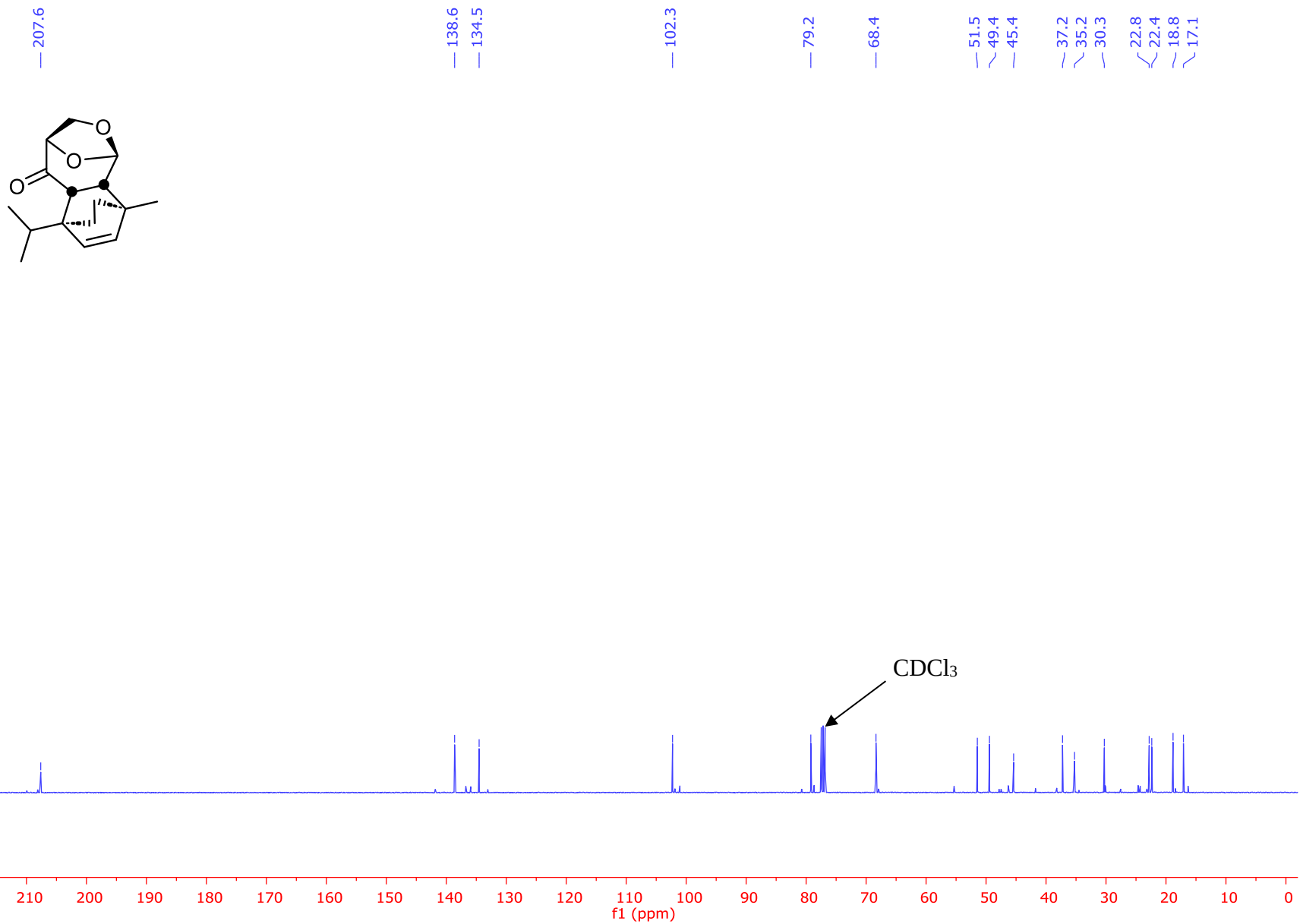

Figure S57: 101 MHz $^{13}C\{^{1}H\}$ NMR Spectrum of Compound **32** (Recorded in $CDCl_3$)

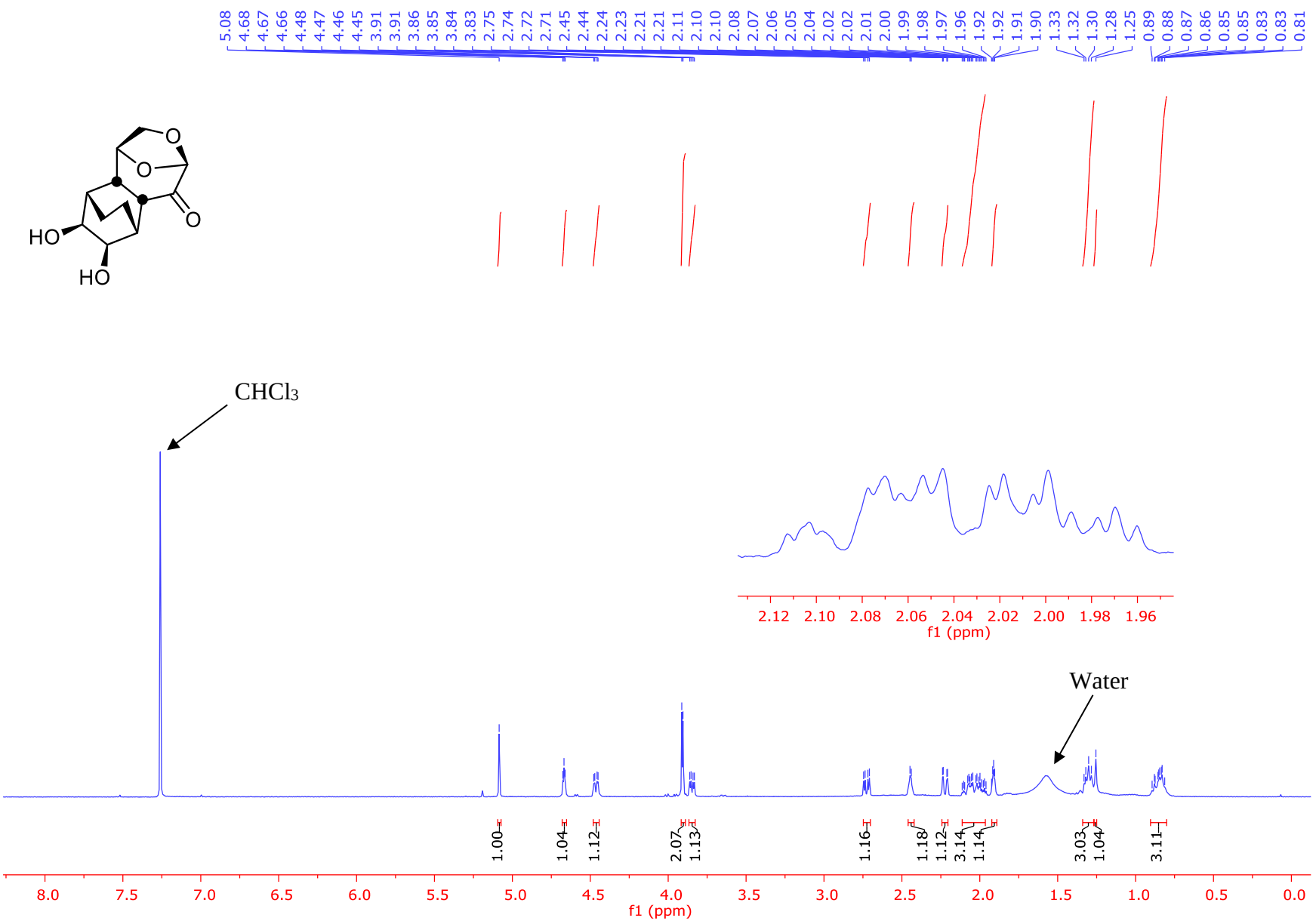

Figure S58: 400 MHz ^{1}H NMR Spectrum of Compound **33** (Recorded in $CDCl_3$)

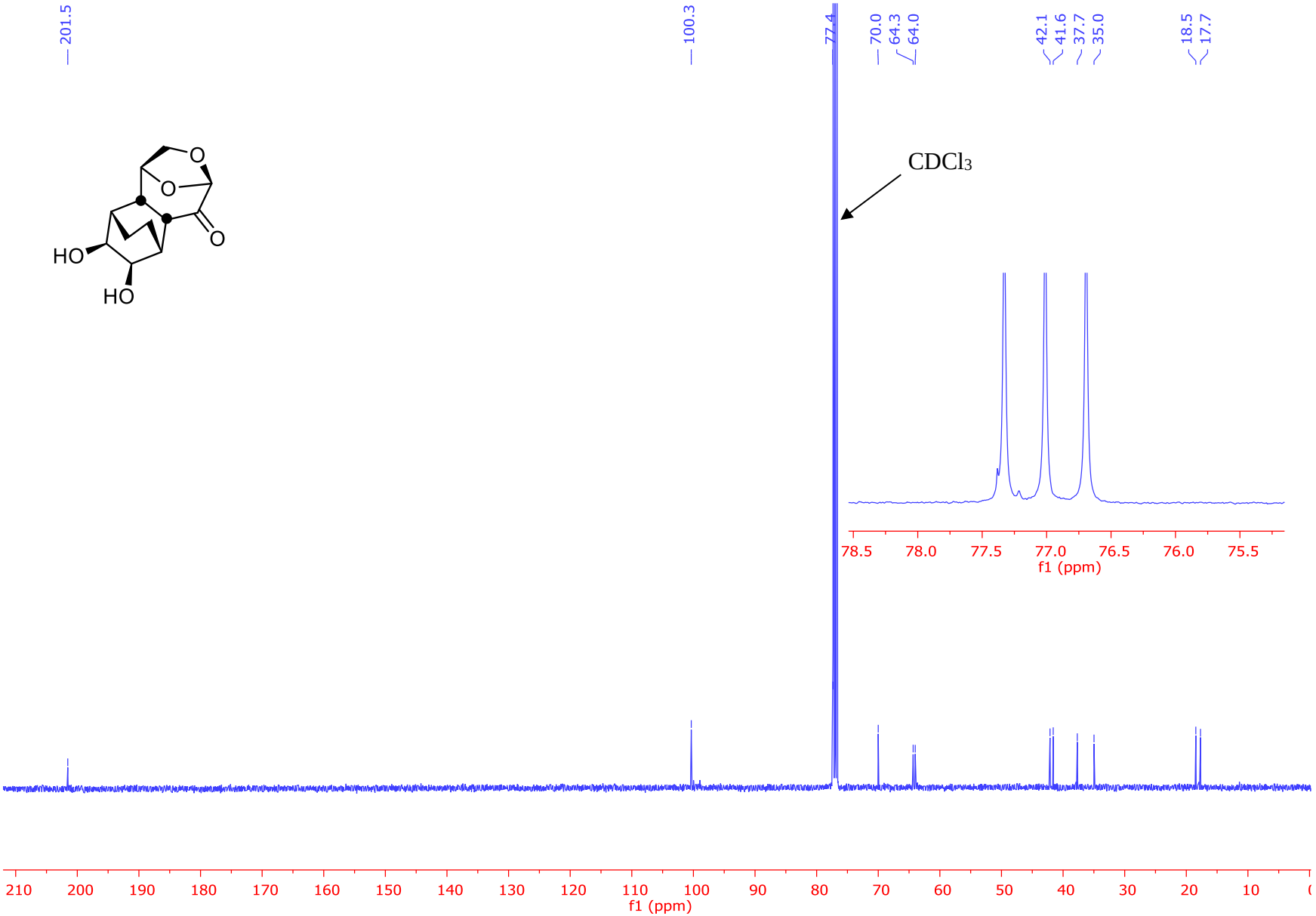

Figure S59: 101 MHz $^{13}C\{^{1}H\}$ NMR Spectrum of Compound **33** (Recorded in $CDCl_3$)

References

1 Horton *et al*. *J. Org. Chem*. **1996**, *61*, 3783.
2 Zurita *et al*. *Carbohydr. Res*. **2015**, *401*, 67.
3 Galimova *et al*. *Russ. J. Org. Chem*. **2014**, *50*, 1848.